WORKING paper

BANQUE DE FRANCE
EUROSYSTÈME

Decomposing the Inflation Response to Weather-Related Disasters[1]

Erwan Gautier & Christoph Grosse-Steffen & Magali Marx & Paul Vertier[2]

December 2023, WP #935
(updated January 2026)

ABSTRACT

This paper estimates the dynamic causal price effects of weather-related disasters in an instrumental-variable approach that links monthly product-category inflation rates with meteorological and disaster data measured in the French overseas territories. We document substantial heterogeneity in price responses across product categories: weather shocks trigger an immediate and pronounced increase in food prices (notably fresh food), while prices of services and manufactured goods partially decline. These extreme weather-induced price effects dissipate within four months. As a result, the overall impact on headline consumer price inflation is moderate and statistically insignificant, peaking at around 0.1%. Additionally, we find a significant reduction in employment following disasters, driven largely by job losses in the food, services, and construction sectors.

Keywords: Natural Disasters; Extreme Weather; Inflation; Disaggregate Inflation

JEL classification: E31, Q54

[1] We would like to thank Eric Strobl for an excellent discussion, as well as Oscar Jordà, Friederike Kuik, Miles Parker, Jeanne Tschopp, and seminar participants at the Toulouse School of Economics, University of Marseille, Université de la Réunion, Banque de France, IEDOM, and participants of the ARUM conference (Paris, 2024), EEA-ESEM Congress (Paris, 2023), the T2M Conference 2023, the Royal Economic Society Annual Conference (Belfast, 2024), EAERE conference (Leuven, 2024) for their useful comments and suggestions. The views and opinions expressed in this paper are those of the authors and not necessarily those of Banque de France or the Eurosystem.

[2] Banque de France, erwan.gautier@banque-france.fr, christoph.grossesteffen@banque-france.fr, magali.marx@banque-france.fr, paul.vertier@banque-france.fr.

NON-TECHNICAL SUMMARY

How do weather-related disasters affect consumer prices? At a time when central banks are considering climate risks in their operational frameworks, this question is becoming relevant for monetary policy. Existing empirical literature has mainly focused on the overall effect on prices, cloaking the complex interplay of supply disruptions following natural disasters that drive up prices in the short run, combined with a shock to the composition of aggregate demand. This paper documents how prices of granular Consumer Price Index (CPI) product categories respond to weather-related natural disasters. The full decomposition across product categories in geographically small regions refines our understanding of the inflation response to extreme weather events. Given that disasters are expected to become more frequent as a result of climate change, our findings help policymakers to address the important challenge posed by uncertain climate change more appropriately.

A challenge for the measurement of causal dynamic effects from weather-related disasters is the imprecise measurement of economic damages resulting from asset impairment and business interruptions following natural disasters, which are not directly observable. We propose an instrumental variable approach for binary disaster events. In a first step, we regress meteorological data on administrative disaster events using a model capturing the non-linear relationship between wind and precipitation intensity and unobserved economic damages during natural disasters. To assess the inflation effects of natural disasters, we then relate the probability of an economic disaster as predicted by the first-step equation to the evolution of prices for different time horizons following the shock. We focus our empirical analysis on prices in four French overseas territories, namely Guadeloupe, Martinique, French Guiana and Réunion.

Figure: Decomposition of the reaction of total inflation to a weather-related disaster

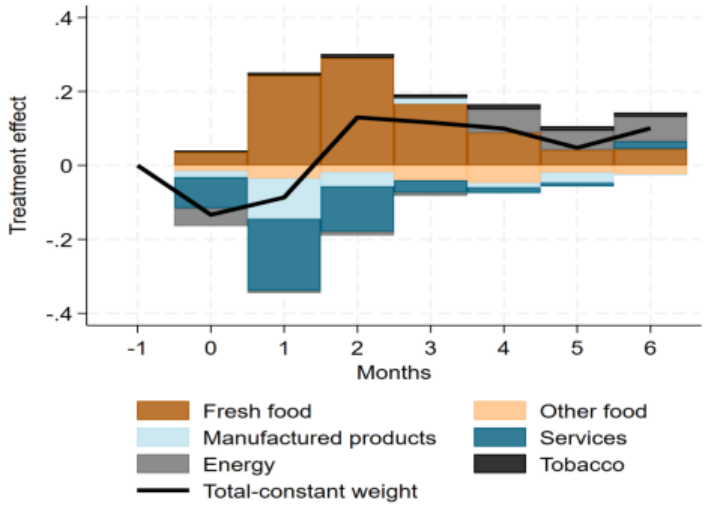

Note: Plotted is the decomposition of the cumulative impulse response of headline CPI to a weather-related disaster obtained from our baseline IV local projection. The contribution of each component is computed as the cumulative response of the CPI of this component times its average weight in the consumer baskets of the four overseas regions between 1999 and 2024. The solid black line reports the price effects obtained for constant-weight headline inflation (in %). Sample period: 1999m01 to 2024m12, excluding the Covid period 2020m03-2021m12, for all four regions.

Our main results are as follows. First, we observe an immediate strong surge in the prices of fresh food products of 8% after two months, which vanishes after four months. This positive inflation effect coincides with a negative impact from natural disasters on agricultural and food processing employment, pointing to a negative supply shock with a displacement of labor supply from the

agricultural and food processing sector to other low-skilled occupations. By contrast, the prices of services and manufactured products decline moderately but in a statistically significant way just after a natural disaster, by about -0.4%. This negative effect coincides with a broad decrease in services and construction employment, suggesting a decrease in aggregate demand. The positive effects on fresh food prices and the negative effects on other components tend to offset each other, yielding an overall slightly positive but non-significant effect on headline inflation. Overall, our results mainly point to a distortion of relative prices, with overall small effects on headline inflation.

A second contribution of the paper is methodological, consisting of a comparison of the two-step IV approach with calibrated damage functions that map meteorological data directly via an explicit functional form into economic damages. In our context, the price effects from the IV approach are slightly larger, suggesting that the IV regression may better address the underlying attenuation bias present when using meteorological data. Our comparison also suggests that, depending on data availability, either of these two methods can be used to provide consistent estimates of the effects of natural disasters. Our IV approach may also be an interesting alternative for applied researchers since it can help to characterize endogenously how extreme weather events affect the occurrence of natural disasters. Relatedly, the findings underline the importance of a careful modeling of regional seasonality, as inflation and weather-induced disaster might share common seasonality patterns that potentially bias the estimator.

Décomposition de la réponse de l'inflation aux catastrophes météorologiques

RÉSUMÉ

Cet article propose une estimation causale des effets dynamiques des catastrophes naturelles sur les prix à l'aide d'une approche par variables instrumentales reliant l'inflation par catégorie de produits aux données météorologiques et aux catastrophes naturelles dans les territoires d'outre-mer français. Nous documentons une forte hétérogénéité des réponses des prix selon les catégories de produits : les chocs météorologiques entraînent une augmentation immédiate et marquée des prix de l'alimentation (notamment des produits frais), tandis que les prix des services et des biens manufacturés diminuent. Ces effets induits par les évenements météorologiques extremes s'estompent à partir de quatre mois. Par conséquent, l'impact global sur l'inflation des prix à la consommation est modéré et statistiquement non significatif, culminant à environ 0,1 %. De plus, nous mesurons une réduction significative de l'emploi à la suite des catastrophes, principalement due à des pertes d'emplois dans les secteurs de l'alimentation, des services et de la construction.

Mots-clés : catastrophes naturelles ; conditions météorologiques extrêmes ; inflation ; inflation désagrégée

1. Introduction

How do natural disasters affect consumer prices? At a time when central banks are considering climate risks in their operational frameworks, this question becomes relevant for monetary policy (e.g. Schnabel, 2021). Existing empirical literature has mainly focused on the overall effect on prices, cloaking the complex interplay of supply disruptions following natural disasters that drive up prices in the short run, combined with a shock to the composition of aggregate demand. This paper documents how prices of granular Consumer Price Index (CPI) product categories respond to weather-related natural disasters. The full decomposition across product categories in geographically small regions refines our understanding of the inflation response to extreme weather events. Given that disasters are expected to become more frequent because of climate change, our findings help policymakers to address upcoming challenges more appropriately (Hansen, 2022).

We focus our empirical analysis on prices in four French overseas territories, namely Guadeloupe, Martinique, French Guiana and La Réunion. These regions are regularly exposed to significant weather-related disasters and are located in different parts of the world, which allows for the study of shocks that are desynchronized across regions. For each of these regions, we use highly harmonized price indices produced by the French statistical office (INSEE), at a disaggregated product level and available at a monthly frequency over the 1999-2024 period. There is a trade-off when considering the optimal size of regions for this type of analysis. While large regions contain the risk that the shock only imperfectly propagates to the economic outcome, small regions might limit the generalizability of the findings regarding the channels of shock propagation. Although the regions considered here are relatively small and isolated, they are comparable to a laboratory experiment, enabling us to precisely identify the effects of extreme weather events on prices by matching data on natural disasters with product-level price indices for each of the four regions.

A challenge in the literature studying causal effects of weather-related disasters is the imprecise measurement of economic damages resulting from asset impairment and business interruptions following natural disasters, which are not directly observable. To overcome measurement issues and identify causal dynamic effects from weather-related natural disasters, we use an instrumental variable (IV) approach. This empirical strategy combines two data sources often separately used in the literature, and which are both imperfect proxies for the unobserved economic damage and suffer systematic biases or measurement issues. The first data type are meteorological data that allow to approach the measurement of economic damages through the arguably objective physical intensity. Meteorological data predict hazardous incidents imperfectly, as events of similar physical amplitude are associated with different levels of destruction depending on regional vulnerabilities.

Consequently, the use of meteorological data often induces an attenuation bias, arising from a significant number of events with high physical magnitude that do not cause economic damages. In the empirical framework, this can lead to an underestimation of true effects arising from weather-related disasters on the economy. The second data type is sourced directly from administrative databases that detect events associated with large economic damages based on several *ad hoc* criteria, sometimes complemented by reporting-based intensity measures e.g. from insurance companies. Administrative databases have the advantage of providing direct evidence on disasters with significant economic damage with a relatively high accuracy. However, they are also known to be subject to various reporting biases, which are likely to generate both attenuation bias (Grislain-Letrémy, 2018) and sampling biases (Felbermayr and Gröschl, 2014), questioning the assumption of exogeneity of the disaster variable with respect to the endogenous outcome.

Our IV strategy uses meteorological data on wind and precipitation as instruments for the occurrence of a reported disaster in a two-step regression approach. In the first step, we regress meteorological data on administrative disaster events using a Logit model which captures the non-linear relationship between wind and precipitation intensity and unobserved economic damages during natural disasters. The instrumented variable combines events reported in the international disaster database (EM-DAT) with a French administrative dataset (GASPAR) that contains information on all disaster events that triggered insurance payments. In the second step, we treat the probability of a disaster predicted from the first step as an exogenous regressor on a set of outcome variables. As we are particularly interested in the dynamic causal effects of weather-related disasters on granular inflation, we use local projections to gauge the effect of economic damages on price indices several months after a disaster for different product categories.

Our main results are as follows. First, we observe an immediate strong surge in the prices of fresh food products of 8% after two months, which vanishes after four months. This positive inflation effect coincides with a negative impact from natural disasters on agricultural and food processing employment, pointing to a negative supply shock with a displacement of labor supply from the agricultural and food processing sector to other low-skilled occupations. By contrast, the prices of services and manufactured products decline moderately but in a statistically significant way just after a natural disaster, by about -0.4%. This negative effect coincides with a broad decrease in services and construction employment, suggesting a decrease in aggregate demand. The positive effects on fresh food prices and the negative effects on other components tend to offset each other, yielding an overall slightly positive but non-significant effect on headline inflation. Overall, our results mainly point to a distortion of relative prices, with overall small effects on headline inflation.

The main contribution of this paper is to show that small aggregate effects of weather-related disasters on headline inflation are the result of quite heterogeneous and partly offsetting price responses across product categories. This has not been documented at this level of granularity in the existing literature before. Parker (2018) and Kabundi et al. (2022) use data from the EM-DAT international disaster database and relate these events to CPI inflation in a large cross-section of countries. These two studies find strong heterogeneity in the impact of disasters on inflation across disaster types and the country development level. They also both emphasize the specific effect of natural disasters on food price inflation. Bao et al. (2023) also document a strong response of fresh food prices after typhoons in China, which drives the overall response in food prices. Heinen et al. (2018) estimate the impact of hurricanes and floods on prices in Caribbean islands via calibrated damage functions. They inspect total headline CPI and three sub-categories, namely food, housing and utilities, and all other items. Their baseline result is an inflationary effect from disasters, lasting one month in response to floods and two months in response to storms. In line with our findings, food price is the sub-component that reacts most strongly to disasters. However, their results show no offsetting effects in product sub-categories, possibly due to the still high level of aggregation of the "other goods" category. Our contribution is the estimation of the price response to natural disasters for a fully exhaustive list of product categories of CPI inflation that covers 12 types of goods and services. A highly balanced panel allows us to interpret our findings as compositional effects of headline inflation with larger granularity. A focus on a homogenous set of relatively small territories regularly exposed to extreme weather events allows us to estimate more precisely dynamic causal effects at monthly frequency. Finally, integrating sectoral economic dynamics enables us to discuss plausible narratives for shifts in sectoral supply and demand.

A second contribution is methodological, consisting of a comparison of the two-step IV approach with calibrated damage functions. Damage functions map meteorological data directly via an explicit functional form into economic damages (Auffhammer, 2018). We show that in our context, price effects obtained with both methods are broadly similar. The effects from the IV approach are slightly larger, suggesting that in our application, the IV regression may better address the underlying attenuation bias present when using meteorological data. Overall, our comparison analysis suggests that, depending on data availability, either of these two methods can be used to provide consistent estimates of the effects of natural disasters. In particular, in our case, the nonlinearity coming from the minimal threshold value in a calibrated damage function contributes a lot to the price effects. Our two-step IV approach may also be an interesting alternative for applied researchers since it can help to characterize endogenously how extreme weather events affect the

occurrence of natural disasters. Another methodological aspect we highlight is the modeling of regional seasonality. Most empirical contributions that evaluate the impact of natural disasters on inflation control for average time-specific fixed effects. This modeling approach ignores the fact that the seasonality of extreme weather events usually varies across territories and thus, is likely correlated with seasonality of inflation or local production. To account for this possible source for omitted variable bias, we include region-specific seasonal dummies. This modeling of seasonality further ensures instrument exogeneity. Quantitative results change significantly if the model does not account for such regional seasonality.

The paper more generally relates to the literature studying the consequences of natural disasters for inflation dynamics. Cavallo et al. (2014) and Doyle and Noy (2015) analyze the reaction of prices to large earthquakes in the form of event studies. Parker (2018) and Kabundi et al. (2022) use a variety of natural disasters, ranging from geophysical events to extreme weather events, distinguishing the intensive margin of disaster-types on prices. A few papers study weather-related disasters only, as we do. One specific strand of papers focuses on temperature variations (Faccia et al., 2021, Ciccarelli et al., 2024, Kotz et al., 2024).

The paper is structured as follows. Section 2 describes the data. Section 3 lays out the empirical strategy. Section 4 contains the main results. Section 5 discusses some methodological issues in particular differences between IV and damage function approaches. Section 6 concludes.

2. Data

In this section, we describe how we combine detailed information on natural disasters and prices for French overseas territories, for the period from January 1999 to December 2024. We exclude observations covering the peak of the Covid-19 episode (March 2020-December 2021) from our baseline sample because of inflation measurement issues and the atypical nature of shocks during the Covid-19 pandemic.

2.1 Product-level inflation data

We use the Consumer Price Index (CPI) produced at monthly frequency by INSEE for each of the four regions in our empirical analysis. Consistent with their administrative designation, we refer to the four overseas territories as DROMs (*départements et régions d'outre-mer*). Overseas territories are the only subnational regions in France for which price indices are specifically calculated using price quotes collected in each region. These consumer price indices have been computed since 1967 in Guadeloupe, Martinique (both Caribbean) and La Réunion (Indian Ocean), and since 1969 in French Guiana (South America). The methodology used for their computation is consistent with

that for metropolitan CPI since 1993 and has been incorporated into the CPI for France since 1998. Price indices are published monthly at a granular level for 12 CPI components, along with their annual weight in the consumption basket. Throughout the paper, we focus on 6 higher-level aggregates based on these 12 CPI components. In Online Appendix A.1, we provide more details on price indices used and Table A.1 displays some summary statistics.

There are some specificities of consumer prices in overseas regions, where prices are set in a distinctive manner compared with metropolitan France. First, price levels are generally higher in overseas regions and the price gap remained broadly constant between 1985 and 2010 (Berthier et al., 2010). Second, as documented in Table A.2 in the Online Appendix, even though inflation in overseas regions is correlated with inflation in metropolitan France, this correlation is lower for food inflation (Hugounenq and Chauvin, 2006), and especially for fresh food.

Second, the heterogeneous correlation of CPIs between metropolitan France and overseas regions is likely to reflect heterogeneous trade prevalence across types of goods and services. Hugounenq and Chauvin (2006) document that about 45% of DROMs' final household consumption was imported in 1999 (of which 60% came from metropolitan France). The share of imported goods was as high as 70% for manufactured products and 90% for durables and fuels. In contrast, the food sector depends much more on local production. In 1995, between 55% and 63% of food needs were covered by local products. Coverage ratios are generally higher for fresh food than for "all food" products (combining fresh and processed food); see Table A.3 in the Online Appendix.

Third, French overseas regions benefit from specific fiscal schemes to compensate for their distance from metropolitan France: VAT is lower and a tax in the form of specific dock dues (*octroi de mer*) on imported products protects local production against external competition. Tobacco and petroleum products are also less taxed in the DROMs than in metropolitan France: no VAT is imposed on petroleum products, and taxes on tobacco are set by local authorities. Petroleum product prices are also set by local authorities.

We complement these monthly data on inflation with monthly data on hotel overnight stays (from 2011), quarterly data on employment (from 2011) and quarterly data on imports and exports (from 2004). To the best of our knowledge, no quarterly data exist in DROMs for consumption or investment (see Online Appendix A.2 for data sources).

2.2 Weather-related disaster data

This section presents the data sources for natural disasters and extreme weather events.[1]

2.2.1 Administrative databases for natural disasters

In this paper, we use two different datasets that collect *ex-post* administrative information on economic losses due to natural events.

Starting point is the EM-DAT international disaster database, produced by the Centre for Research on the Epidemiology of Disasters (CRED). It has global coverage, a standardized approach to disaster thresholds, and marks a *de facto* standard for natural-disaster shock identification in the literature. The events recorded in the database are aggregated from several sources, namely insurance companies, UN agencies, NGOs, research institutes and press agencies. Events recorded in EM-DAT must respect at least one of three criteria: (i) 10 or more people killed; (ii) 100 or more people affected/injured/homeless; and (iii) declaration by the country of a state of emergency and/or an appeal for international assistance. Throughout the analysis, we focus on disasters classified as "storms", "floods" or "landslides" (since the latter are often caused by heavy rainfall). For each region, we create a monthly binary variable equal to 1 if at least one such natural disaster was reported in a region during a calendar month, 0 otherwise.

These data are supplemented by the French administrative dataset GASPAR (*Gestion Assistée des Procédures Administratives relatives aux Risques*) that is assembled by the French Ministry of Ecological Transition. A disaster is recorded upon declaration by the French government of a state of "natural disaster", after consultation by an inter-ministerial commission. Importantly, under French law, the declaration of state of natural disaster conditions the eligibility of households to an insurance payout. We therefore consider that events registered in this database are a strong indicator for economic damages. The GASPAR dataset, starting in 1990, contains various information, such as the start date and the end date of events, municipality, region, and type of disaster. We collect events that include designations of floods, tropical storms or cyclones and landslides.[2] Then, for each region, we construct a binary indicator by assigning each disaster reported in GASPAR to the month corresponding to its reported start date.

[1] Following the literature, we would refer to climate as moments of the distribution underlying longer periods of realizations of weather data. Our focus is on weather realizations in the tails of the distribution of precipitation and wind speed data, and not in effects of changes in the moment of this distribution (see e.g. Dell et al. (2012) for the latter).

[2] These types of events include tropical phenomena, storms, and cyclones, damages due to waves or tidal waves, and floods. A natural disaster can combine several events of this type at the same time. We exclude events that are not directly related to weather extreme events, such as volcanic eruptions, damages due to lava and earthquakes, or for which there is no occurrence in our sample, such as snowstorms or avalanches.

Combining these two datasets leads us to 100 disaster events over the period 1999-2024 in the four regions. Most of the events in EM-DAT are also reported in GASPAR, but a smaller proportion of GASPAR events are reported in EM-DAT, since GASPAR reports a significantly higher total number of events (Table A.5 in the Online Appendix). The events can be categorized along different criteria. Out of the 100 events, 92 entailed either high wind or high rain (33 of which were associated with landslides), and 8 were landslides not associated with high wind or high rain. Out of the events entailing either wind or rain, 14 were due to both floods and storms, 76 events were floods unrelated to a storm, and 2 were storms not associated with floods (Tables A.6 and A.7 in the Online Appendix).

Both data sources have well-documented reporting biases. A heterogeneous insurance pattern across French overseas territories likely leads to misreporting in the GASPAR database due to a charity hazard. Grislain-Letrémy (2018) shows that the probability that local authorities declare the state of emergency depends on the insurance coverage of households in their community. If this coverage is large, authorities have an incentive to declare an emergency, a prerequisite in French law for insurance payouts. If the coverage is low, however, local communities might be better off calling for direct financial assistance from the French government. This introduces a misreporting bias into the GASPAR database. For EM-DAT, Felbermayr and Gröschl (2014) find a different bias. They conclude that news-driven and insurance-based datasets generally raise a selection bias issue with a potential correlation between intensity measures and error terms in economic growth regressions. Such a selection bias would also most likely affect our results on inflation responses.

To overcome these potential biases, we complement our natural disaster datasets with information from meteorological records. When we estimate the effects of disasters on prices or real variables, this will allow us to use an IV approach where reporting-based natural disaster events are instrumented by meteorological records. Instrument *exogeneity* holds if the weather-related disaster is unrelated to any other unobserved shocks that affect the inflation rate in a systematic way. In other words, weather-related extreme events should affect prices only through the economic damages they create. As it is standard in the literature, we argue that natural disasters captured by meteorological data alone are plausibly exogenous to economic outcomes (Strobl, 2012, Felbermayr and Gröschl, 2014).

2.2.2 Meteorological records

The meteorological information was collected by remote sensing systems based on satellites. Wind speed is taken from the National Oceanic and Atmospheric Administration (NOAA) Cross-Calibrated Multi-Platform (CCMP) wind vector analysis that allows us to compute wind speed over

the ocean surface in meters per second. Each vector summarizes the average wind speed in a cell of 0.25 degrees of latitude longitude coordinates within a six-hour interval.

Figure 1. Data from remote sensing

a) Wind speed, La Réunion

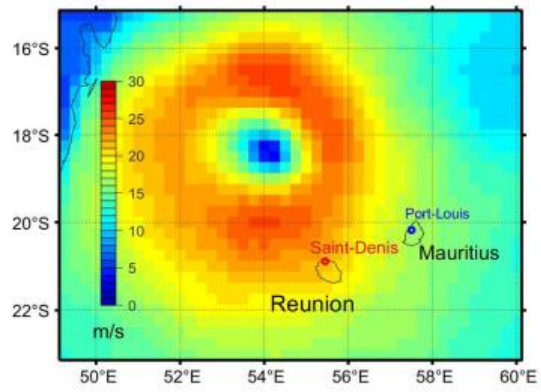

b) Precipitation, Guadeloupe

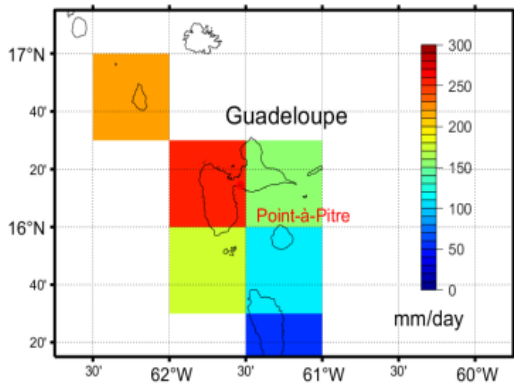

Note: Panel a) Maximum wind speed in La Réunion on 25 February 2007 is 27.76 m/s, which is associated with the passing of Cyclone Gamède. Data from NOAA Cross-Calibrated Multi-Platform (CCMP); 0.25-degree grid in m/s; range from 0 to 30. Panel b) Maximum daily rainfall in Guadeloupe: 252.59 mm on 19 November 1999. The chart illustrates a high degree of regional concentration of precipitation. Data from NOAA CPC Global Unified Gauge-Based Analysis of Daily Precipitation; 0.5-degree grid in mm in a day.

Figure 1a provides an illustration of the data for the case of cyclone Gamede passing La Réunion in February 2007. Precipitation data are taken from the NOAA CPC Global Unified Gauge-Based Analysis of Daily Precipitation, which provides daily cumulative precipitation in millimeters over horizontal surface at a resolution of 0.5 degrees of latitude longitude coordinates. Figure 1b illustrates an episode of extreme precipitation in Guadeloupe in November 1999. For aggregation, we convert gridded observations to a region–month value x_{it} by taking the monthly maximum: for region i and month t i.e., the maximum over all grid cells intersecting region i and all six-hourly slots (wind) or days (rain) in month t. Table A.9 in the Online Appendix reports summary statistics, showing that La Réunion is the region with the highest average wind speed maximum, while French Guiana is the region with the highest average precipitation maximum.

Figure 2 illustrates the correlation between administrative disaster data and the physical intensity of rainfall and wind. Specifically, it plots the occurrence of administrative events against the joint distribution of maximum monthly precipitation and wind speed. When we compare discrete events with the physical intensity of wind and precipitation, we find that many events lie in the upper tail of the distribution. EM-DAT events are almost systematically located above the median of either wind or precipitation records, and most of them are in the top quartile. Conversely, GASPAR events are mainly located in the center of the distribution. This can be due to the charity bias in GASPAR, or due to true economic damage from natural

disasters associated with low meteorological intensity due to heterogeneous regional vulnerability. As we cannot detect the reason from available data alone, this complicates empirical identification of causal effects from extreme weather events on the economy. The next section presents our instrumental variable approach to overcome this identification issue.

Figure 2. Administrative shocks and joint distribution of precipitation and wind speed

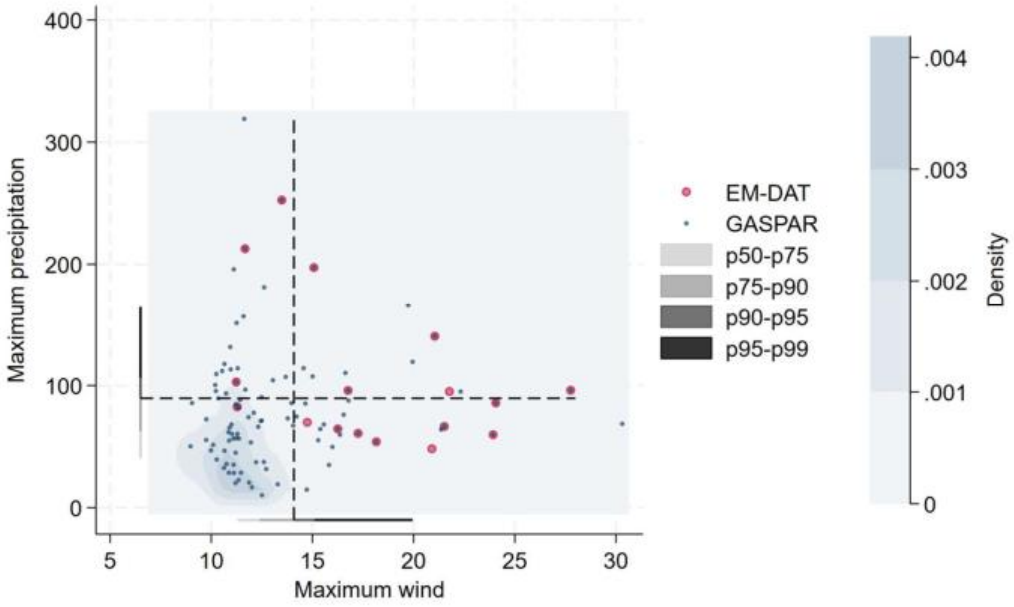

Note: Plotted are the month-region wind speed maxima (measured in meters/second) and month-region precipitation maxima (measured in mm/day) associated with each EM-DAT event (red dots) and GASPAR events (blue dots), as well as their joint distribution (blue shaded density) between 1999m01 to 2024m12, excluding the Covid period 2020m03-2021m12, and pooled across all regions. Dashed lines mark top-decile (p90) wind speed and precipitation maxima. Grey and black rectangles represent, for each variable, the range of values between median (p50), top quartile (p75), top decile (p90), top 5% (p 95) and top percentile (p99).

3. Empirical strategy

This section documents our IV empirical strategy to estimate the effects of weather-related disasters on prices and real variables. Our strategy relies on instrumenting disasters reported as binary variables in EM-DAT or GASPAR datasets with wind speed and rainfall variables. However, the relationship between weather data and economic damages is highly nonlinear (Emanuel, 2011) and a standard 2SLS regression cannot capture this non-linearity. Moreover, Antoine and Lavergne (2023) argue that an inadequate functional form in the first stage of an IV regression could give rise to weak instrument issues for inference. To account for this nonlinearity in our IV approach, we thus follow the two-step method proposed by Wooldridge (2010). In a first step, we estimate by maximum likelihood a Logit model relating the binary disaster variable with weather data. In a second step, we estimate a 2SLS regression where in the first stage equation, we use the estimated probability predicted by the Logit model as an

instrument for natural disasters and in the second stage of the 2SLS regression, we relate product-category inflation to disasters as predicted by the first stage equation. Xu (2021) shows that this two-step IV estimation method outperforms a linear 2SLS estimator (i.e. with a linear probability model as first-stage IV equation).

3.1 Logit regression

As described above, we first estimate a Logit model where the dependent variable $\omega_{i,t}$ is a binary variable that is equal to one if a natural disaster related to a storm, a flood or a landslide is reported in GASPAR or EM-DAT at date *t* in region *i*, and 0 otherwise and $p_{i,t}$ the probability of disaster at date *t* in region *i*. Our estimated non-linear model can be written as follows:

$$p_{i,t} = P(\omega_{i,t} = 1) = P(\omega_{it}^{*} \geq 0) = \frac{1}{(1+\exp(-\omega_{it}^{*}))}, \quad (1)$$

where $\omega_{it}^{*} = a + bX_{i,t} + cZ_{i,t} + dY_t + e_q + f_i + e_q \times f_i + h_y + u_{it}.$

The vector $X_{i,t}$ contains meteorological data on wind speed and precipitation. $Z_{i,t}$ is a vector of controls that are specific to each region and date, which contains the monthly variation of a business climate indicator, three lags of monthly variations of CPI for fresh food, other food, manufactured products, services and energy. Y_t is a vector of aggregate controls common to all regions at period *t*, consisting of monthly variation of CPI for metropolitan France and monthly variation of the ECB deposit rate. We also include several fixed effects to control for unobservable heterogeneity: region fixed effects f_i, year fixed effects h_y, calendar quarter fixed effects e_q, and interacted fixed effects between region and calendar quarter to account for differences of weather seasonality across the three regions where overseas territories are located, notably the Caribbean, South America, and the Indian Ocean (see Section 5.2 for a discussion on the role of seasonality controls). Finally, u_{it} denotes residuals, which we assume to be independent and identically distributed and drawn from a standard logistic distribution. The model is estimated by maximum likelihood.

To illustrate the highly nonlinear relationship between wind/rain and natural disaster events, we compute the simulated probabilities of a natural disaster for wide ranges of wind and rain values - relying on estimates of a simplified version of our Logit model with only rain, wind and regional dummies as exogenous variables. Figure 3 plots these simulated predicted probabilities as a function of rain and wind speed for the case of La Réunion.

Figure 3. Simulated probabilities from the Logit model relating natural disasters and meteorological data

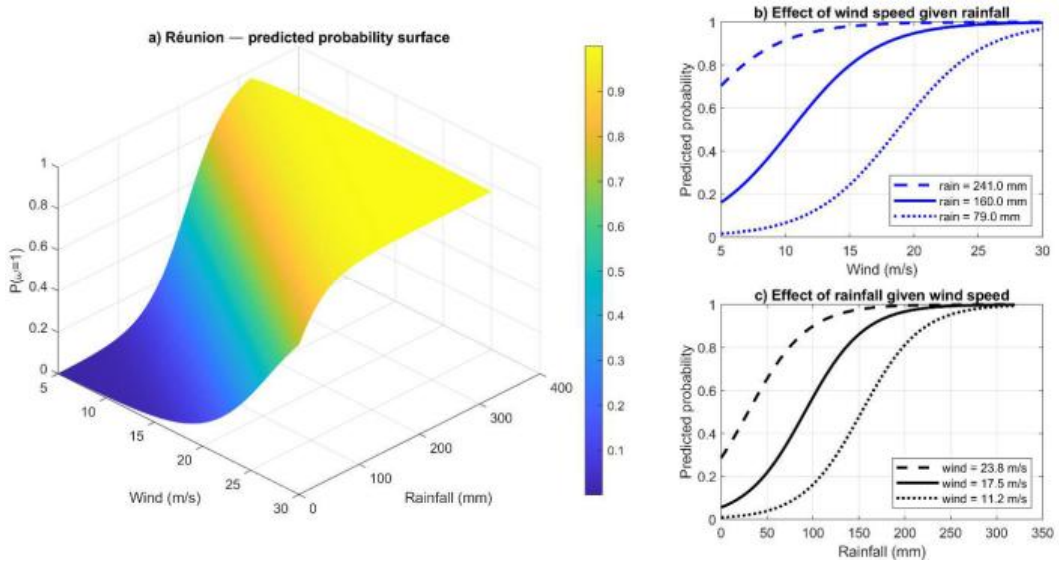

Note: Plotted are predicted probabilities obtained from a logistic cumulative distribution function (CDF) for a simplified version of model (1) relating wind speed and rainfall to the occurrence of an administrative weather-related disaster: $P(\omega_{i,t} = 1|wind, rain) = \frac{1}{1+\exp(-(a+b_1 wind+ b_2 rain+f_i))}$. The s-shaped sigmoid is determined by estimated coefficients for wind intensity (b_1), rainfall intensity (b_2) and the regional dummies (f_i). The model is estimated over the sample period 1999m01 to 2024m12, excluding the Covid period 2020m03-2021m12, covering the four regions.

The relationship between the probability of a natural disaster and wind speed or rainfall is S-shaped, reflecting the logistic functional form underlying the Logit model. For a large range of low values of wind speed or rainfall this probability is close to 0 (dark blue region in Panel a) whereas for another wide range of high values of wind and rainfall the probability is close to 1 (yellow region). Whenever the latent variable ω_{it}^* (which depends on wind and rain values but also on the estimated coefficients associated with these variables) goes above 0, the probability gets closer to 1. The marginal effects of wind and rain on the probability of a disaster will vary with the levels of wind speed and rainfall. The marginal effects are small at very low values of meteorological intensity, where the probability of a disaster is very low anyways, or at very high values of meteorological intensity, where a disaster is almost certain. In contrast, the marginal effect (or the slope of the sigmoid) is steepest at intermediate levels for rainfall and wind (as illustrated in Panel b and Panel c of Figure 3). One important feature of this model is that the shape and the location of the non-linearity are determined by the empirical estimation, and we do not rely on *ad hoc* thresholds for wind speed or rainfall above which we consider meteorological events start to cause economic damage, or above which disasters are certain.[3]

[3] These estimated thresholds are characterized by a joint effect of wind speed and rainfall, meaning that the marginal effect of each variable varies with respect on the level of the other.

This also allows us to fully characterize how wind and rain values affect the occurrence of a disaster event reportedly having led to economic damages in a given region.

Panel A of Table 1 reports the average marginal effects estimated from our Logit model from equation (1). Each column corresponds to a different model where we consider linear, square or cubic specifications of wind speed and precipitation, with or without the lower order terms. First, we find positive and significant marginal effects of both wind speed and rainfall on the occurrence of a natural disaster, see column (1). When we include in separate regressions squared or cubic values of rainfall and wind speed in columns (2) and (3), the parameters are also significant but comparing pseudo-R^2 values, the fit of the model slightly worsens. When we include all meteorological data in levels plus higher-order terms, most of the regression coefficients become insignificant and the fit of the model only marginally improves, as can be seen in columns (4) and (5). We use the model presented in column (1) as baseline specification since we have a concern for weak instruments due to non-significant regressors for models with higher-order terms. Our results suggest that the nonlinearity of the relationship between meteorological data and our binary outcome variable is sufficiently captured by the logistic CDF if wind speed and rainfall enter in levels.[4]

3.2 2SLS regression

In a second step, we implement a standard 2SLS regression, where the predicted probability of a disaster obtained from the Logit model (equation 1) serves as an instrument for the dummy variable of administrative events. The first stage of the 2SLS can be written as follows:

$$\omega_{i,t} = \alpha_1 + \varphi_1 \hat{p}_{i,t} + \rho_1 Z_{i,t} + \tau_1 Y_t + \delta_{1y} + \mu_{1q} + \gamma_{1i} + \mu_{1q} \times \gamma_{1i} + \varepsilon_{1i,t}, \qquad (2)$$

where $\hat{p}_{i,t}$ is the predicted probability of a natural disaster $\omega_{i,t}$ as a function of meteorological data estimated from equation (1).[5] We include the same control variables and include the same type of fixed effects as in equation (1). Panel B of Table 1 reports the results from this first stage of IV regression. All specifications show a very strong first-stage relationship, with F-statistics typically above 100.[6] This underlines the high relevance of meteorological data for particularly destructive disaster events in an IV setup.

[4] We run robustness regressions including higher order terms for wind speed and rain as instrumental variables. Results are discussed in Section 4.2 below.

[5] We use subindex 1 for parameters of the first stage equation and subindex 2 for parameters of the second stage equation.

[6] We assess the strength of the first stage regression with the robust F-stat, which relies on the assumption that the residuals from the first stage are i.i.d. Figure B.1 in the Online Appendix illustrates that the residuals are not autocorrelated.

Consistent with the Logit estimation, considering probabilities obtained from a logistic CDF fitted to meteorological data in levels entails a slightly stronger explanatory power (both in terms of F-stat and R^2) than considering them in square or cubic transformations of wind speed or rainfall (columns 2 and 3), but a lower explanatory power than combining higher- with lower-order terms. However, in the latter specifications, the gains in terms of explanatory power are small, while the model in column (1) shows already a highly significant F-statistic. We therefore adopt the most parsimonious model as our baseline.[7]

Table 1. Regressing administrative disasters on sensing meteorological data

	(1)	(2)	(3)	(4)	(5)
Panel A: Logit model – Marginal effects					
Wind	0.024***			-0.016	0.189
	(5.36)			(-0.55)	(1.07)
Rain	0.002***			0.003***	0.03**
	(7.17)			(4.21)	(2.00)
$Wind^2$		0.0009***		0.001	-0.013
		(5.66)		(1.36)	(-1.06)
$Rain^2$		9.57e-6***		-5.26e-6	-8.30e-6
		(5.90)		(-1.57)	(-0.48)
$Wind^3$			0.0004***		0.0003
			(5.68)		(1.17)
$Rain^3$			4.31e-8***		8.82e-9
			(4.65)		(0.18)
Pseudo R^2	0.378	0.358	0.336	0.385	0.388
N	904	904	904	904	904
Panel B: First Stage – 2SLS					
$\hat{p}_{i,t}$.	1.034***	1.027***	1.022***	1.033***	1.035***
	(11.13)	(11.07)	(10.89)	(11.62)	(12.31)
Adj.R2	0.330	0.309	0.282	0.336	0.339
N	904	904	904	904	904
F-Stat	123.78	122.53	118.59	135.1	151.61

Note: Panel A contains the estimation results of the Logit model in equation (1). Panel B presents the first stage of the IV regression from equation (2), where the dependent variable is $\omega_{i,t}$ a binary variable equal to 1 if a weather-related disaster has been reported by EM-DAT or GASPAR, and 0 otherwise. *Wind* corresponds to the month-region maximum wind speed (in m/s) from the CCMP database. *Rain* is the month-region maximum daily precipitation (in mm) as reported by the CPC Global Unified Gauge-Based Analysis of Daily Precipitation. T-stats are reported in parentheses. Standard errors are heteroskedasticity-robust and computed using a White-correction routine. The model is estimated over the sample period 1999m01 to 2024m12, excluding the Covid period 2020m03-2021m12, covering the four regions. Significant at ***0.01, **0.05, *0.10.

[7] Table B.1 in the Online Appendix provides some alternative specifications with dummies for top deciles of wind and rain used as instruments or using a standard 2SLS regression (using a linear probability model as a first stage), but F-stats are much lower than in our baseline specification.

Figure B.2 in Online Appendix plots the distribution of predicted probability obtained from the Logit model while Figures B.3 to B.5 plot a decomposition of the latter conditioning on the occurrence of actual administrative natural disasters. The entire distribution conditional on an observed administrative shock is shifted to the right compared with the distribution when there is no administrative disaster reported in the data. We take this as evidence for a good predictive property achieved in model (1). Overall, we find that the average predicted probability of a weather-related disaster conditional on observing no administrative disaster as reported in EM-DAT or GASPAR is 7%, while it is 43% conditional on observing an administrative disaster.

Estimation for the second stage of the IV regression relies on a local projection method (Jordà, 2005). We relate the log of the price index evolution between date (year-month) *t-1*, and date *t+h* (where *h=0...6* months) to the estimated probability of a natural disaster $\widehat{\omega}_{i,t}$ recovered from the first stage of the 2SLS estimation (equation 2). For each price index of interest (headline CPI or product-level CPI), the second stage regression can be written as follows:

$$\log\left(\frac{P_{i,t+h}}{P_{i,t-1}}\right) = \alpha_{2h} + \theta_h \widehat{\omega}_{i,t} + \rho_{2h} Z_{i,t} + \tau_{2h} Y_t + \delta_{2hy} + \mu_{2hq} + \gamma_{2hi} + \mu_{2hq} \times \gamma_{2hi} + \varepsilon_{2h,i,t}, \quad (3)$$

where $\widehat{\omega}_{i,t}$is the fitted value of the reported disaster $\omega_{i,t}$ derived from the first stage of the 2SLS (equation 2). All control variables and fixed effects are identical to those included in equations (1) and (2). In particular, the regression includes three lags of the endogenous variable, namely the product-level monthly inflation rates. This modeling approach is recommended by Montiel-Olea and Plagborg-Møller (2021) in the context of local projections to obtain robust estimation and take care of potential autocorrelation in the error terms, which can be problematic in time-series models that feature high persistence in the underlying data. Equation (3) is estimated separately for each horizon *h*, and the parameters of interest are θ_h, they capture the cumulative effect on prices of a natural disaster *h* months after a weather-related disaster. Standard errors are heteroskedasticity-robust and computed using a White-correction routine, as suggested by Montiel-Olea and Plagborg-Møller (2021) and Inoue et al. (2025).

We estimate equations (2) and (3) using a standard 2SLS estimator. Since $\widehat{\omega}_{i,t}$ is the continuous predicted probability defined in the range [0,1], our parameter of interest θ_h should be interpreted as the effect of the predicted probability $\widehat{\omega}_{i,t}$ going from 0 to 1 on cumulative price variation *h* months after a weather-related disaster event.

4. Main results

In this section, we present the results of our baseline estimation strategy for the headline CPI and the six main product-level components but also for the real activity variables.

4.1 Baseline specification

Figure 4 plots the results from the second stage of our baseline 2SLS regression. We first find that the effect of weather-related disasters on prices is heterogeneous across CPI product components. On the one hand, inflation of fresh food increases strongly and rapidly, up to 8% two months after a weather-related disaster. This effect is particularly strong, as it typically represents about 3.2 standard deviations of fresh food CPI on average across the four regions. This positive effect then decays progressively, until reaching values close to zero after 5 months. On the other hand, prices of other components decrease moderately after weather-related disasters. Prices of services decrease by a maximum of 0.5% (after one month), those of manufactured products by a maximum of 0.4% (after one month) and those of other food by a maximum of 0.3% (after 4 months). The negative reactions of these components are significant at the 5% level at least once over the 6 months of the projection horizon, but overall decay to zero quickly after the disaster. For services, the negative effect is broad-based across all subcomponents, though the effects are significant only for health services, and to a lesser extent for communication services (Table B.2 in the Online Appendix). For food, manufactured goods or services, the price effects are transitory: it is significant just after the disaster but disappears after some months. Weather-related disasters lead to transitory relative price effects but not to permanent or broad-based price increases. Finally, prices of energy or tobacco products do not react significantly to weather-related disasters, which is expected since they are strongly administered. When we compare the effects obtained with our 2SLS regression to the ones obtained by OLS, i.e. by using $\omega_{i,t}$ as exogenous variable in equation (3), we find similar qualitative results, but the price effects obtained from OLS regressions are smaller (Figure B.6 and Table B.3 in the Online Appendix). This confirms that relying only on administrative data to measure economic damages tends to underestimate the effects of disasters on inflation, since a significant share of these natural disasters does not correspond to extreme weather events and are therefore likely to be related to less severe real economic damages.

Figure 4. Impact of weather disasters on prices – CPI components and headline CPI

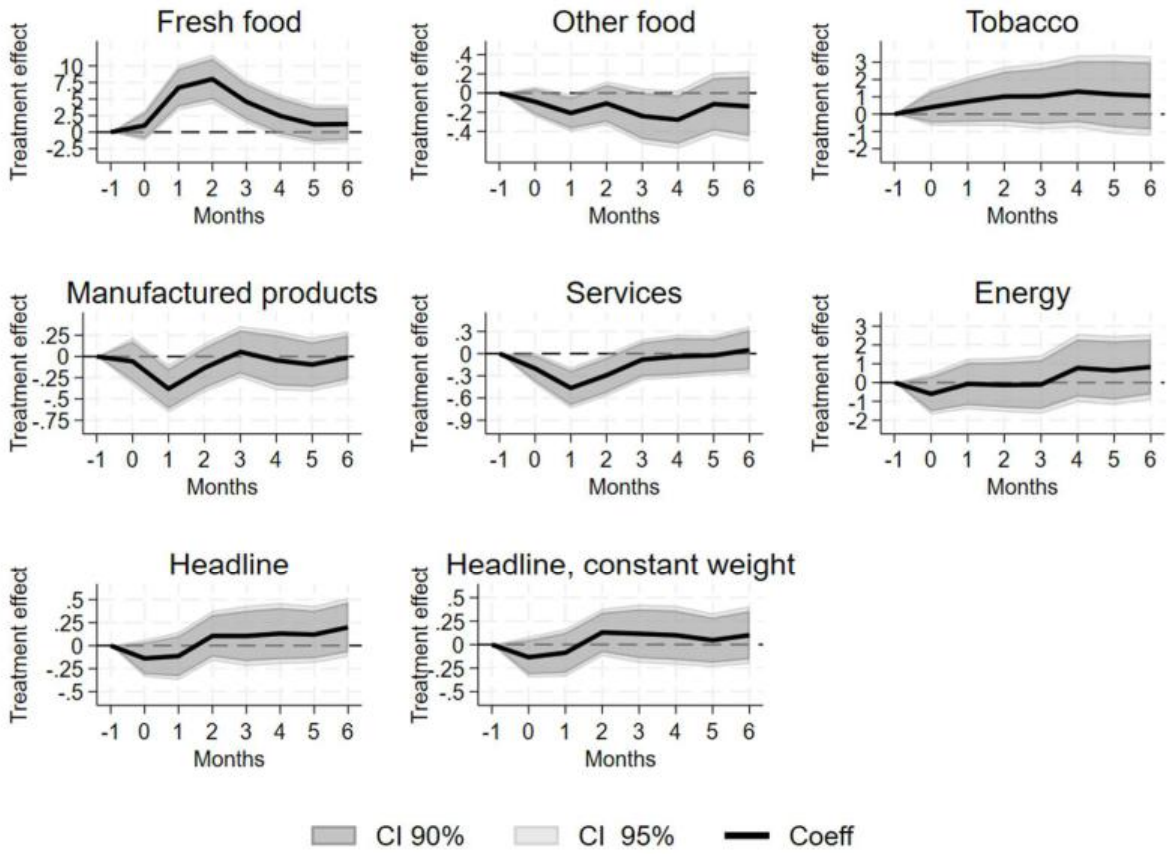

Note: Plotted are the cumulative impulse responses of CPI product components and headline to weather-related disasters obtained from our 2SLS baseline model; price effects (solid black line) are reported in percent; shaded areas show 90% (dark grey) and 95% (light grey) confidence intervals. Standard errors are heteroskedasticity-robust and computed using a White-correction routine. Months are expressed in distance to the natural disaster. Sample period: 1999m01 to 2024m12, excluding the Covid period 2020m03-2021m12, for all four regions.

Our second main result shows the dynamic propagation of weather-related disasters on headline inflation over time (bottom panel of Figure 4). We evaluate this effect in two different ways. First, we directly use the headline CPI as dependent variable. Second, we compute a constant-weight headline CPI in which each of the 6 CPI subcomponents described above is weighted by its average weight over time and space. This latter index will also allow us to evaluate the contribution of each component to the overall effect controlling for time-varying CPI composition effects. The effect on headline CPI first decreases modestly and temporarily by about 0.1% after one month, then becomes positive after two months, and stabilizes at around 0.15%. The effect is however not statistically significant. Our IV estimates for total CPI are in the range of those found in the existing literature. Heinen et al. (2018) find that an average hurricane or flood causes a temporary rise in CPI by about 0.1 pp. Parker (2018) finds that a

natural disaster among the top quintile leads to an increase in total CPI of about 0.6 pp after a year, and 0.9 pp after two years.[8]

Figure 5. Decomposition of the reaction of total inflation in the baseline specification

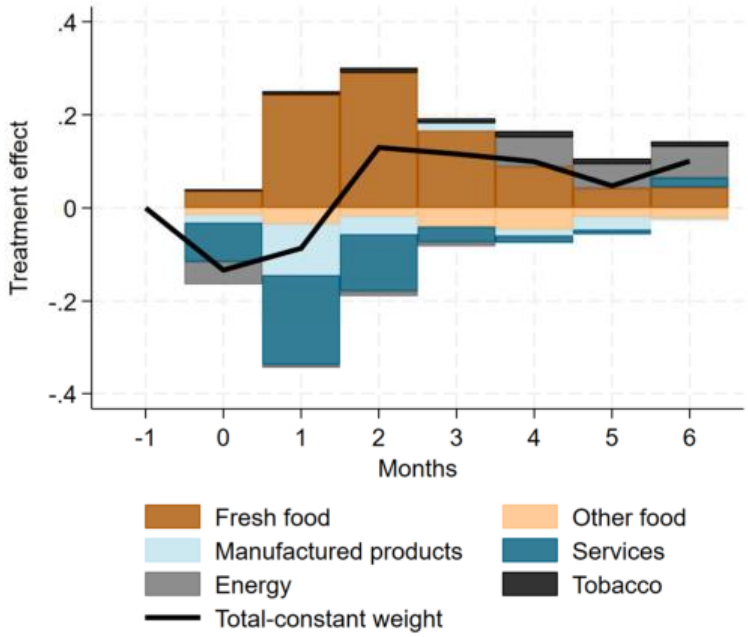

Note: Plotted is the decomposition of the cumulative impulse response of headline CPI to a weather-related disaster obtained from our baseline IV local projection. The contribution of each component is computed as the cumulative response of the CPI of this component times its average weight in the consumer baskets of the four overseas regions between 1999 and 2024. The solid black line reports the price effects obtained for constant-weight headline inflation (in %). The x-axis corresponds to the time horizon expressed in months since the disaster. Sample period: 1999m01 to 2024m12, excluding the Covid period 2020m03-2021m12, for all four regions.

Figure 5 decomposes the effect on total inflation based on the effects estimated for the six sub aggregates taken separately, namely fresh food, other food, tobacco services, manufactured products and energy. Each contribution is computed as the observed pass-through multiplied by the average weight of the component over 1999-2024. The sum of the contributions is compared to the reaction of the constant-weight CPI headline. The results indicate offsetting contributions of fresh food on the inflationary side, and of manufactured products and services on the deflationary side, resulting in a more muted response of headline CPI.

Since natural disasters affect very differently CPI categories, the impact of disasters on headline inflation will depend on the CPI weight of each component. Since the weight of fresh food in CPI tends to decrease over time, from 5.9% in 1999 to 2.7% in 2024 in our sample, the CPI effect of disasters would decrease over time. If we assume that the weight of fresh food had

[8] Both papers find stronger positive effects on food, and rather negative effects on other components (such as housing). However, there is no available data to compute a decomposition (Heinen et al., 2018) and data coverage is not homogenous across countries (Parker, 2018).

stayed the same over the period 1999-2024 at its value in 1999, the disaster effect on overall prices would have reached 0.5%.[9]

4.2 Robustness

Our results are robust to several alternative specifications even if the magnitude of the price effects can vary somewhat (see Table B.4 in the Online Appendix). We consider several alternative specifications where i) we exclude La Réunion where fresh food prices are more volatile and extreme events are more frequent, ii) we control for lags of the dependent variable $\omega_{i,t}$, iii) we exclude administrative disasters occurring less than six months after a previous administrative disaster, iv) we use combinations of higher order meteorological data in the first-step Logit regression, v) we use dummies in the Logit regression indicating whether wind and rain are in the top decile of the distribution. For all these specifications, we find a positive and significant effect for fresh food 2 months after the disaster and negative price effects for services and manufacturing goods one month after the disaster. Additionally, we show that pre-trends are unlikely to drive our results, both through visual evidence for the two main events that hit La Réunion, the cyclones Dina in 2002 and Gamède in 2007, and by estimating backward local projections (Figures B.7 and B.8).

In Online Appendix C, we consider alternative measures based on meteorological records from ground stations and document that our results hold (Table C.1). In Online Appendix D, we exploit the continuous nature of the first-stage Logit fitted probability $\hat{p}_{i,t}$. We re-estimate local projections after discretizing $\hat{p}_{i,t}$ at increasing thresholds *T*. This exercise shows that price effects for fresh food are near zero when the threshold is close to 0, and rise monotonically with the threshold, reaching large values for very high predicted probabilities. Our baseline IV effect lies in the upper part of the distribution of effects obtained across thresholds, consistent with the idea that $\hat{p}_{i,t}$ embeds information about event severity (only 5.8% of tested specifications yield higher estimates). In other words, high values of the instrument predict episodes that are both more likely to be administratively recognized and economically more disruptive. Finally, placebo exercises that randomize instruments and treatment yield effects centered near zero and well below our baseline estimates (Figure E.1 in the Online Appendix).

[9] Online Appendix F provides details of these calculations and some additional results on possible distributional effects across households of weather-related disasters arising from varying budget shares of fresh food along the income distribution. Specifically, this share is larger for low-income households than for high-income households.

4.3 Effects on real economic activity

Turning to the interpretation of these results on prices, the positive effects on the prices of food are likely driven by supply-side factors, while the negative effects on other CPI items are likely driven by demand factors. To shed light on these mechanisms, we estimate reactions of sector-level employment in the four regions to weather-related disasters. The main results are reported in Table 2 while Table B.10 in the Online Appendix provides more detailed results. Note that these effects for real activity are less precisely estimated since data are available only at a quarterly frequency and for shorter time horizons.

Table 2. Main effects of meteorological extreme events on selected real variables (2SLS)

	T=0	T=1	T=2	T=3	T=4	T=5	T=6
Overnight hotel stays	-21.08**	-3.88	-2.31	-17.43***	-1.83	1.38	-10.45
	(8.3)	(7.25)	(7.95)	(6.6)	(5.51)	(7.45)	(6.85)
Employment							
Total	-0.07	-0.37*	-0.61**	-0.82***	-1.02***	-1.18***	-1.20***
	(0.13)	(0.2)	(0.24)	(0.28)	(0.29)	(0.33)	(0.37)
Agriculture (AZ)	-.34	-1.69**	-1.58	-1.24	-1.02	-.81	-1.83
	(.61)	(.82)	(.96)	(1.06)	(1.17)	(1.27)	(1.3)
Food manuf. (C1)	.67**	.78	-.06	-.54	-1.29*	-1.18	-1.54**
	(.32)	(.5)	(.67)	(.83)	(.77)	(.77)	(.75)
AZ+C1	.54*	.01	-.39	-.55	-1.01	-.89	-1.54***
	(.31)	(.42)	(.53)	(.59)	(.62)	(.64)	(.59)
Construction (FZ)	-.31	-.95	-1.39**	-1.92***	-1.98**	-2.27**	-2.76***
	(.36)	(.59)	(.66)	(.73)	(.84)	(.91)	(.95)
Car repair (GZ)	-.15	-.29*	-.41**	-.34	-.43*	-.51**	-.63**
	(.11)	(.17)	(.19)	(.22)	(.23)	(.25)	(.25)
Transports (HZ)	-.34	-.46	-.83*	-.88*	-1.13**	-1.51***	-1.88***
	(.26)	(.39)	(.44)	(.49)	(.53)	(.57)	(.6)
Accom. – restaurants (IZ)	-.43	-.72	-1.31**	-1.87***	-2.15***	-2.26***	-2.27***
	(.41)	(.57)	(.62)	(.69)	(.71)	(.81)	(.84)
Real estate (LZ)	.15	-.22	-.09	-.35	-1.09*	-1.55**	-1.03
	(.27)	(.44)	(.51)	(.55)	(.59)	(.66)	(.78)
Scientific – admin (MN)	-.24	-.57	-.81*	-.81*	-1.14**	-1.29**	-1.32**
	(.28)	(.38)	(.42)	(.44)	(.48)	(.53)	(.58)
Public admin (OQ)	-.01	-.39*	-.56**	-.77***	-.98***	-1.18***	-.96**
	(.16)	(.2)	(.23)	(.3)	(.31)	(.37)	(.41)
Other services (RU)	-.66	-1.66*	-2.05**	-2.67**	-2.83***	-2.73**	-2.43**
	(.55)	(.92)	(.99)	(1.09)	(1.04)	(1.12)	(1.17)
Imports	2.84	2.57	6.29	4.92	5.26	2.14	3.39
	(2.25)	(3.37)	(4.08)	(4.15)	(3.79)	(3.7)	(3.39)

***Note*:** Coefficients based on 2SLS local projections providing cumulative impulse response functions of real activity data in the four regions estimated for month horizon *h=0…6* between 2011m01 and 2024m12 for employment, and between 2014m01 and 2024m12 for external trade. Heteroskedasticity-robust standard errors in parentheses, computed using a White-correction routine. Significant at ***0.01, **0.05, *0. 10. The sample excludes the Covid period 2020m03 to 2021m12.

Our main finding is a decrease of overall employment immediately after the disaster with the effect reaching its maximum at a 1.2 % drop after six months and this downturn is widespread across

sectors. This result is consistent with previous findings by Barattieri et al. (2023) after hurricanes in Puerto Rico. Specifically, we find sustained decrease in agricultural and food manufacturing employment following a natural disaster reaching a maximum and significant drop of -1.5% after six months. This finding is in line with previous studies documenting a drop in agricultural labor supply after natural disasters (Kirchberger, 2017). It suggests that the price increase in fresh food, which is more likely to be produced locally than other food products, results from a predominant negative supply shock related to the destruction of crops in fields.

Employment in most services sectors also decreases significantly, in particular for construction (- 2.8% after 6 months), accommodation and restaurants (-2.3%), other services (-2.4%) and transports (-1.9%). Relatedly, we estimate negative effects of weather-related disasters on overnight hotel stays of up to -17% after three months, but these effects are much less persistent. In this context, the combination of downward effects on services prices and downward effects on employment in services suggests a predominant negative demand effect. This result is in line with recent contributions showing that natural disasters decrease demand, notably through higher risk aversion (Cantelmo et al., 2023 and Cassar et al., 2017).

We do not find significant effect of weather-related disaster on employment in the manufacturing sector or on imports, one main source of supply for manufactured products in overseas territories.[10] These results suggest that the negative effect on the prices of manufactured products is also likely to stem from predominant negative demand. Relatedly, the absence of reaction of imports suggests that the drop in the prices of other food products mostly come from a negative demand effect, as other food products are mostly imported.

5. Robustness results and methodological discussion

This section compares our results with the ones obtained from a damage function approach which is an alternative empirical strategy to measure economic effects of weather-related disasters. We also discuss how the controls for seasonality affect the results.

5.1 Comparison with results from damage functions

One alternative empirical approach often used in the literature to assess the effect of weather-related disasters on inflation is to rely on damage functions. This approach defines a functional form using as inputs weather and climate data and assumes a direct mapping between this function and economic outcomes in the sense of a "dose response function". For applications,

[10] Table B.11 in the Online Appendix reports estimated sectoral import responses.

see in particular Emanuel (2011), Strobl (2011, 2012) and Heinen et al. (2018); for methodological reviews, see Auffhammer (2018) and Kolstad and Moore (2020). In this section, we compare our baseline results to estimates obtained with damage functions as proposed by Heinen et al. (2018) and we discuss the methodological differences and parallels with our IV approach.

To obtain a time-series of wind damage for each region, we first compute a wind destruction index. Specifically, for gridded cell *j* of weather data in one of our four regions *i* and within a day *d*, we compute the monthly wind-destruction as follows:

$$H_{it} = \max \left[\sum_{j=1}^{J} \xi_{ij} \sum_{d=1}^{D} \left(W_{ijd}^{max} \right)^3 \times \mathbb{1}_{\left\{ W_{ijd}^{max} > W^* \right\}} \right]_{d \in t}, \quad (4)$$

where ξ_{ij} are exposure weights for grid cell *j* in region *i*, which aggregate to one at the regional level, W_{ijd}^{max} is the maximum sustained wind speed for one minute in an intraday window *d* of six hours from the CCMP, and $\mathbb{1}_{\{W > W^*\}}$ is an indicator variable equal to one if the recorded wind speed exceeds a threshold value W^* (0, otherwise). In our case, we set this value at 15 m/s, which corresponds to the 95th percentile of the wind distribution in our sample. We discuss below results of robustness exercises where we vary the wind speed threshold. Maximum sustained wind speed enters the damage function in cubic form, as it has been found that the local destructive power of wind is roughly in cubic form related to wind speed (Emanuel, 2011). Exposure weights ξ_{ij} are constructed from satellite nighttime light data. Nighttime light has a high predictive power for economic activity (see Henderson et al., 2012, Chen and Nordhaus, 2019 and Pérez-Sindín et al., 2021 for applications), which makes it particularly suited for the construction of weights in our case, as we are interested in detecting areas of more intensive economic activity.

Regarding possible economic destruction due to excessive rainfall, we also follow Heinen et al. (2018) and define region-specific flood destruction as

$$F_{it} = \max \left[\sum_{j=1}^{J} \xi_{ij} \times r_{ijdt} \times \mathbb{1}_{\{ r_{ijdt} > r^* \}} \right]_{d \in t}, \quad (5)$$

where r_{ijdt} is the cumulative sum of rainfall in millimeters over a three-day backward-looking window in region *i*, weather cell *j*, on day *d,* in month *t*. The exposure weights ξ_{ij} follow the same logic as above and are also constructed from satellite nighttime light data. Following

Heinen et al. (2018), we set r^* at 112 mm which corresponds to the top 98th percentile of the distribution of rainfall in our sample (see Online Appendix G for more details on the construction of damage functions).

To evaluate the effect of disasters on prices, we run the same local projection method as in our baseline model but using damage functions as exogenous variables:

$$\log\left(\frac{P_{i,t+h}}{P_{i,t-1}}\right) = \alpha_h + \theta_{H,h}H_{it}^S + \theta_{F,h}F_{it}^S + \rho_h Z_{i,t} + \tau_h Y_t + \delta_{hy} + \mu_{hq} + \gamma_{hi} + \mu_{hq} \times \gamma_{hi} + \varepsilon_{h,i,t} \quad (6)$$

where H_{it}^S and F_{it}^S are standardized values of H_{it} and F_{it}, and control variables and fixed effects are the same as the ones included in our baseline model (3). Results of this estimation are reported in Table B.5 in the Online Appendix. Damage functions have positive and significant effects on prices of fresh food products, and overall negative effects on the prices of manufactured products, services, and other food products; these results are broadly consistent with our baseline IV specification. Price effects mainly come from the wind damage function, while the rain damage function contribution is more muted. Some diverging results can be observed compared to the 2SLS specification: rain damage functions entail some short-lived positive effects on energy and services, while wind damage functions yield short-lived positive effects for manufactured products.

Quantitively, we cannot directly compare the magnitude of the price effects obtained from the two types of regressions - one derived from damage functions and the other one based on the predicted probability of a disaster as an exogenous variable. In particular, the two types of explanatory variables are not expressed in the same units: in the 2SLS model, the predicted probability lies in the [0, 1] interval, whereas the damage functions are based on linear (for rainfall) or cubic (for wind speed) values derived from meteorological records. To compare quantitatively the price effects obtained in the two distinct exercises, we estimate how damage functions are related to the Logit predicted probability to ensure comparability of units across specifications. To do so, we first estimate the slope of the regression linking the damage functions (H_{it}^S and F_{it}^S) to the predicted probability of a disaster ($\hat{p}_{i,t}$), as follows:

$$H_{it}^S = \alpha_H + \beta_H \hat{p}_{i,t} + \varepsilon_{i,t,h} \quad (7)$$

$$F_{it}^S = \alpha_F + \beta_F \hat{p}_{i,t} + \varepsilon_{i,t,h} \quad (8)$$

The results of these regressions (reported in Table B.6 in the Online Appendix) show a strong positive correlation between the predicted probabilities and the standardized damage

functions.[11] Estimates of β_H and β_F give us the damage function variation consistent with a predicted probability of a disaster ranging from 0 to 1 so that we can easily compute the predicted price response combining these two parameters ($\widehat{\beta}_H$ and $\widehat{\beta}_F$) with the ones estimated from equation (6). We compute price effects obtained from damage functions that would be consistent in terms of units with our IV estimates as follows:

$$\hat{\theta}_{H,h} \times \widehat{\beta}_H + \hat{\theta}_{F,h} \times \widehat{\beta}_F \quad (9)$$

This predicted price response therefore corresponds to the effect of the wind and rain damage functions when their variation is such that they entail a shift of the 2SLS predicted probability from 0 to 1.

Figure 6. Price effects estimated using damage functions or IV regressions for headline CPI and three main CPI product categories

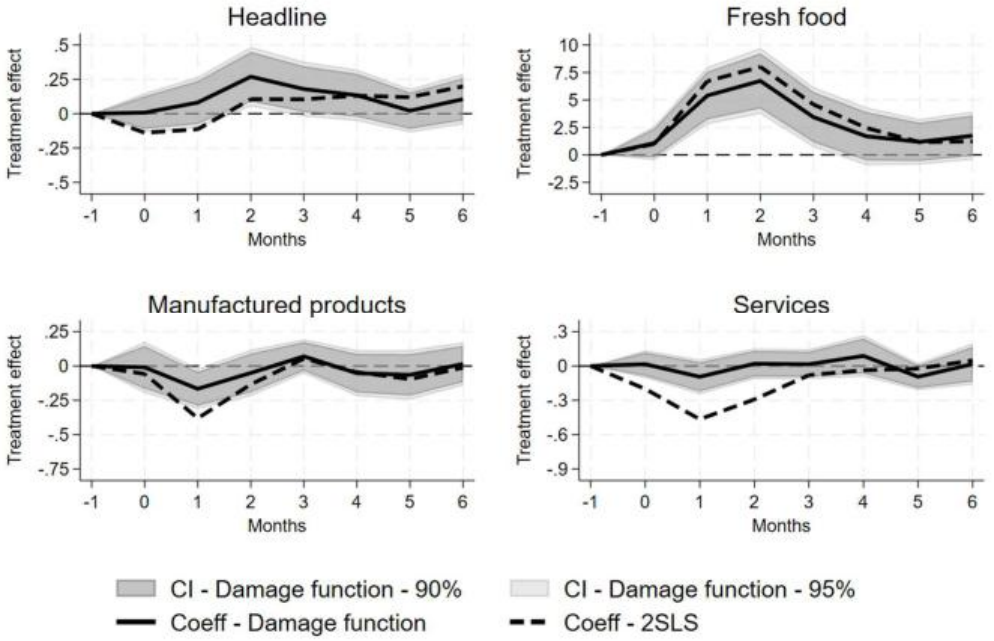

Note: Plotted are the cumulated impulse response functions obtained from the baseline 2SLS model (dashed black lines) and using the wind and rain damage functions in OLS regressions (solid black lines). The price response (in %) to damage functions is computed for a variation of the damage functions equivalent to a 0-to-1 increase in the 2SLS predicted probability of a disaster. Shaded areas represent 90% and 95% confidence intervals associated with the coefficients of the damage functions. Standard errors are heteroskedasticity-robust and computed using a White-correction routine. The x-axis corresponds to the time horizon expressed in months since the disaster. Sample period: 1999m01 to 2024m12, excluding the Covid period 2020m03-2021m12, for all four regions.

Figure 6 compares our baseline 2SLS estimates for total CPI and fresh food, manufactured products and services CPI (dashed lines) to estimates obtained from damage functions (solid lines), using the normalization described above. The results using damage functions are

[11] Additionally, Tables B.7 and B.8 in the Online Appendix show that higher predicted probabilities of disasters $\hat{p}_{i,t}$ are associated with much higher shares of non-null damage functions, and that predicted probabilities are higher when wind or rain are above the thresholds we set for the baseline damage function (W^*=15 m/s and r^*=112 mm).

coherent with those of our baseline 2SLS methodology. In most cases, estimated reactions are close, though a bit lower in absolute values. As a complementary analysis, we report results of separated regressions for the wind damage function and rain damage function in Figure B.9 in the Online Appendix. Results appear to be driven by the wind damage function, with only limited effects from the rain damage function. This is consistent with our finding of a higher average marginal effect of wind over precipitation on the disaster probability in the Logit regression model (1). To further test the respective role of rain and wind extreme events, we have estimated the price effects of the different weather-related disasters including dummy variables corresponding to different types of events (storms with or without floods, floods without storms, landslides) in OLS local projections.[12] We find the price effects mainly come from storms (Table B.9 in the Online Appendix). This conclusion is also in line with results obtained by Heinen et al. (2018).

In both damage function and IV approaches, economic damages or occurrence of reported damages are expressed as a nonlinear function of weather data. The nonlinearities in the damage function come from the dummy variable based on wind or rain thresholds, but also the use of cubic terms. In contrast, the nonlinearity in the IV approach comes only from the probability of weather-related disasters. This probability is endogenous and is estimated using a Logit model that links wind speed and rainfall to recorded administrative disasters, while in the damage function approach, disaster occurrence is determined by an exogenous threshold. We investigate how the two sources of nonlinearities in the damage function contribute to the estimation of the results and how they compare with the IV approach. We run this comparison exercise for fresh food prices since the effects of weather-related disasters are maximal for this product category and using the damage function computed with wind speed which is the most important meteorological dimension for economic damages in our sample. Our comparison exercise consists of using different damage functions where we vary the threshold of the dummy variable entering the damage function and we also test damage functions where wind is introduced linearly (instead of the cubic term). Results are plotted on Figure 7. In columns, we vary the threshold values, while in rows we vary how wind speed is incorporated into the damage function (cubic transformation, levels, or a simple dummy variable). Our baseline scenario (with a threshold at 15m/s and a cubic transformation of wind speed) is represented in panel (a) for comparison.

[12] Estimating our 2SLS model would require using three different instruments for the three types of weather events. We prefer to keep the empirical model simple, as our focus is on the relative contribution of the different weather-related events to price effects.

Figure 7. Effects of alternative wind damage functions on fresh food prices

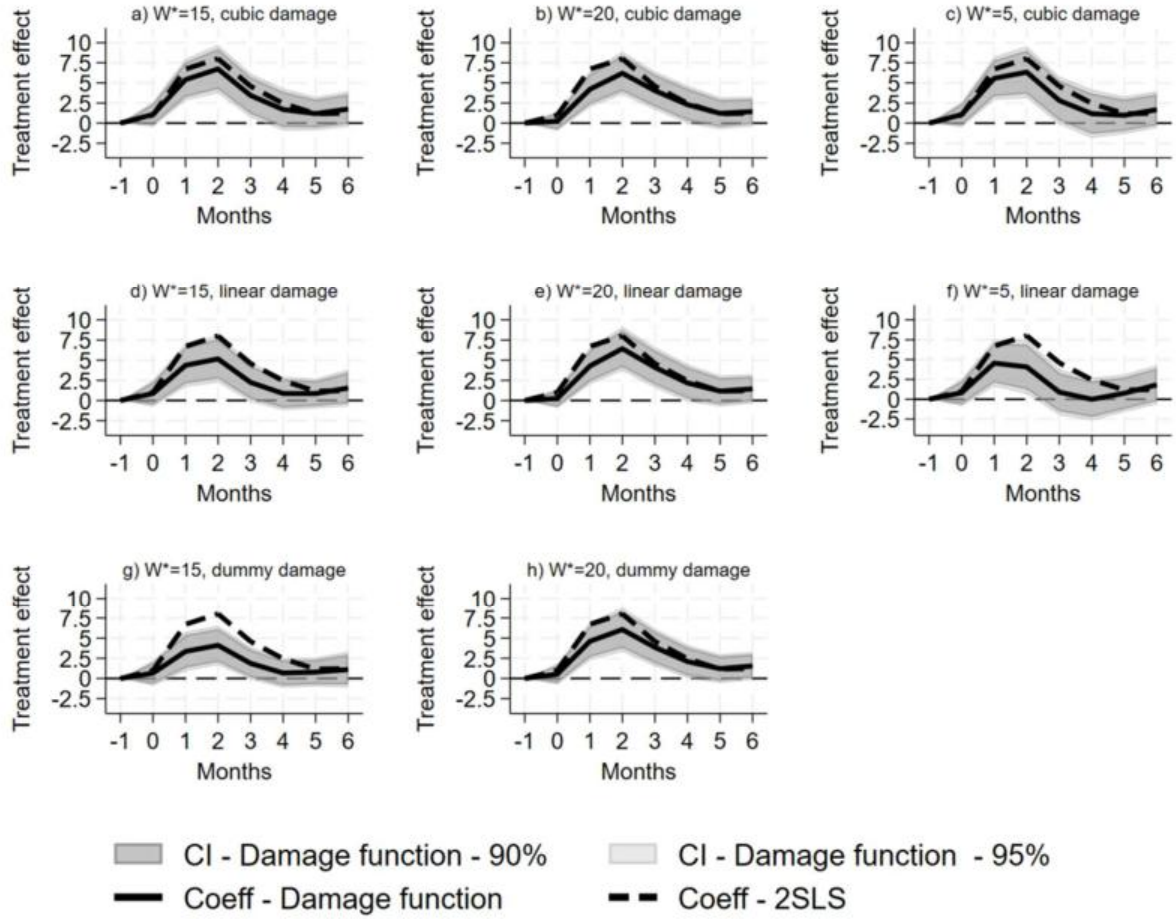

Note: Plotted are the dynamic responses of alternative wind damage functions on the prices of fresh food. In columns, we report results where we vary the threshold under which the damage function is 0. In column (1), we consider a threshold of 15 m/s as in our baseline scenario (95th percentile). In column (2), the threshold is set to 20 m/s (99th percentile) and in column (3), we set this threshold to 5 m/s implying that the damage function is always different from 0. In rows, for a given max threshold of wind, we report results of regressions where we modify the functional form of the damage function when it is different from 0 (i.e. above the max threshold). In the first row, we report results using the baseline damage function using the cubic term transformation. In the second row, we use wind in levels in the damage function. In the third row, we report results where the damage function is reduced to a dummy variable equal to 1 if the wind speed is above the max threshold at date *t* and 0 otherwise. Dashed lines in all the graphs report our baseline 2SLS estimates for comparison. The shaded area represents the 90%- and 95% confidence intervals. Standard errors are heteroskedasticity-robust and computed using a White-correction routine. All price effects are expressed in percent. The x-axis corresponds to the time horizon expressed in months since the disaster. Sample period: 1999m01 to 2024m12, excluding the Covid period 2020m03-2021m12, for all four regions.

First, we consider two polar cases of the damage function: one where we use a very low threshold such that the only source of nonlinearity arises from the cubic transformation of wind speed (panel c) and another one where the threshold is larger (set at 20 m/s, i.e., the 98th percentile of the wind speed distribution) but where we do not include the cubic transformation of wind speed. In that case, the damage function is reduced to a dummy variable equal to 1 when wind speed exceeds the threshold and 0 otherwise (panel h). When we compare results using these two alternative damage functions, the results are almost identical. This suggests that the two types of nonlinearities in the damage function capture the same price effects. Moreover, for a threshold of 20m/s, the cubic transformation of wind speed does not provide additional

price effects (panel b). Put differently, when the threshold in the damage function is set at a relatively high value, the price effects estimated with a simple dummy damage function (panel h) are similar to those obtained with the baseline damage function that includes both types of nonlinearities (panels a and b).

Keeping the threshold at 15 m/s but with a damage function where wind is introduced in levels (panel d), we find that more than half of price effects are captured (5.2% at *t+2* versus 6.7% with the cubic term) and the dummy threshold still captures a significant share of price effects (Figure 7, panel g). This result is consistent with our IV regression: when we introduce cubic terms of rain and wind, we also find somewhat stronger price effects for fresh food (10.3% at *t+2* instead of 8.0% in our baseline, see Table B.4 in the Online Appendix). Overall, in both approaches, results are quite similar, the main difference comes from modelling choices: in the IV model, thresholds are determined by the estimation of the model whereas in the damage functions, the thresholds are set by the econometrician and are justified by physics laws or expert judgment. In our context, the comparison between damage functions and our IV approach suggests that the price effects are mainly driven by the nonlinearity coming from the binary threshold defining the occurrence of a disaster event rather than by whether the weather data are introduced in levels or in cubic terms.

Finally, we test whether results of damage functions differ because of the explicit exposure measure (Figure B.10 in the Online Appendix). There are potentially many factors that shape the impact of meteorological events at the local level. The existing literature refers to geological features such as the degree of urbanization and land use in the affected area (Noy, 2009), or the shape of the continental shelf and coast (Bertinelli and Strobl, 2013). Nightlight imagery, the exposure weight we adopted from the literature, is notably ill-suited to capture agricultural value-added (Keola, 2015), and its predictive power for services value-added can be heterogeneous across territories (Bluhm and McCord, 2022). If we compute damage functions (4) and (5) without exposure weights, we find very similar results (panels d to f of Figure B.10 in the Online Appendix).

5.2 The role of seasonal factors and year fixed effects

This section documents the importance of accounting for regional seasonality in estimating the effects of weather-related extreme events. Indeed, such events in overseas territories are often related to hurricanes and cyclones. The occurrence of storms is more likely during periods when the difference between air temperature and sea surface temperature is at its peak, resulting in a seasonal phenomenon. This matters for two reasons. First, it highlights the need to model regional seasonality in the empirical framework to prevent possible omitted variable bias. Second,

instrument exogeneity requires that instruments and outcome variables are uncorrelated conditional on all control variables. Possibly overlapping seasonality between inflation and wind speed can be controlled for with regional time dummies. Next, we discuss sources and patterns of seasonality in the data and show how the treatment of this seasonality affects quantitatively our results.

Seasonality in extreme weather events differs across the territories. Table A.8 in the Online Appendix shows that weather-related disasters in La Réunion are concentrated during the first half of the year. In contrast, Guadeloupe, Martinique, located in the Caribbean, are affected by the North Atlantic hurricane season, which runs from June to November. There is also regional heterogeneity in the absolute exposure to weather-related disasters. While Guadeloupe, La Réunion and Martinique have a comparable number of administrative shocks, French Guiana has a much smaller number of shocks (all based on GASPAR data), which are mainly concentrated in the month of May (Tables A.5 and A.8 in the Online Appendix). Similarly, seasonal patterns in inflation differ across the regions. Figure A.1 in the Online Appendix plots the average monthly variation for the main components of CPI across regions. Seasonal variation in La Réunion appears to differ from that of the other overseas regions, both in timing and in magnitude. The difference mainly reflects that La Réunion is the only southern hemisphere region in our sample, affecting the seasonal timing of agriculture and tourism.

In our baseline regression, we have included quarter fixed effects interacted with regional fixed effects to capture the seasonal effects specific to each region. In Table 3, we compare our baseline 2SLS specification with alternative 2SLS specifications controlling differently for seasonal patterns. Panel (A) reports our baseline estimates for comparison. Panel (B) reports results from a specification excluding quarterly region-specific fixed effects (but including year fixed effects common to all regions). The product-level price reactions differ substantially. Not controlling for region-specific seasonality yields much stronger effects for fresh food products, which go up to 18.6% after two months, driven by the distinct seasonality of La Réunion. Stronger effects for fresh food prices are partially offset by stronger negative price effects for manufactured products, down to a minimum of -0.7% after two months. Additionally, the prices of services increase more substantially at the end of the horizon, by up to 0.9% after 6 months.[13] Eventually, in this specification, the effects for headline CPI are positive and significant. In Table B.12 in the Online Appendix, we report that controlling only for seasonal effects and excluding year fixed effects yields results closer to our baseline specification. Overall, these

[13] This specific effect appears to be entirely driven by the disasters and price seasonality of French Guiana, in which 60% of shocks occur in the month of May.

results imply that controlling for region-specific seasonal patterns is important for the precise and unbiased estimation of dynamic causal effects of weather-related extreme events on prices.

Table 3. Alternative specifications regarding seasonality for the 2SLS strategy

	T=0	T=1	T=2	T=3	T=4	T=5	T=6
(A) Baseline							
Headline	-0.14	-0.11	0.11	0.11	0.13	0.12	0.20
Fresh food	0.99	6.71***	8.01***	4.59***	2.45	1.16	1.23
Other food excl. tobacco	-0.09	-0.21**	-0.11	-0.24	-0.28*	-0.11	-0.14
Manufactured products	-0.06	-0.38***	-0.13	0.05	-0.05	-0.10	-0.01
Services	-0.20*	-0.47***	-0.29**	-0.08	-0.04	-0.02	0.05
(B) No seasonal effect							
Headline	-0.09	0.08	0.46***	0.42**	0.41**	0.52***	0.56***
Fresh food	6.05***	16.28***	18.59***	12.45***	6.37**	2.69	0.25
Other food excl. tobacco	-0.03	-0.07	0.01	-0.15	-0.24	-0.09	-0.10
Manufactured products	-0.17	-0.71***	-0.32*	0.06	0.07	0.29	0.25
Services	-0.40***	-0.51***	-0.13	0.17	0.53***	0.77***	0.90***

***Note*:** Results for alternative specifications of local projections of consumer prices from a 2SLS model. Panel (A) shows results for our baseline specification, panel (B) shows results for a 2SLS specification controlling for year-quarter fixed effects, but not for region-specific quarter fixed effects. Significant at ***0.01, **0.05, *0.10. Standard errors are heteroskedasticity-robust and computed using a White-correction routine. Sample period: 1999m01 to 2024m12, excluding the Covid period 2020m03-2021m12, for all four regions.

6. Conclusion

This paper estimates the sectoral effects on prices of weather-related natural disasters in the four French overseas territories between 1999 and 2024. The response of inflation to weather-related disasters is heterogeneous across CPI components both in terms of timing and amplitude, with a quick and positive response of food inflation, especially fresh food, which is partly offset by a negative contribution of inflation in services and manufactured products. This leads to a moderate, non-significant effect on headline inflation. We provide complementary evidence on real activity. While lower employment in the food sector points toward dominant supply effects in the price response of fresh food, lower demand for manufactured goods and services in conjunction with lower employment are likely to contribute to the negative price response of manufactured goods and services.

Finally, the paper makes a methodological contribution of interest for follow-up empirical work. Namely, it proposes an IV approach to overcome the measurement problems related to economic damage resulting from physical disaster risk. Instrumenting disaster occurrence in administrative databases with meteorological data leads to comparable results as the direct specification damage functions. Relatedly, the findings underline the importance of a careful modeling of regional seasonality, as inflation and weather-induced disaster might share common seasonality patterns that potentially bias the estimator.

References

Antoine, Bertille, and Pascal Lavergne. (2023). "Identification-Robust Nonparametric Inference in a Linear IV Model." *Journal of Econometrics*, *235*(1), 1-24.

Auffhammer, Maximilian. (2018). "Quantifying Economic Damages from Climate Change." *Journal of Economic Perspectives*, 32(4), 33-52.

Bao, Xiaojia, Puyang Sun, and Jianan Li. (2023). "The Impacts of Tropical Storms on Food Prices: Evidence from China." *American Journal of Agricultural Economics,* 105(2), 576-596.

Barattieri, Alessandro, Patrice Borda, Alberto Brugnoli, Martino Pelli, and Jeanne Tschopp. (2023). "The Short-Run, Dynamic Employment Effects of Natural Disasters: New Insights from Puerto Rico." *Ecological Economics*, *205*, 107693.

Berthier, Jean-Pierre, Jean-Louis Lhéritier, and Gérald Petit. (2010). "Comparaison des Prix entre les DOM et la Métropole en 2010", *Insee première*, Juillet 2010, n°1304.

Bertinelli, Luisito, and Eric Strobl. (2013). "Quantifying the Local Economic Growth Impact of Hurricane Strikes: An Analysis from Outer Space for the Caribbean." *Journal of Applied Meteorology and Climatology*, 52(8), 1688–97.

Bluhm Richard, and Gordon C. McCord. (2022). "What Can We Learn from Nighttime Lights for Small Geographies? Measurement Errors and Heterogeneous Elasticities." *Remote Sensing,* 14(5):1190.

Cantelmo, Alessandro, Giovanni Melina, and Chris Papageorgiou. (2023). "Macroeconomic Outcomes in Disaster-Prone Countries." *Journal of Development Economics,* 161(2023), 103037.

Cassar, Alessandra, Andrew Healy, and Carl Von Kessler. (2017). "Trust, Risk, and Time Preferences after a Natural Disaster: Experimental Evidence from Thailand." *World Development,* 94(2017): 90-105.

Cavallo, Alberto, Eduardo Cavallo, and Roberto Rigobon. (2014). "Prices and Supply Disruptions during Natural Disasters," *Review of Income and Wealth,* 60(S2), 449-471.

Chen, Xi, and William D. Nordhaus. (2019). "VIIRS Nighttime Lights in the Estimation of Cross-Sectional and Time-Series GDP." *Remote Sensing*, 11(9), 1057.

Ciccarelli, Matteo, Friderike Kuik, and Catalina Martínez Hernández. (2024). "The Asymmetric Effects of Temperature Shocks on Inflation in the Largest Euro Area Countries." *European Economic Review*, 168 (September 2024), 104805.

Dell, Melissa, Benjamin F. Jones, and Benjamin A. Olken. (2012). "Temperature Shocks and Economic Growth: Evidence from the Last Half Century." *American Economic Journal: Macroeconomics*, 4(3), 66-95.

Doyle, Lisa, and Ilan Noy. (2015). "The Short-Run Nationwide Macroeconomic Effects of the Canterbury Earthquakes." *New Zealand Economic Papers,* 49(2), 134-156.

Emanuel, Kerry. (2011). "Global Warming Effects on U.S. Hurricane Damage." *Weather, Climate, and Society*, 3(4), 261–268.

Faccia, Donata, Miles Parker, and Livio Stracca. (2021). "Feeling the Heat: Extreme Temperatures and Price Stability." ECB Working Paper, 2626.

Felbermayr, Gabriel, and Jasmin Gröschl. (2014). "Naturally Negative: The Growth Effects of Natural Disasters." *Journal of Development Economics,* 111(2014), 92-106.

Grislain-Letrémy, Céline. (2018). "Natural Disasters: Exposure and Underinsurance." *Annals of Economics and Statistics*, 129(March 2018), 53-83.

Hansen, Lars Peter. (2022). "Central Banking Challenges Posed by Uncertain Climate Change and Natural Disasters." *Journal of Monetary Economics*, 125(2022), 1-15.

Heinen, Andréas, Jeetendra Khadan, and Eric Strobl. (2018). "The Price Impact of Extreme Weather in Developing Countries." *Economic Journal*, 129(619), 1327-1342.

Henderson, J. Vernon, Adam Storeygard, and David N. Weil. (2012). "Measuring Economic Growth from Outer Space." *American Economic Review*, 102(2), 994-1028.

Hugounenq, Réjane, and Valérie Chauvin. (2006). "Les Évolutions Comparées des Prix à la Consommation dans les DOM et en Métropole". *Bulletin de la Banque de France*, n°151. 33-46.

Inoue, Atsushi, Òscar Jordà, and Guido M. Kuersteiner. (2025). "Inference for Local Projections." *Econometrics Journal*, 00, 1–25.

Jordà, Òscar. (2005). "Estimation and Inference of Impulse Responses by Local Projections." *American Economic Review*, 95(1), 161-182.

Kabundi, Alain, Montfort Mlachila, and Jiaxiong Yao. (2022). "How Persistent are Climate-Related Price Shocks? Implications for Monetary Policy." IMF Working Paper, 2022/207.

Keola, Souknilanh, Magnus Andersson, and Ola Hall. (2015). "Monitoring Economic Development from Space: Using Nighttime Light and Land Cover Data to Measure Economic Growth." *World Development*, *66*, 322-334.

Kirchberger, Martina. (2017). "Natural Disasters and Labor Markets." *Journal of Development Economics,* 125 (2017), 40-58.

Kolstad, Charles D., and Frances C. Moore. (2020). "Estimating the Economic Impacts of Climate Change Using Weather Observations." *Review of Environmental Economics and Policy*, 14(1), 1-24.

Kotz, Maximilian, Friderike Kuik, Eliza Lis, and Christiane Nickel. (2024). "Global Warming and Heat Extremes to Enhance Inflationary Pressures." *Communications Earth & Environment*, 5(116).

Montiel-Olea, José Luis, and Mikkel Plagborg-Møller. (2021). "Local Projection Inference is Simpler and More Robust than You Think." *Econometrica,* 89(4), 1789-1823.

Noy, Ilan. (2009). "The Macroeconomic Consequences of Disasters." *Journal of Development Economics*, 88(2), 221-231.

Parker, Miles. (2018). "The Impact of Disasters on Inflation." *Economics of Disasters and Climate Change*, 2(1), 21-48.

Pérez-Sindín, Xaquín S., Tzu-Hsin Karen Chen, and Alexander V. Prishchepov. (2021). "Are Night-Time Lights a Good Proxy of Economic Activity in Rural Areas in Middle and Low-Income Countries? Examining the Empirical Evidence from Colombia." *Remote Sensing Applications: Society and Environment*, 24(2021), 100647.

Schnabel, Isabel. (2021). "A New Strategy for a Changing World." Speech delivered at the virtual Financial Statements series hosted by the Peterson Institute for International Economics, 14 July 2021.

Strobl, Eric. (2011). "The Economic Growth Impact of Hurricanes: Evidence from U.S. Coastal Counties." *Review of Economics and Statistics*, 93(2), 575-589.

Strobl, Eric. (2012). "The Economic Growth Impact of Natural Disasters in Developing Countries: Evidence from Hurricane Strikes in the Central American and Caribbean Regions." *Journal of Development Economics*, 97(2012), 130-141.

Wooldridge, Jeffrey M. (2010). *Econometric Analysis of Cross Section and Panel Data*. Cambridge, MA: MIT Press.

Xu, R. (2021). "On the Instrument Functional Form with a Binary Endogenous Explanatory Variable." *Economics Letters*, *206*, 109993.

ONLINE APPENDIX

Decomposing the Inflation Response to Weather-Related Disasters

Erwan Gautier, Christoph Grosse-Steffen, Magali Marx, Paul Vertier

Appendix A. Data sources and descriptive statistics

A.1 Consumer prices in French DROMs

A.1.1 CPI data

CPI data are downloaded from INSEE website. We use monthly raw CPI data. INSEE publishes these data for several levels of aggregation (or "regroupements conjoncturels"), all based on the COICOP classification. The indicators can be classified into 4 aggregates, for which there exists 12 subindicators (whose composition can be found here):

- Food including tobacco, which is broken down between fresh food, other food and tobacco
- Manufactured products, which is broken down between footwear and garment, other manufactured products and pharmaceutical products
- Energy, for which INSEE produces a subindex on petroleum products (but no other subindices)
- Services, which includes transportation, communication, health, rents and other services

In our baseline analysis, we focus on manufactured products, energy and services without breaking them down, but we break down food including tobacco into its three components, because of their very different nature (fresh food products being largely produced locally, other food being largely imported, and tobacco being administered).

Headline CPI is significantly correlated between overseas regions and France with an average correlation of 0.29, except for La Réunion (Table A.2). On average, the correlation is strong and positive for services (0.7) but smaller for manufactured products and energy (about 0.3), and this holds true for all overseas regions except for La Réunion in which the CPI of manufactured products is negatively correlated with that of France. While the CPI of other food products and tobacco is positively correlated between overseas regions and France (0.3 to 0.6), this is not the case for the CPI of fresh food products, which is not significantly correlated between overseas regions and France (-0.02 on average).

Table A.1. Descriptive statistics of monthly inflation rate (1999m01-2024m12)

	Guadeloupe		French Guiana		La Réunion		Martinique		DROMs		France	
Component	mean	sd	mean	sd	mean	sd	mean	sd	mean	sd	mean	sd
Headline	0.14	0.49	0.13	0.42	0.14	0.59	0.14	0.40	0.13	0.34	0.14	0.35
Fresh products	0.35	3.38	0.32	3.07	0.69	8.91	0.32	2.72	0.42	2.48	0.30	3.39
Other food	0.18	0.47	0.17	0.33	0.19	0.40	0.20	0.41	0.19	0.28	0.16	0.31
Tobacco	0.70	2.54	0.61	2.71	0.70	3.52	0.73	2.55	0.68	1.67	0.51	1.74
Manufactured products	0.05	0.91	-0.02	0.27	0.04	0.89	0.04	0.63	0.03	0.45	0.02	1.06
Energy	0.27	2.19	0.28	2.26	0.27	2.14	0.28	2.20	0.27	1.93	0.35	1.87
Services	0.15	0.58	0.15	0.75	0.14	0.78	0.14	0.51	0.14	0.49	0.15	0.48

Note: the table reports the mean and standard deviation of monthly inflation rates in each overseas territory and in France mainland. The sample excludes the Covid period 2020m03-2021m12.

Table A.2. Correlations between headline monthly CPI inflation in DROMs and in France (1999m01-2024m12)

Component	Guadeloupe	French Guiana	La Réunion	Martinique	All DROMs
Headline	0.296 [0.000]	0.287 [0.000]	0.058 [0.328]	0.247 [0.000]	0.291 [0.000]
Fresh food	0.039 [0.507]	0.027 [0.652]	-0.009 [0.883]	-0.110 [0.061]	-0.016 [0.781]
Other food	0.287 [0.000]	0.433 [0.000]	0.466 [0.000]	0.454 [0.000]	0.582 [0.000]
Tobacco	0.235 [0.000]	0.116 [0.050]	0.239 [0.000]	0.135 [0.022]	0.313 [0.000]
Manufactured products	0.339 [0.000]	0.393 [0.000]	-0.183 [0.002]	0.360 [0.000]	0.266 [0.000]
Energy	0.294 [0.000]	0.285 [0.000]	0.308 [0.000]	0.333 [0.000]	0.346 [0.000]
Services	0.422 [0.000]	0.692 [0.000]	0.519 [0.000]	0.47 [0.000]	0.723 [0.000]

Note: the table reports correlation coefficients between headline CPI monthly inflation in each overseas territory and headline CPI monthly inflation in France mainland, p-values in parentheses. The sample excludes the Covid period 2020m03-2021m12.

Table A.3 – Share of consumption covered by local production

	Fruit		Vegetables	
	Fresh	**All**	**Fresh**	**All**
Guadeloupe	44%	16%	55%	43%
Martinique	31%	13%	39%	26%
French Guiana	94%	79%	90%	81%
La Réunion	62%	34%	68%	48%

Note: Coverage ratios of local production for fruit and vegetables in the four regions, both for fresh food (Fresh) and the sum of fresh and non-fresh food (All).

Source: Observatoire des économies agricoles ultramarines (2021) – La couverture des besoins alimentaires dans les DCOM.

Figure A.1. Seasonal variations of regional monthly CPI inflation

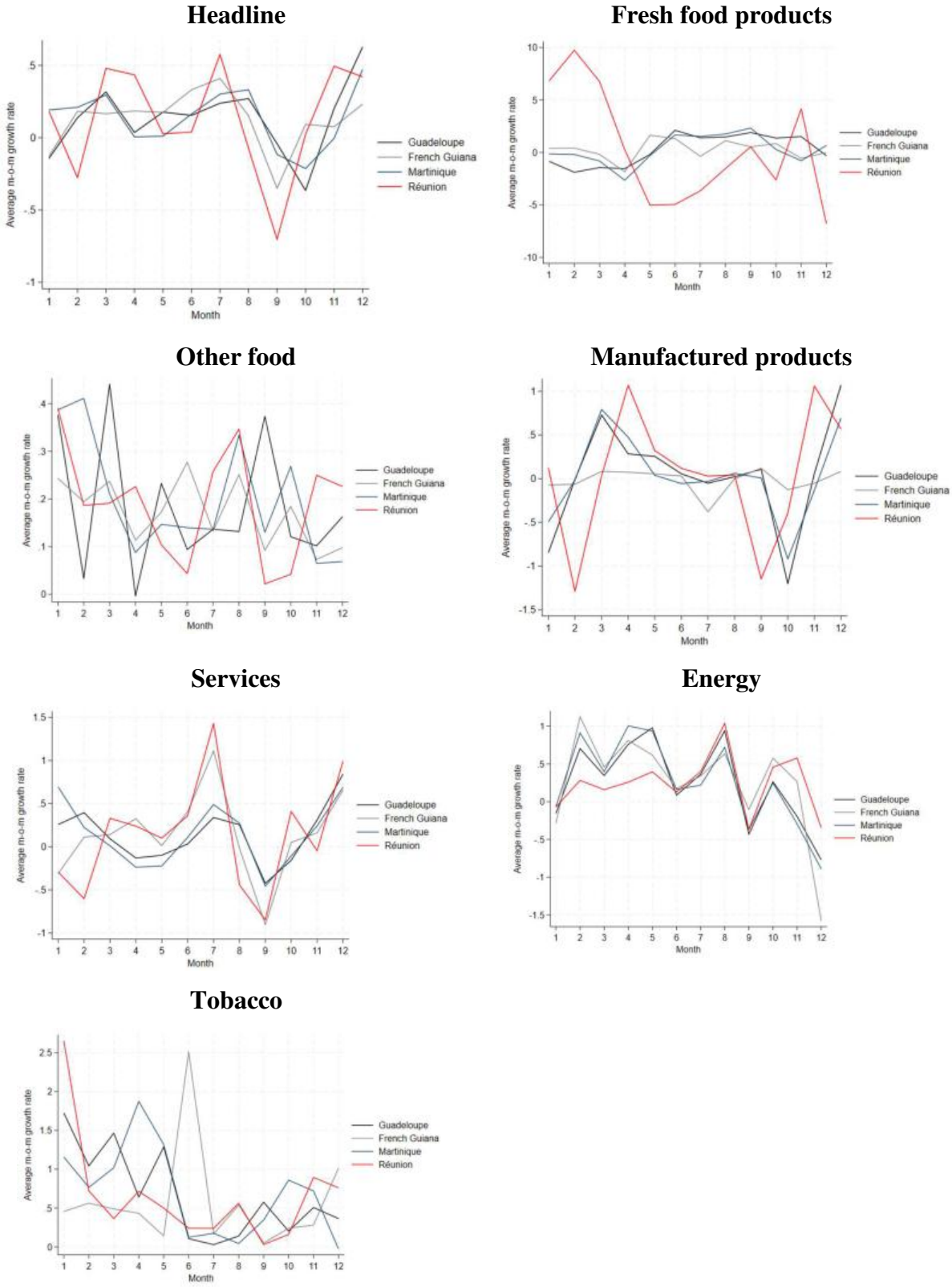

Note: the figure plots for each calendar month the average month-on-month variations (in %) of headline CPI and of CPI by broad product categories. The x-axis reports calendar month (1 for January, 2 for February…). The sample excludes the Covid period 2020m03-2021m12.

A.1.2 Composition of CPI baskets across overseas regions

Annual CPI weight data for each aggregate are also downloaded from the INSEE website. The composition of consumer baskets is heterogeneous across French territories and varies over time. Table A.4 reports the weights of each aggregate according to the French statistical office (INSEE) over our sample period, in each region, and the unweighted mean over the sample. Food including tobacco represents about 17% of the consumer basket in the considered region at the end of the sample, with a weight that is declining over time. Fresh food represents roughly 16% of the food basket in 2024 (2.7% of the CPI basket), and its weight strongly decreased over time from 5.9% in 1999. Services represent about 45% of the consumer basket at the end of the sample, with a maximum weight of 46% in La Réunion and a minimum weight of 43% in Martinique. Contrary to food, the weight of services increases over time in all territories. Manufactured products represent 30% of the CPI basket in 2024, only slightly above the sample mean.

Table A.4. Weight of the main aggregates of Consumer Price Index (Total=10,000)

Geographical area	**Guadeloupe**			**French Guiana**			**La Réunion**			**Martinique**			**DROMs**			**France**		
Period	**1999**	**2024**	**99-24**	**1999**	**2024**	**99-24**	**1999**	**2024**	**99-24**	**1999**	**2024**	**99-24**	**1999**	**2024**	**99-24**	**1999**	**2024**	**99-24**
Food	2882	1654	2110	2729	1705	2224	2675	1708	2091	2538	1626	2061	2706	1673	2121	1973	1687	1843
Fresh food	813	345	410	499	245	359	432	195	240	615	311	415	590	274	356	225	185	217
Other food	1999	1252	1625	2139	1384	1752	2121	1407	1686	1895	1263	1585	2039	1327	1662	1550	1323	1432
Tobacco	71	57	75	91	76	113	122	106	165	29	52	61	78	73	103	198	179	195
Manuf. products	3065	3049	3057	2526	2822	2601	3200	2925	3010	2868	3174	2870	2915	2993	2885	3011	2305	2821
Footwear and garment	779	388	590	613	548	618	618	470	614	673	400	632	671	452	613	541	343	447
Other manuf. prod.	2012	2040	2111	1775	1889	1732	2376	2104	2159	1964	2273	1944	2032	2077	1987	2093	1564	1939
Pharma. products	274	621	355	139	385	251	205	351	238	232	501	294	213	465	284	377	398	435
Energy	822	912	882	707	962	761	758	749	738	793	866	855	770	872	809	717	831	783
Petroleum prod.	600	548	665	459	530	523	533	434	522	561	532	637	538	511	587	408	428	444
Services	3232	4385	3951	4042	4511	4413	3370	4618	4162	3801	4334	4215	3611	4462	4185	4144	5177	4490
Transportation*	0	62	338	0	232	401	0	196	371	0	131	216	0	155	332	228	296	252
Communication*	0	439	333	0	433	392	0	352	413	0	444	377	0	417	378	197	199	247
Health	331	805	447	147	548	302	278	974	506	280	736	418	259	766	418	507	614	552
Rents	723	817	812	1470	1406	1552	874	835	962	934	878	988	1000	984	1078	776	794	744
Other services	1757	2262	2096	2141	1892	1901	1786	2261	2035	2188	2145	2262	1968	2140	2073	2444	3274	2699

* Data only available since 2010 for all regions (DROMs).

***Note*:** Weight of the main components of CPI in the four regions, and in metropolitan France, for year 1999, year 2024 and the average overt the 1999-2024 period. The average for the four DROMs is an unweighted mean. The sample excludes the Covid period 2020m03-2021m12.

Comparing the weights in overseas regions to those in metropolitan France, three facts stand out. First, the weight structure is more stable over time in metropolitan France. Second, the weights in overseas regions and in France differ mainly with respect to food excluding fresh food (which is

higher in DROMs) and services (which is lower in DROMs). Thirdly, the composition of consumption baskets in overseas regions are converging to the composition measured in metropolitan France.

A.2 Real activity and external sector

We complement our empirical analysis with some sectoral data on real activity. We include sectoral employment published at quarterly frequency by INSEE since 2011. Employment in overseas regions is dominated by services: non-commercial services (public administration) represent about 45% of employment, and commercial services represent about 39% of employment. In contrast, the manufacturing industry represents only about 7% of total employment, and the construction sector about 5%, followed by the agricultural sector with 2%. To assess the effect of natural disasters on the tourism sector, we also include monthly hotel overnight stays ("*nuitées dans l'hôtellerie*") in our analysis, published at monthly frequency by INSEE since 2011. They amount to 83,000 on average every month, which roughly corresponds to about 15% of the average population of overseas regions. Finally, we also explore the effects of natural disasters on imports, which are provided by the French customs on a quarterly basis since 2004. Food imports represent about 10% of all imports, refined oil about 25%, and transport materials about 20%. In our analysis, these quarterly data are merged with our main monthly dataset assuming constant monthly values of employment and imports within a quarter. We tested an alternative way of merging the data, assuming that quarterly data refer to the last month of each quarter and using a linear interpolation within the quarter. The results are robust.

A.3 Administrative disaster databases

Table A.5. Overlap between the administrative measures of disasters

		Number of reported disasters (and %) in			
	Total	**Guadeloupe**	**French Guiana**	**La Réunion**	**Martinique**
GASPAR	97	27 (27.8%)	8 (8.2%)	31 (32.0%)	31 (32.0%)
EM-DAT	17	4 (23.5%)	1 (5.9%)	8 (47.1%)	4 (23.5%)
All admin.*	100	27 (27.0%)	8 (8.0%)	34 (34.0%)	31 (31.0%)
GASPAR & EM-DAT	14	4 (28.6%)	1 (7.1%)	5 (35.7%)	4 (28.6%)

Note: Descriptive statistics on the distribution of natural disasters (including storms, floods and landslides) in the four French overseas territories. The percentages in brackets sum to 100% over the columns (ie for a given data source). "All admin" is the union between GASPAR and EM-DAT events. The sample excludes the Covid period 2020m03-2021m12.

Table A.6. Types of disasters – Floods and storms

Number of observations		Flood		Total
		No	Yes	
Storm	No	1,068	***76***	1,144
	Yes	***2***	***14***	16
Total		1,070	90	1,160

Note: this table reports the distribution of events with our sample period (1999-2024, excluding the Covid period 2020m03-2021m12) In bold, 92 administrative disasters as reported in EM-DAT or GASPAR datasets including either floods or storms.

Table A.7 – Types of disasters - Landslides

Number of events	**Flood or storm events**		**No flood or storm events**
	without landslides	with landslides	with landslides
	59	33	
Total	92		8

Note: Number of disaster events (storm or flood) in which landslides occur or not in columns (2) and (3). Column (4) reports the number of landslides events in periods without storms or floods.

Table A.8. Share of total administrative disasters (in %) by month of the year

Month	La Réunion	Guadeloupe	Martinique	French Guiana
January	23.5	7.4	3.2	12.5
February	32.4	0.0	0.0	12.5
March	5.9	3.7	0.0	12.5
April	17.7	3.7	9.7	25.0
May	2.9	11.1	12.9	37.5
June	2.9	7.4	3.2	0.0
July	0.0	0.0	3.2	0.0
August	0.0	7.4	9.7	0.0
September	0.0	18.5	16.1	0.0
October	0.0	14.8	19.4	0.0
November	2.9	18.5	12.9	0.0
December	11.8	7.4	9.7	0.0

Note: Share of total number of administrative disasters by calendar month, in each of the different regions. 32.4% of all administrative disasters in La Réunion occurred in February. The sample excludes the Covid period 2020m03-2021m12.

A.4 Meteorological data

The Appendix A.4 illustrates the meteorological data used in the empirical model and provides summary statistics.

Figure A.2. Wind speed from remote sensing

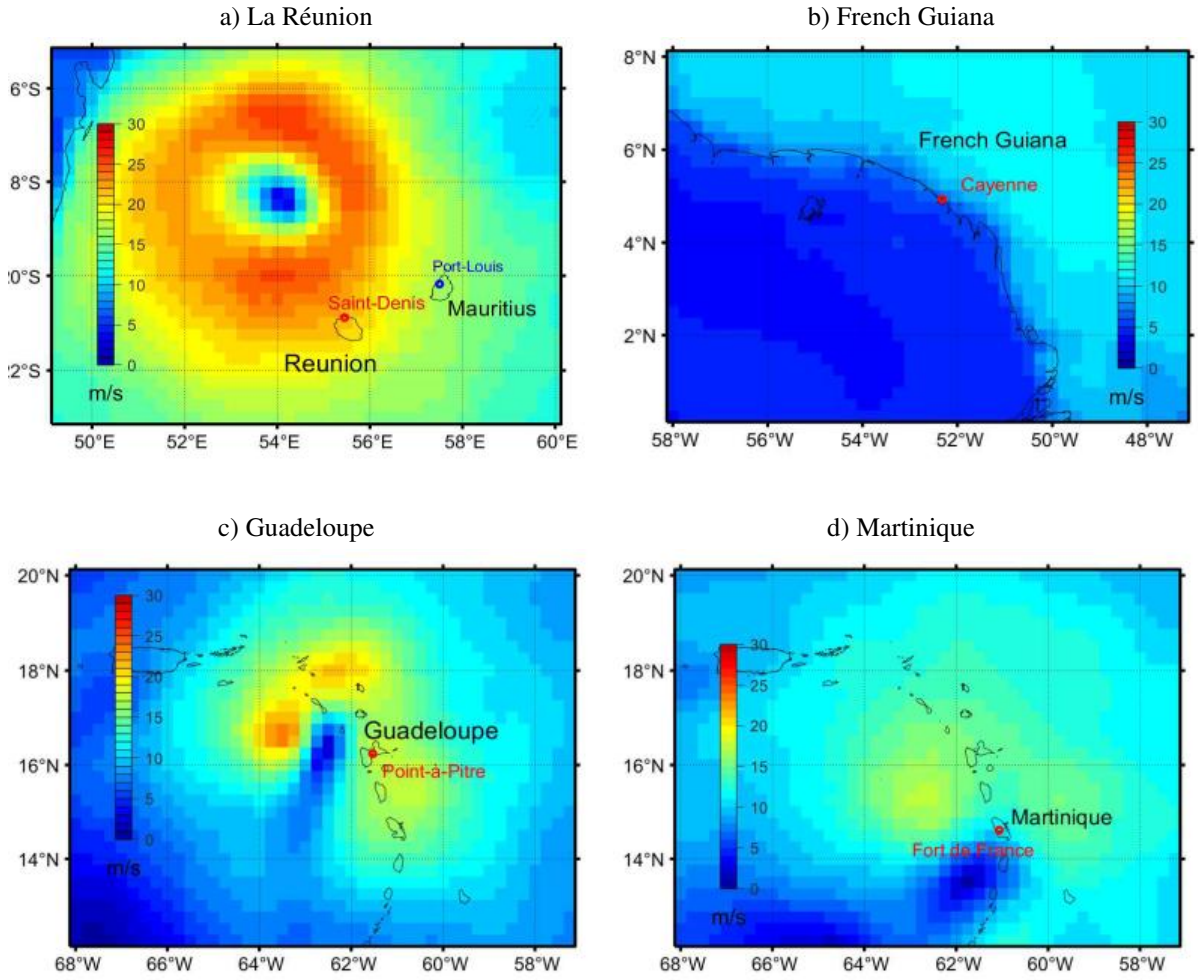

Note: Wind speed from NOAA's Cross-Calibrated Multi-Platform (CCMP) provided on a global scale on a 0.25° latitude/longitudinal grid. Wind speed is measured as maximal sustained wind for one minute during a 6-hour window. Its unit is in m/s on a range from 0 to 30. Panels a–d show the maximum wind speed observations for days with regionally large events:(a) La Réunion, Cyclone Gamede, 27.76 m/s on 2007-Feb-25 12 am, (b) Martinique, Hurricane Dean, 17.26 m/s on 2007-Aug-17 6 pm. (c) Guadeloupe, Hurricane Maria, 21.52 m/s on 2017-Sep-19 6 pm. (d) French Guiana, 13.52 m/s on 2015-Mar-10 12 pm.

Figure A.3. Precipitation from remote sensing

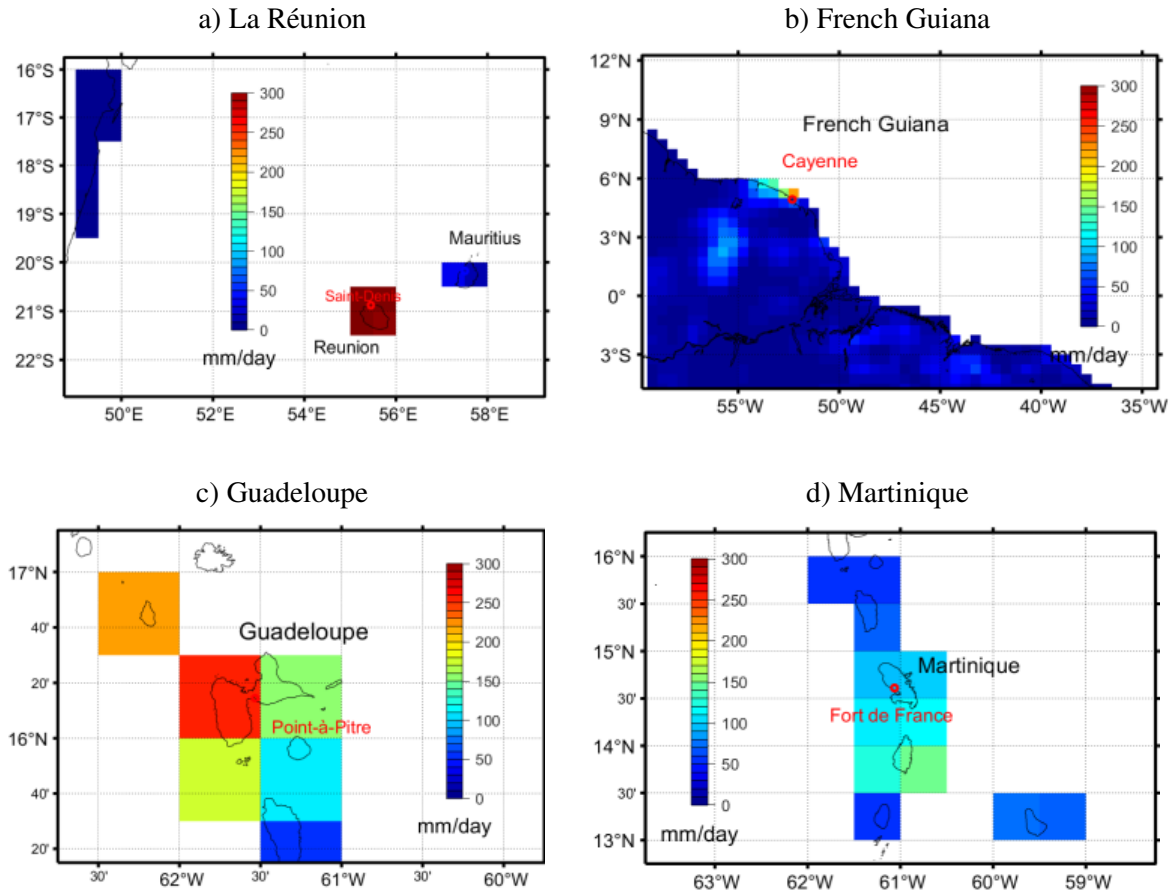

Note: Precipitation from CPC Global Unified Gauge-Based Analysis of Daily Precipitation. The data is defined on a 0.5° longitude/latitude grid and its unit is measured in mm/day with global realizations in the interval [0,300]. Panels a–d show the corresponding observations on days with regionally extreme precipitation events. (a) La Réunion, 319.11 mm on 2011-01-29, (b) Martinique, 141.06 mm on 2016-09-28, (c) Guadeloupe, 252.59 mm on 1999-11-19, (d) French Guiana, 212.79 mm on 2000-04-08.

Table A.9. Summary statistics of meteorological data

	Rain (mm/day)		**Wind speed** (m/s)	
	Mean	SD	Mean	SD
La Réunion	41.06	43.29	13.33	2.71
French Guiana	67.54	30.34	10.13	1.30
Guadeloupe	37.30	24.78	11.68	1.64
Martinique	41.18	24.64	11.20	1.35
Unweighted average	46.77	33.88	11.59	2.17

Note: Precipitation is measured in cumulative mm/day. Wind speed is measured in m/s as maximum sustained wind speed for one minute. The sample excludes the Covid period 2020m03-2021m12.

Appendix B. Additional results

Figure B.1 Partial autocorrelation of the 2SLS first-stage residual.

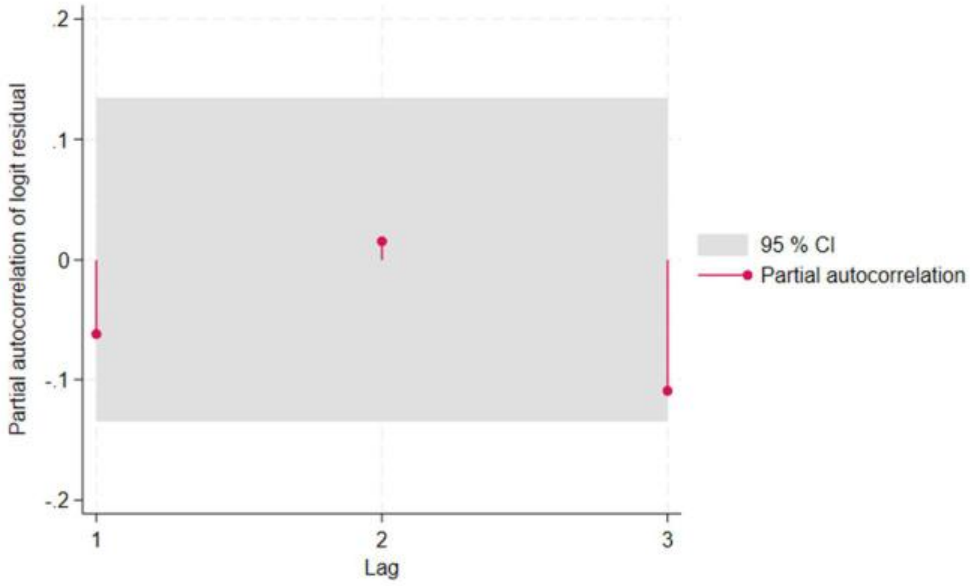

Note: Average partial autocorrelation of the Logit residual obtained over the 4 regions. The partial autocorrelation and the related 95 % confidence interval are computed using the Stata *pac* command for each of the 4 regions. The confidence interval is computed as the standard error of $1/\sqrt{n}$, where n is the sample size. The results are then averaged using equal weights. The shaded area represents the average confidence interval.

Figure B.2. First-stage fitted values: predicted probability of a significant natural disaster

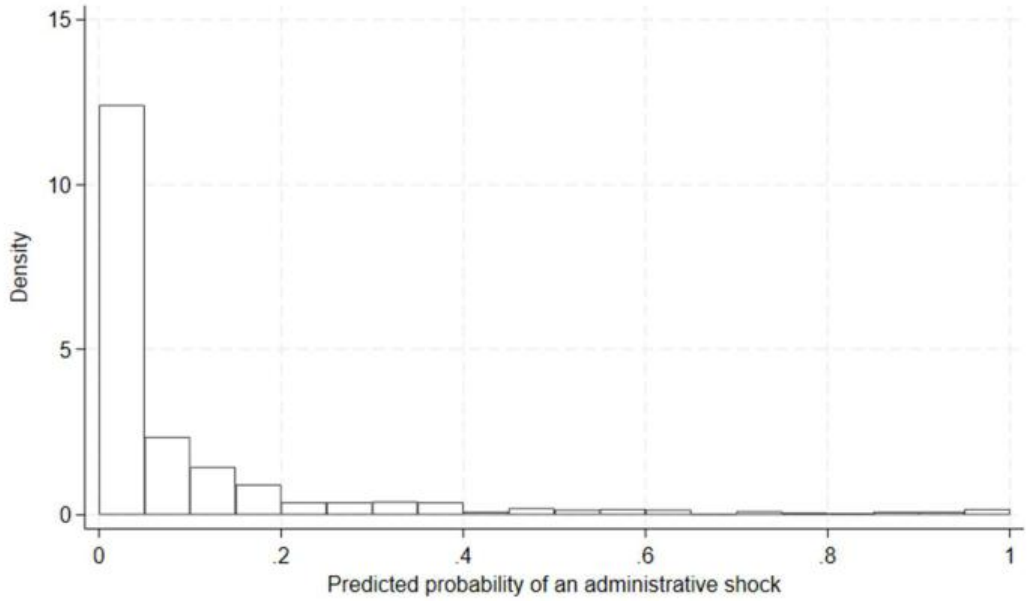

Note: Density plot of predicted probabilities $\hat{p}_{i,t}$ obtained from Logit model (1). Since the dependent variable is an indicator variable associated with natural disaster events with large economic damages, we interpret p_{it} as the predicted probability of an economically significant natural disaster as a function of meteorological data. The sample excludes the Covid period 2020m03-2021m12.

Figure B.3. First-stage fitted values: predicted probability conditional on the occurrence of an administrative disaster (GASPAR or EM-DAT)

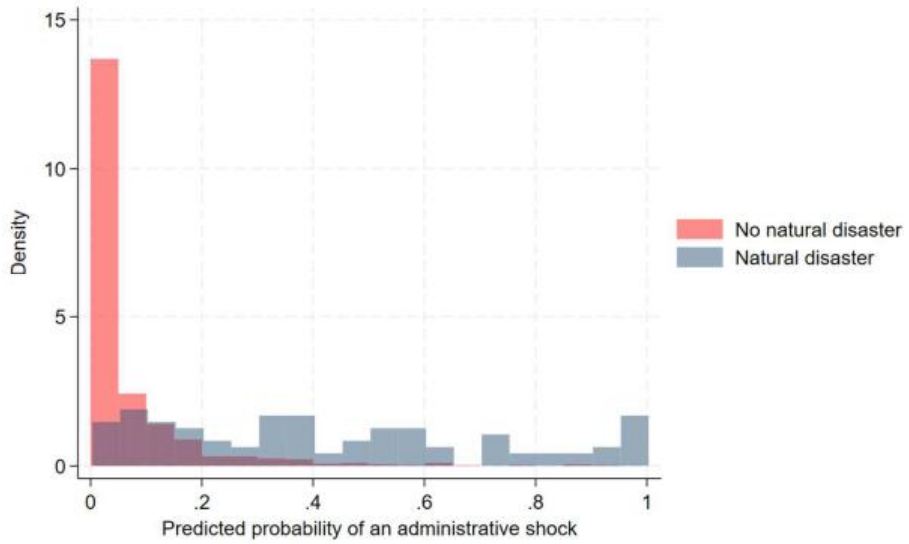

Note: Density of predicted probabilities, computed on two separate subsamples of dates where an administrative weather-related disaster was reported (in blue) and dates with no reported disaster (in red), (decomposition of previous Figure B.2). Sample excludes the Covid period (2020m03–2021m12).

Figure B.4. First-stage fitted values: predicted probability conditional on the occurrence of GASPAR disaster

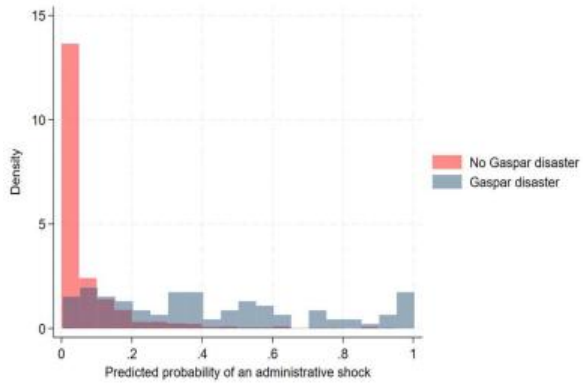

Note: Density of predicted probabilities, computed on two separate subsamples of dates where an administrative weather-related disaster was reported in **GASPAR** (in blue) and dates with no reported disaster (in red), (decomposition of previous Figure B.2). Sample excludes the Covid period (2020m03–2021m12).

Figure B.5. First-stage fitted values: predicted probability conditional on the occurrence of EM-DAT disaster

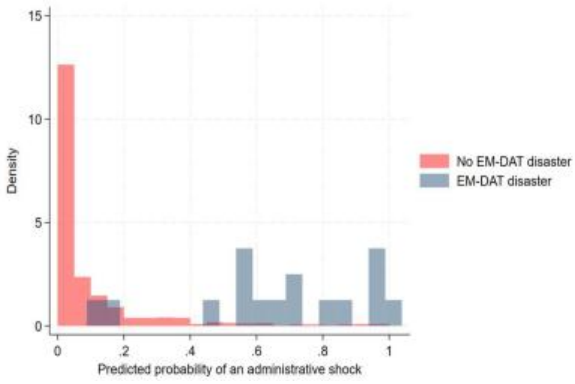

Note: Density of predicted probabilities, computed on two separate subsamples of dates where an administrative weather-related disaster was reported in **EM-DAT** (in blue) and dates with no reported disaster (in red), (decomposition of previous Figure B.2). Sample excludes the Covid period (2020m03–2021m12).

Table B.1. First stage regressions - alternative specifications

Endogenous variable: ω_{it}	**(1)** **Logit model**	**(2)** **Linear prob. model**
Logit model		
Dummy top decile wind	0.139***	
	(5.12)	
Dummy top decile rain	0.153***	
	(5.71)	
Pseudo R^2	0.311	
N	904	
2SLS - first stage equation		
Predicted probability ($\hat{p}_{it}$)	1.022***	
	(9.32)	
Wind		0.041***
		(6.49)
Rain		0.003***
		(6.58)
Adj.R2	0.250	0.230
N	904	904
F-Stat	86.83	48.651

Note: Column (1) presents the estimation results for Logit stage eq. (1) and first stage eq. (2) with dependent variable all natural disasters reported in EM-DAT and GASPAR as a binary variable. *Dummy top decile wind* is a dummy variable indicating whether the maximum wind speed from the CCMP database in a given region and month is in the top decile of the distribution computed across the 4 regions. *Dummy top decile rain* is a dummy variable indicating whether the maximum daily precipitation in a region and month as reported by the Climate Prediction Center (CPC) is in the top decile of the distribution computed across the 4 regions. Column (2) presents the results of a linear probability model as a first stage regression in the IV approach. Sample period: 1999m01 to 2024m12, excluding the Covid period 2020m03-2021m12, for all four regions. T-stats are reported in parentheses. Standard errors are heteroskedasticity-robust and computed using a White-correction routine. Significant at ***0.01, **0.05, *0.10.

Table B.2. Effects on CPI cumulated inflation for all available product components (2SLS)

	T=0	T=1	T=2	T=3	T=4	T=5	T=6
Food excl. tobacco	0.03	0.90***	1.28***	0.54	0.23	0.18	0.17
	(0.20)	(0.30)	(0.36)	(0.36)	(0.36)	(0.34)	(0.31)
Other food	-.09	-0.21**	-0.11	-0.24	-0.28*	-0.11	-0.14
	(.08)	(0.10)	(0.12)	(0.15)	(0.15)	(0.17)	(0.19)
Fresh food	0.99	6.71***	8.01***	4.59***	2.45	1.16	1.23
	(1.20)	(1.74)	(1.88)	(1.64)	(1.63)	(1.52)	(1.50)
Tobacco	0.39	0.73	1.02	1.03	1.30	1.15	1.05
	(0.55)	(0.72)	(0.88)	(0.98)	(1.07)	(1.17)	(1.18)
Energy	-0.60	-0.07	-0.13	-0.11	0.78	0.64	0.83
	(0.56)	(0.69)	(0.73)	(0.80)	(0.93)	(0.94)	(0.89)
Petroleum products	-0.82	-0.15	-0.15	-0.31	0.55	0.45	0.89
	(0.76)	(0.93)	(0.99)	(1.05)	(1.21)	(1.26)	(1.21)
Manufactured products	-0.06	-0.38***	-0.13	0.05	-0.05	-0.10	-0.01
	(0.14)	(0.14)	(0.15)	(0.15)	(0.18)	(0.16)	(0.16)
Other manuf.	0.05	-0.12	-0.08	-0.07	-0.02	0.09	-0.06
	(0.08)	(0.09)	(0.11)	(0.13)	(0.13)	(0.10)	(0.11)
Footwear and garments	-0.37	-1.53**	-0.46	0.40	-0.44	-1.04	0.04
	(0.60)	(0.65)	(0.63)	(0.60)	(0.74)	(0.74)	(0.57)
Pharmaceutical products	-0.05	-0.02	0.04	-0.11	-0.13	0.02	-0.12
	(0.09)	(0.12)	(0.14)	(0.15)	(0.15)	(0.16)	(0.18)
Services	-0.20*	-0.47***	-0.29**	-0.08	-0.04	-0.02	0.05
	(0.11)	(0.14)	(0.15)	(0.14)	(0.15)	(0.14)	(0.16)
Other services	-0.07	-0.15	-0.05	0.10	0.12	0.12	0.24
	(0.11)	(0.13)	(0.17)	(0.17)	(0.18)	(0.19)	(.21)
Rents	0.04	-0.13	-0.03	-0.05	0.00	0.02	0.08
	(0.09)	(0.11)	(0.13)	(0.14)	(0.15)	(0.16)	(0.16)
Communication services	-0.28*	-0.30	-0.37	-0.30	-0.33	-0.02	-0.06
	(0.16)	(0.23)	(0.26)	(0.30)	(0.36)	(0.42)	(0.45)
Health services	-0.26**	-0.14	-0.30*	-0.38**	-0.33*	-0.14	-0.10
	(0.11)	(0.14)	(0.16)	(0.16)	(0.20)	(0.19)	(0.26)
Transportation services	-2.63	-4.02	-1.02	0.04	-2.20	1.84	0.02
	(2.92)	(3.17)	(2.87)	(2.53)	(3.05)	(2.65)	(3.17)
Total	-0.14	-0.11	0.11	0.11	0.13	0.12	0.20
	(0.10)	(0.13)	(0.14)	(0.17)	(0.17)	(0.16)	(0.16)
Total, constant weight	-0.13	-0.09	0.13	0.12	0.10	0.05	0.10
	(0.11)	(0.13)	(0.13)	(0.16)	(0.16)	(0.15)	(0.16)

***Note*:** This table reports the estimated coefficients of the cumulative impulse responses of CPI product components and headline inflation to weather related disasters obtained from the 2SLS local projections model (coefficients θ_h in the equation (3)). Heteroskedasticity-robust standard errors in parentheses are computed using a White-correction routine. Sample period: 1999m01 to 2024m12, excluding the Covid period 2020m03-2021m12, for all four regions. Significant at ***0.01, **0.05, *0.10.

Table B.3. Main results – CPI headline and product components – OLS regressions

OLS estimates	T=0	T=1	T=2	T=3	T=4	T=5	T=6
Total	-0.07	-0.03	0.01	0.10	0.10	0.05	0.05
	(0.05)	(0.07)	(0.08)	(0.09)	(0.08)	(0.08)	(0.08)
Total, constant weight	-0.07	-0.04	0.02	0.12	0.11	0.05	0.03
	(0.05)	(0.07)	(0.07)	(0.08)	(0.08)	(0.07)	(0.07)
Fresh food	0.61	3.00***	3.73***	2.24**	1.26	0.52	0.26
	(0.55)	(0.87)	(1.06)	(0.97)	(0.82)	(0.75)	(0.64)
Other food excl. tobacco	-0.08**	-0.08	-0.05	-0.14*	-0.08	-0.06	-0.07
	(0.04)	(0.06)	(0.08)	(0.08)	(0.08)	(0.09)	(0.10)
Manufactured products	-0.09	-0.12	-0.05	0.08	0.11	-0.05	-0.03
	(0.08)	(0.08)	(0.09)	(0.09)	(0.09)	(0.09)	(0.08)
Services	-0.09	-0.23***	-0.16**	0.12	0.07	0.05	0.06
	(0.07)	(0.08)	(0.07)	(0.08)	(0.08)	(0.08)	(0.09)
Energy	-0.21	-0.10	-0.55	-0.48	-0.20	0.13	0.07
	(0.23)	(0.35)	(0.42)	(0.46)	(0.53)	(0.56)	(0.54)
Tobacco	0.05	0.30	0.25	0.13	0.61	0.45	0.28
	(0.33)	(0.40)	(0.45)	(0.48)	(0.58)	(0.62)	(0.64)

***Note*:** This table reports the estimated coefficients of the cumulative impulse responses of CPI product components and headline inflation to weather related disasters (using ω_i as exogenous variable) obtained from an OLS local projection. Heteroskedasticity-robust standard errors in parentheses, computed using a White-correction routine. Sample period: 1999m01 to 2024m12, excluding the Covid period 2020m03-2021m12, for all four regions. Significant at ***0.01, **0.05, *0.10.

Figure B.6. Main results – CPI headline and product components – 2SLS vs OLS

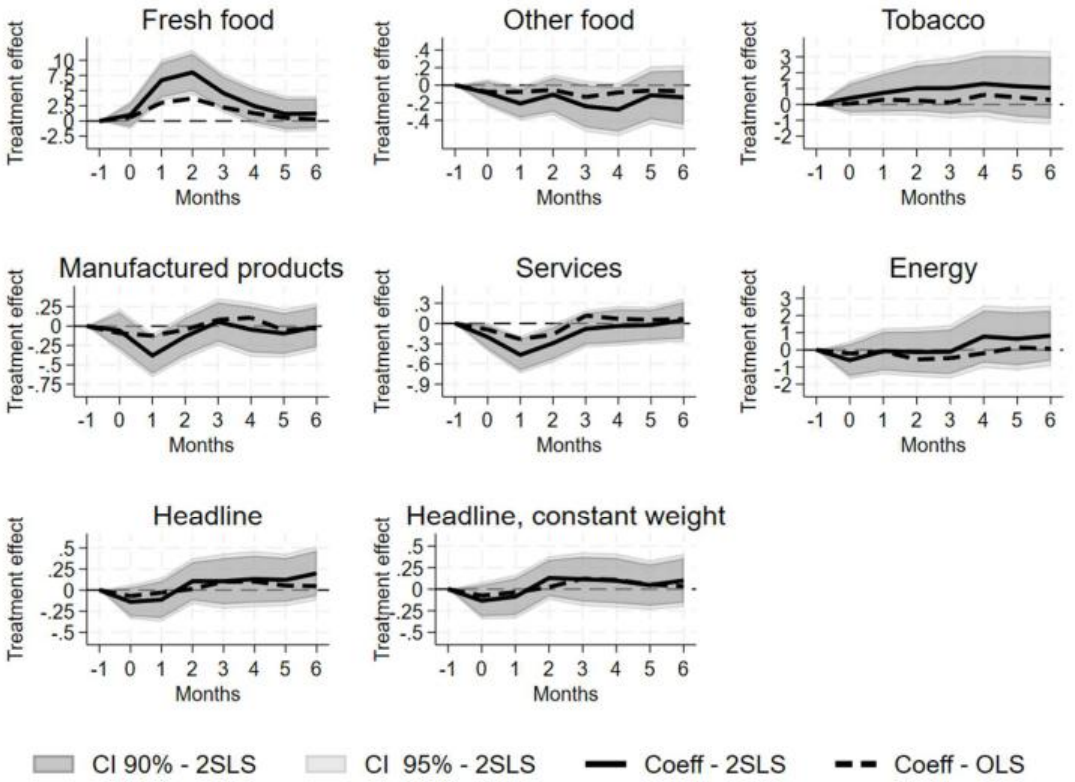

Note: Cumulated impulse response functions of CPI components in our baseline 2SLS (solid lines) and using an OLS specification (dashed lines). Treatment effects are expressed in percent. 90% and 95% confidence intervals for the 2SLS estimate in the shaded areas. Standard errors are heteroskedasticity-robust and computed using a White-correction routine. The x-axis corresponds to the time horizon expressed in months since the disaster. Sample period: 1999m01 to 2024m12, excluding the Covid period 2020m03-2021m12, for all four regions.

Table B.4. Robustness analysis for headline CPI and its components (2SLS regressions)

	T=0	T=1	T=2	T=3	T=4	T=5	T=6
(A) Total							
2SLS - Baseline	-0.14	-0.11	0.11	0.11	0.13	0.12	0.20
2SLS – Baseline – excl. La Réunion	-0.23**	-0.19	-0.23	-0.16	-0.22	-0.12	-0.13
2SLS – Baseline, 3 lags shock	-0.11	-0.06	0.13	0.11	0.15	0.15	0.22
2SLS – Baseline excl. shock < 6months	-0.20	-0.11	0.23	0.20	0.26	0.26	0.38
2SLS – 6 lags forward	-0.12	-0.08	0.16	0.15	0.16	0.13	0.22
2SLS – Wind and rain ^3	-0.07	0.02	0.31	0.25	0.14	0.13	0.25
2SLS – Wind and rain ^1 & 2 & 3	-0.10	-0.01	0.21	0.20	0.14	0.13	0.23
2SLS – Top decile wind or rain	-0.19	-0.31*	-0.02	0.09	0.18	0.27	0.33*
(B) Fresh food							
2SLS - Baseline	0.99	6.71***	8.01***	4.59***	2.45	1.16	1.23
2SLS – Baseline – excl. La Réunion	0.31	3.22***	2.75**	1.05	0.17	0.02	-0.35
2SLS – Baseline, 3 lags shock	1.50	7.41***	8.59***	4.89***	2.45	1.16	1.52
2SLS – Baseline excl. shock < 6months	2.62	12.89***	14.93***	8.48***	4.24	1.96	2.57
2SLS – 6 lags forward	0.87	6.65***	8.14***	4.54***	1.81	0.52	0.84
2SLS – Wind and rain ^3	1.82	9.16***	10.31***	5.23**	2.54	1.63	1.95
2SLS – Wind and rain ^1 & 2 & 3	1.43	8.02***	10.06***	6.58***	3.68**	2.13	1.90
2SLS – Top decile wind or rain	0.31	5.29**	6.95***	4.74**	3.36*	2.82	2.43
(C) Other food excl. tobacco							
2SLS - Baseline	-0.09	-0.21**	-0.11	-0.24	-0.28*	-0.11	-0.14
2SLS – Baseline – excl. La Réunion	-0.12	-0.24**	-0.15	-0.31*	-0.27	-0.14	-0.14
2SLS – Baseline, 3 lags shock	-0.09	-0.17*	-0.09	-0.23	-0.25	-0.10	-0.13
2SLS – Baseline excl. shock < 6months	-0.15	-0.30*	-0.15	-0.40*	-0.43*	-0.16	-0.22
2SLS – 6 lags forward	-0.08	-0.17*	-0.07	-0.21	-0.27*	-0.08	-0.13
2SLS – Wind and rain ^3	-0.14	-0.19*	-0.15	-0.25	-0.34*	-0.19	-0.22
2SLS – Wind and rain ^1 & 2 & 3	-0.08	-0.20**	-0.11	-0.23	-0.25	-0.12	-0.15
2SLS – Top decile wind or rain	-0.02	-0.21	-0.10	-0.21	-0.35*	-0.12	-0.07
(D) Manufactured products							
2SLS - Baseline	-0.06	-0.38***	-0.13	0.05	-0.05	-0.10	-0.01
2SLS – Baseline – excl. La Réunion	-0.18	-0.36**	-0.16	-0.08	-0.31	-0.38*	-0.17
2SLS – Baseline, 3 lags shock	-0.05	-0.36**	-0.13	0.04	-0.04	-0.07	-0.02
2SLS – Baseline excl. shock < 6months	-0.09	-0.62**	-0.22	0.07	-0.07	-0.12	-0.03
2SLS – 6 lags forward	-0.06	-0.43***	-0.17	0.01	-0.02	-0.09	-0.02
2SLS – Wind and rain ^3	-0.10	-0.42***	-0.15	0.17	-0.11	-0.11	0.03
2SLS – Wind and rain ^1 & 2 & 3	-0.04	-0.32**	-0.14	0.00	-0.08	-0.14	-0.03
2SLS – Top decile wind or rain	0.01	-0.47**	-0.26	0.00	-0.06	-0.09	0.10
(E) Services							
2SLS - Baseline	-0.2*	-0.47***	-0.29**	-0.08	-0.04	-0.02	0.05
2SLS – Baseline – excl. La Réunion	-0.34***	-0.50***	-0.34**	0.03	-0.12	0.02	-0.15
2SLS – Baseline, 3 lags shock	-0.2*	-0.43***	-0.29*	-0.09	-0.05	0.01	0.05
2SLS – Baseline excl. shock < 6months	-0.35*	-0.75***	-0.50*	-0.16	-0.08	0.02	0.09
2SLS – 6 lags forward	-0.15	-0.40***	-0.25*	-0.01	0.03	0.00	0.10
2SLS – Wind and rain ^3	-0.13	-0.40***	-0.20	-0.05	-0.06	-0.07	0.07
2SLS – Wind and rain ^1 & 2 & 3	-0.18*	-0.44***	-0.28*	-0.02	-0.05	0.00	0.12
2SLS – Top decile wind or rain	-0.29**	-0.59***	-0.29*	-0.08	-0.06	0.08	0.09

***Note*:** Coefficients of the cumulative impulse response functions of consumer prices to weather-related disasters using alternative specifications of local projections. "2SLS baseline" is our baseline 2SLS specification. "2SLS – Baseline – excl. La Réunion" is the baseline specification excluding La Réunion. "2SLS – Baseline, 3 lags shock" controls for up to 3 lags of the shock. "2SLS – 6 lags forward" controls for up to 6 forward lags of the shock. "Baseline excl. shock < 6 months" is the baseline specification, excluding shocks that occur less than 6 months after a previous shock. "2SLS – Baseline, weather station data" is the baseline specification, but with instruments taken from weather station data rather than remote sensing data. "2SLS – Rain and wind ^3" uses as instruments cubic values of wind and rain. "2SLS – Wind and rain ^1 & 2 & 3" uses as instruments cubic values of wind and rain, as well as lower order terms. "2SLS – Top decile wind or rain" uses as instruments dummies indicating whether wind and rain records are in the top decile of the distribution. Sample period: 1999m01-2024m12, excluding the Covid period 2020m03-2021m12. Significant at ***0.01, **0.05, *0.10. Standard errors are heteroskedasticity-robust and computed using a White-correction routine. Results for tobacco and energy are not reported since disasters have no significant effects in the baseline regression.

Figure B.7. Evolution of fresh food prices around two major natural disasters in La Réunion

"Cyclone Gamède" – Feb. 2007 **"Cyclone Dina" – Jan. 2002**

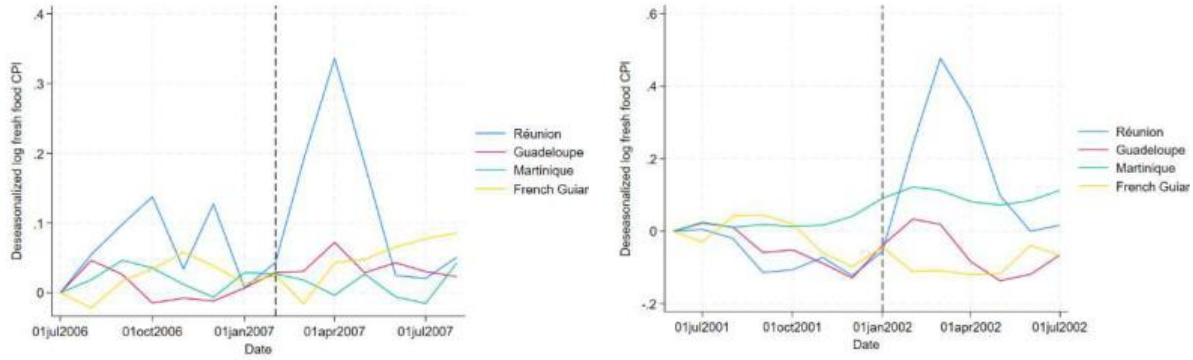

Note: Plotted is the log CPI of fresh food for each region, 6 months before and 6 months after cyclones Gamède (Feb. 2007 in La Réunion) and Dina (Jan. 2002 in La Réunion), that correspond to the two largest events in terms of wind speed in our dataset. The series are seasonally adjusted (at monthly frequency) for each region and expressed in deviation from their value in July 2006 (for Gamède) and June 2001 (for Dina).

Figure B.8. Baseline estimated price effects for fresh food CPI, including pre-trends up to 6 months

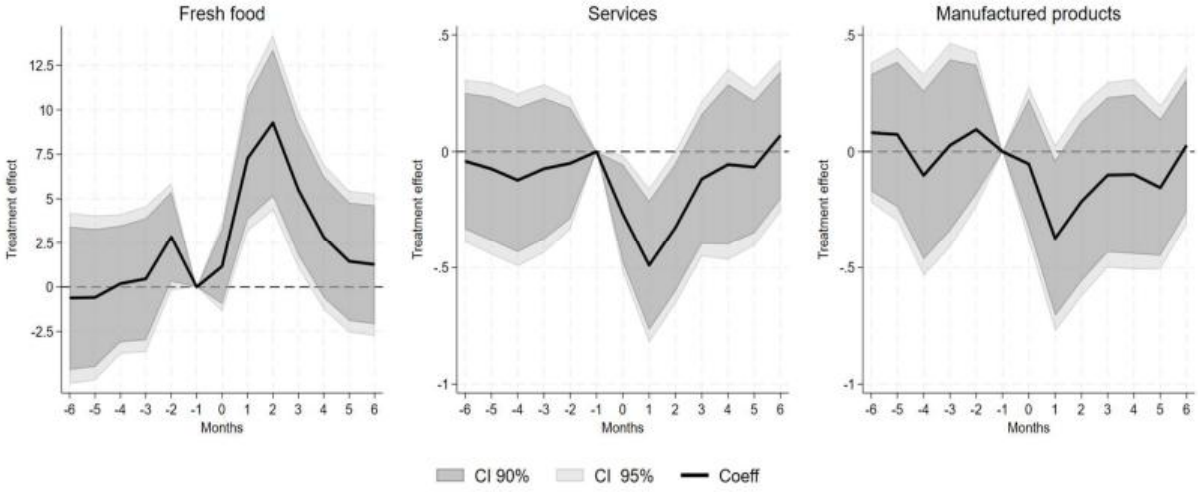

Note: Cumulated impulse response function for the CPI of fresh food obtained from the 2SLS specification, with no controls for lagged values of shocks and of the outcome variable. Treatment effects are expressed in percent. 90% and 95% confidence intervals for the 2SLS estimate in the shaded areas. Standard errors are heteroskedasticity-robust and computed using a White-correction routine. The x-axis corresponds to the time horizon expressed in months since the disaster. Sample period: 1999m01 to 2024m12, excluding the Covid period 2020m03-2021m12, for all four regions.

Table B.5. Price effects of disasters proxied using damage functions - OLS regressions

	T=0	T=1	T=2	T=3	T=4	T=5	T=6
Total – headline CPI							
Rain damage function	0.00	-0.01	0.01	0.02	0.05***	0.03	0.03
	(0.02)	(0.02)	(0.02)	(0.02)	(0.02)	(0.02)	(0.02)
Wind damage function	0.01	0.03	0.08**	0.04	0.00	-0.02	0.01
	(0.02)	(0.03)	(0.04)	(0.03)	(0.03)	(0.02)	(0.03)
Fresh food							
Rain damage function	-0.27	0.20	0.41	0.36	0.21	0.07	0.10
	(0.20)	(0.36)	(0.32)	(0.28)	(0.27)	(0.29)	(0.30)
Wind damage function	0.63***	1.65***	1.90***	0.83*	0.37	0.34	0.50*
	(0.18)	(0.34)	(0.51)	(0.49)	(0.45)	(0.29)	(0.27)
Other food							
Rain damage function	0.00	-0.03**	-0.02	-0.02	-0.03	-0.01	-0.03
	(0.01)	(0.01)	(0.01)	(0.02)	(0.02)	(0.02)	(0.02)
Wind damage function	-0.02*	-0.02	0.00	-0.01	-0.02	-0.01	-0.02
	(0.01)	(0.01)	(0.02)	(0.02)	(0.02)	(0.03)	(0.03)
Tobacco							
Rain damage function	-0.06	-0.07	-0.03	-0.01	0.05	0.08	0.10
	(0.08)	(0.09)	(0.11)	(0.12)	(0.14)	(0.16)	(0.15)
Wind damage function	0.13	0.17	0.15	0.09	0.05	-0.04	-0.06
	(0.12)	(0.14)	(0.16)	(0.18)	(0.19)	(0.21)	(0.20)
Energy							
Rain damage function	0.08	0.15	0.15	0.20	0.27*	0.22	0.21*
	(0.10)	(0.13)	(0.13)	(0.14)	(0.14)	(0.14)	(0.12)
Wind damage function	-0.18**	-0.09	0.02	0.04	0.07	0.01	0.05
	(0.07)	(0.11)	(0.14)	(0.15)	(0.17)	(0.17)	(0.15)
Manufactured products							
Rain damage function	0.00	-0.01	0.00	0.01	0.02	0.02	-0.01
	(0.02)	(0.02)	(0.02)	(0.02)	(0.02)	(0.02)	(0.02)
Wind damage function	-0.01	-0.05***	-0.01	0.02	-0.04*	-0.04*	0.01
	(0.02)	(0.02)	(0.02)	(0.02)	(0.02)	(0.02)	(0.02)
Services							
Rain damage function	0.01	-0.01	0.01	0.00	0.06**	0.01	0.03
	(0.01)	(0.02)	(0.01)	(0.01)	(0.02)	(0.01)	(0.02)
Wind damage function	-0.01	-0.02	0.00	0.01	-0.03	-0.04***	-0.02
	(0.02)	(0.02)	(0.02)	(0.02)	(0.02)	(0.02)	(0.03)

***Note*:** This table reports the estimated coefficients of the cumulative impulse responses of CPI product components and headline inflation to weather related disasters (using standardized damage functions of wind and rain H_{it}^{S} and F_{it}^{S} as exogenous variables) obtained from an OLS local projection. For fresh food products, an increase of the wind damage function by one SD increases prices by 1.65% one month after the shock. Heteroskedasticity-robust standard errors in parentheses, computed using a White-correction routine. Significant at ***0.01, **0.05, *0.10.

Table B.6. OLS regressions relating damage functions to predicted probability of a disaster (from the Logit model)

	Standardized **wind** damage function	Standardized **rain** damage function
Predicted probability ($\hat{p}_{i,t}$) from the Logit model	2.93***	2.84***
	(0.65)	(0.62)
Constant	-0.13***	-0.14***
	(0.04)	(0.04)
Adj. R2	0.234	0.214
N	904	904

Note: Results of OLS regressions relating the damage functions H_{it}^{S} and F_{it}^{S}, given by equations (7) and (8) to the predicted probability of a weather-related disaster obtained from the Logit model ($\hat{p}_{i,t}$). Sample period: 1999m01 to 2024m12, excluding the Covid period 2020m03-2021m12, for all four regions. Heteroskedasticity-robust standard errors in parentheses, computed using a White-correction routine. Significant at ***0.01, **0.05, *0.10.

Table B.7. Characteristics of wind and rain damage functions depending on the predicted probabilities of disasters

	$\hat{p}_{i,t} \in [0 ; 0.25[$			$\hat{p}_{i,t} \in]0.25 ; 0.5]$			$\hat{p}_{i,t} \in]0.5 ; 0.75]$			$\hat{p}_{i,t} \in]0.75 ; 1]$		
	Share of dam. funct. >0	Mean of dam. funct.	Mean of dam. funct. if >0	Share of dam. funct. >0	Mean of dam. funct.	Mean of dam. funct. if >0	Share of dam. funct. >0	Mean of dam. funct.	Mean of dam. funct. if >0	Share of dam. funct. >0	Mean of dam. funct.	Mean of dam. funct. if >0
Wind damage function (W*=15 m/s)	1.8 %	41.0	2,313.4	7.7 %	333.0	4,329.3	39.3 %	1,299.8	3,308.6	57.1 %	3,922.9	6,865.1
Rain damage function (r*=112 mm)	0.1 %	0.3	216.7	10.8 %	16.4	151.9	17.9 %	46.9	262.9	57.1 %	148.1	259.2

Note: This table presents, for different values of the predicted probability from the Logit model ($\hat{p}_{i,t}$), the share of observations for which the wind and rain damage functions are strictly positive ("Share of dam. funct. >0"), the average value of the damage function ("Mean of dam. funct.") and the average value of the damage function conditional on being strictly positive ("Mean f dam. funct. if >0"). The results are reported for the baseline wind damage function (with W*=15 m/s) and for the baseline rain damage function (r*=112 mm).

Table B.8. Average values of predicted probability from the Logit model depending on maximum monthly wind speed and rainfall

	Average probability ($\hat{p}_{i,t}$) below threshold	Average probability ($\hat{p}_{i,t}$) above threshold
Maximum monthly wind speed (threshold=15 m/s)	8.3 %	47.7 %
Maximum monthly rainfall (threshold=112 mm)	9.1 %	40.5 %

Note: Average values of the predicted probability from the Logit model ($\hat{p}_{i,t}$), conditional on whether monthly maximum wind speed and rainfall are below the threshold set for the baseline damage functions (respectively 15 m/s and 112 mm). The average probability when wind speed is below the threshold of 15 m/s is 8.3%, and it is equal to 47.7% when maximum monthly wind speed is above the threshold of 15 m/s.

Table B.9. Local projection estimations (OLS) relating consumer prices to the different types of administrative disasters

	T=0	T=1	T=2	T=3	T=4	T=5	T=6
(A) Headline							
Storms (with or without floods)	-0.06	0.19	0.47	0.30	-0.13	-0.08	0.10
Floods (without storms)	-0.08	-0.08	-0.06	0.05	0.14	0.09	0.06
Landslides only	0.13	0.05	-0.23	0.08	0.15	-0.05	-0.31
(B) Fresh food							
Storms (with or without floods)	4.10**	12.06***	13.69***	8.65**	4.19	3.38	4.32**
Floods (without storms)	-0.01	0.80	1.41	1.04	1.00	0.21	-0.37
Landslides only	-1.54	2.53	1.48	-2.34	-4.31*	-3.69*	-2.98**
(C) Other food							
Storms (with or without floods)	-0.06	0.01	0.05	-0.07	-0.19	-0.14	-0.18
Floods (without storms)	-0.06	-0.06	-0.02	-0.09	0.01	0.03	0.01
Landslides only	-0.20*	-0.38***	-0.61***	-0.61***	-0.74***	-0.78***	-0.59***
(D) Manufactured products							
Storms (with or without floods)	-0.14	-0.35**	-0.27	-0.04	-0.21	-0.26	0.10
Floods (without storms)	-0.11	-0.12	0.00	0.06	0.10	-0.02	-0.04
Landslides only	0.27	0.46***	0.06	0.48*	0.85***	0.18	-0.14
(E) Services							
Storms (with or without floods)	-0.10	-0.16	-0.02	0.17	-0.11	-0.05	0.11
Floods (without storms)	-0.09	-0.22**	-0.16**	0.08	0.08	0.05	0.06
Landslides only	0.07	-0.22	-0.32	0.28	0.26	0.26	-0.07
(F) Energy							
Storms (with or without floods)	-0.74	-0.53	-0.52	-0.30	-0.94	-0.02	0.16
Floods (without storms)	-0.16	-0.01	-0.52	-0.50	-0.05	0.15	0.10
Landslides only	0.71	0.04	-0.41	-0.15	0.16	0.19	-0.58
(G) Energy							
Storms (with or without floods)	-0.19	0.02	1.16	1.22	1.42	1.22	1.12
Floods (without storms)	0.11	0.33	-0.03	-0.24	0.32	0.22	0.08
Landslides only	-0.10	0.23	0.92	1.47*	1.15*	0.63	0.14

***Note*:** This table reports the estimated coefficients of the cumulative impulse responses of CPI product components and headline inflation to weather related disasters obtained from an OLS local projections where we include simultaneously three dummies for administrative disasters as reported in EM-DAT or GASPAR: one indicating storms (with or without floods), another one for floods (without storms) and a last for landslides only. In each column, Panels (A) to (G) report the results of one regression relating price changes to the three dummy variables for disasters (control variables and fixed effects are also included as in our baseline exercise). Sample period: 1999m01 to 2024m12, excluding the Covid period 2020m03-2021m12, for all four regions. Standard errors are heteroskedasticity-robust and computed using a White-correction routine. Significant at ***0.01, **0.05, *0.10

Figure B.9. Comparison of baseline damage functions with wind-only and rain-only damage functions

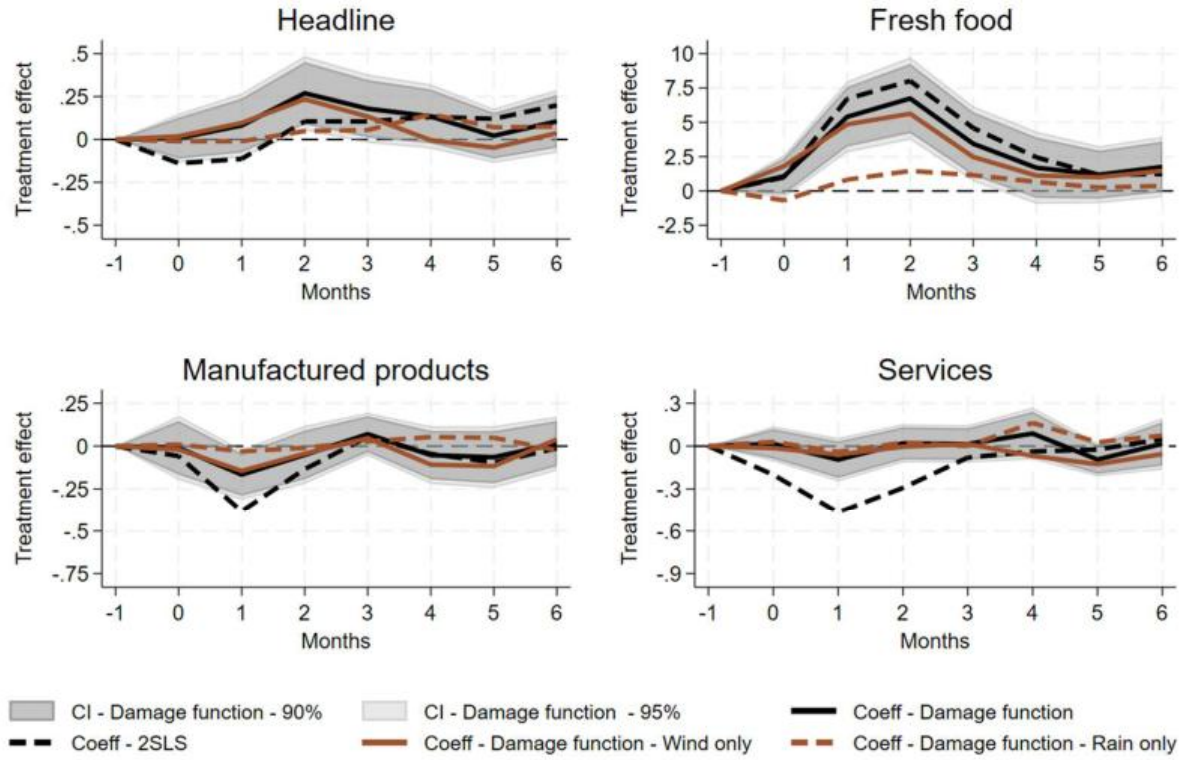

Note: Plotted are the cumulated impulse response function for the baseline 2SLS (dashed line) and for damage functions evaluated "at predicted probability", i.e. for a variation of the damage functions equivalent to a switch from a predicted probability equal to 0 to a predicted probability equal to 1. In solid black, the price reaction is estimated through a regression including both wind and rain damage functions, and the shaded area represent the 90% and 95% confidence interval for this estimation. Standard errors are heteroskedasticity-robust and computed using a White-correction routine. In solid brown, the price reaction is estimated through a regression including only wind damage functions. In dashed brown, the price reaction is estimated through a regression including only rain damage functions. All effects are expressed in percent. The x-axis corresponds to the time horizon expressed in months since the disaster. Sample period: 1999m01 to 2024m12, excluding the Covid period 2020m03-2021m12, for all four regions.

Figure B.10. Effects of wind damage functions on fresh food prices: the role of the nighttime light weights

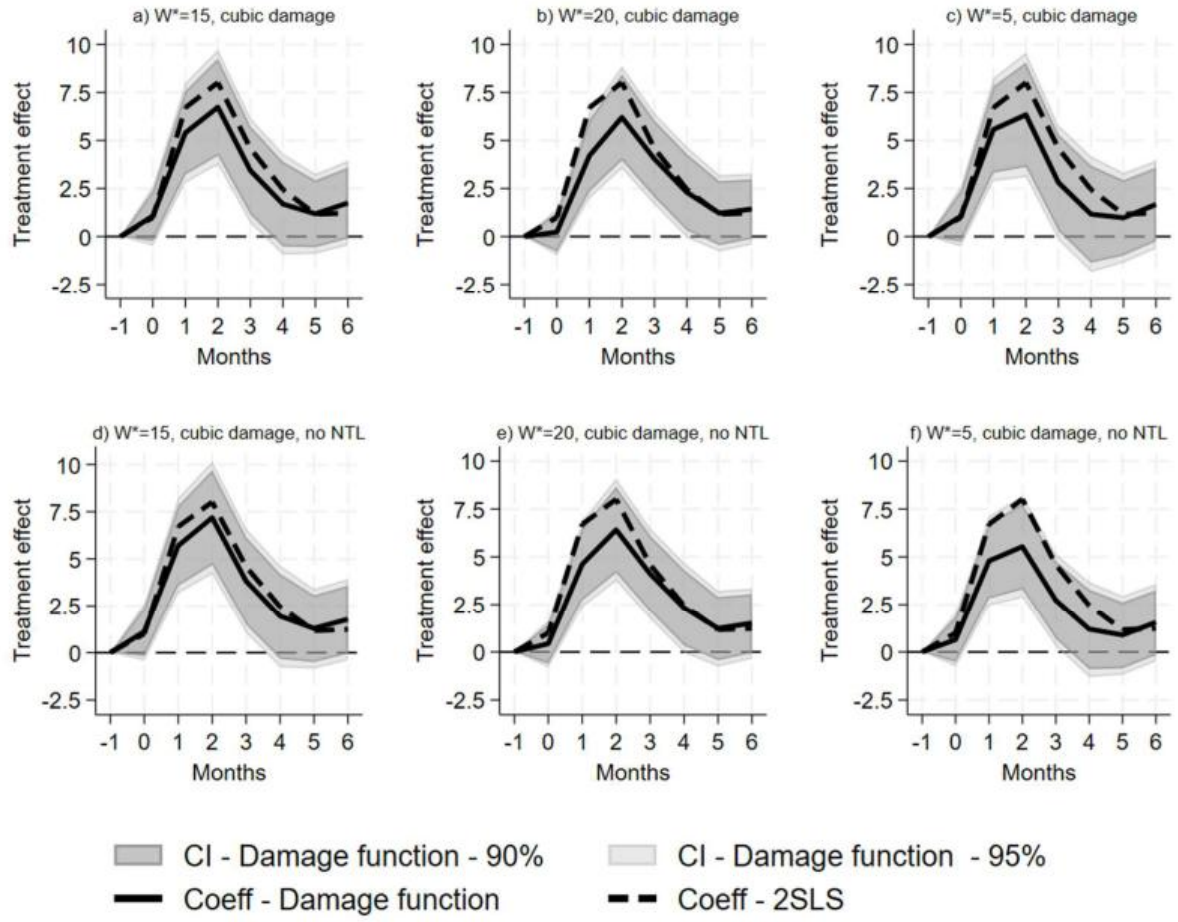

Note: Results of alternative wind damage functions on the prices of fresh food. In columns, we report results where we vary the threshold under which the damage function is 0. We consider a threshold of 15m/s as in our baseline scenario (95th percentile of win distribution in our sample) (column 1), in column (2), the threshold is set to 20m/s (99th percentile of the wind distribution) and in column (3), we set this threshold at 5m/s implying that the damage function is always different from 0 (there is no nonlinearity due the max threshold). In rows, for a given max threshold of wind, we report results of regressions where we weight or not the observations by nighttime light or not. In the first row, we report results using the baseline damage function using the cubic term transformation weighted by nighttime light 'with NTL'). In the second row, we do not weight for nighttime light ('no NTL'). Dashed lines in all the graphs report our baseline 2SLS estimates. The shaded area represents the 90%- and 95% confidence intervals for the effects of the damage function. Standard errors are heteroskedasticity-robust and computed using a White-correction routine. All price effects are expressed in percent. The x-axis corresponds to the time horizon expressed in months since the disaster. Sample period: 1999m01 to 2024m12, excluding the Covid period 2020m03-2021m12, for all four regions.

Table B.10. Effects of weather-related disasters on real variables (2SLS)

	T=0	T=1	T=2	T=3	T=4	T=5	T=6
Hotel stays							
Overnight hotel stays	-21.08**	-3.88	-2.31	-17.43***	-1.83	1.38	-10.45
	(8.30)	(7.25)	(7.95)	(6.6)	(5.51)	(7.45)	(6.85)
Employment							
Total	-0.07	-0.37*	-0.61**	-0.82***	-1.02***	-1.18***	-1.20***
	(0.13)	(0.20)	(0.24)	(0.28)	(0.29)	(0.33)	(0.37)
Agriculture (AZ)	-0.34	-1.69**	-1.58	-1.24	-1.02	-0.81	-1.83
	(0.61)	(0.82)	(0.96)	(1.06)	(1.17)	(1.27)	(1.30)
Food manuf. (C1)	0.67**	0.78	-0.06	-0.54	-1.29*	-1.18	-1.54**
	(0.32)	(0.50)	(0.67)	(0.83)	(0.77)	(0.77)	(0.75)
AZ+C1	0.54*	0.01	-0.39	-0.55	-1.01	-0.89	-1.54***
	(0.31)	(0.42)	(0.53)	(0.59)	(0.62)	(0.64)	(0.59)
Industry (C2 to C5)	0.06	0.00	-.13	-0.19	-0.30	-0.50	-0.46
	(0.16)	(0.25)	(0.30)	(0.32)	(0.37)	(0.38)	(0.47)
Construction (FZ)	-0.31	-0.95	-1.39**	-1.92***	-1.98**	-2.27**	-2.76***
	(0.36)	(0.59)	(0.66)	(0.73)	(0.84)	(0.91)	(0.95)
Car repair (GZ)	-0.15	-0.29*	-0.41**	-0.34	-0.43*	-0.51**	-0.63**
	(0.11)	(0.17)	(0.19)	(0.22)	(0.23)	(0.25)	(0.25)
Transports (HZ)	-0.34	-0.46	-0.83*	-0.88*	-1.13**	-1.51***	-1.88***
	(0.26)	(0.39)	(0.44)	(0.49)	(0.53)	(0.57)	(0.60)
Accom. – restaurants (IZ)	-0.43	-0.72	-1.31**	-1.87***	-2.15***	-2.26***	-2.27***
	(0.41)	(0.57)	(0.62)	(0.69)	(0.71)	(0.81)	(0.84)
Info. – comm (JZ)	-0.30	-0.61	-0.34	-0.15	-0.26	-0.53	-1.21
	(0.37)	(0.58)	(0.70)	(0.76)	(0.83)	(0.84)	(0.84)
Finance – insurance (KZ)	0.02	0.12	-0.07	-0.06	-0.15	-0.24	-0.48
	(0.29)	(0.37)	(0.41)	(0.44)	(0.45)	(0.46)	(0.50)
Real estate (LZ)	0.15	-0.22	-0.09	-0.35	-1.09*	-1.55**	-1.03
	(0.27)	(0.44)	(0.51)	(0.55)	(0.59)	(0.66)	(0.78)
Scientific – admin (MN)	-0.24	-0.57	-0.81*	-0.81*	-1.14**	-1.29**	-1.32**
	(0.28)	(0.38)	(0.42)	(0.44)	(0.48)	(0.53)	(0.58)
Public admin (OQ)	-0.01	-0.39*	-0.56**	-0.77***	-0.98***	-1.18***	-0.96**
	(0.16)	(0.20)	(0.23)	(0.30)	(0.31)	(0.37)	(0.41)
Other services (RU)	-0.66	-1.66*	-2.05**	-2.67**	-2.83***	-2.73**	-2.43**
	(0.55)	(0.92)	(0.99)	(1.09)	(1.04)	(1.12)	(1.17)
Interim	1.53	-0.27	-2.67	-2.92	-0.52	3.48	-0.99
	(2.80)	(3.92)	(4.74)	(5.18)	(5.06)	(5.10)	(5.34)

***Note*:** This table reports the estimated coefficients of the cumulative impulse responses of real activity measures to weather related disasters obtained from the 2SLS local projections model (coefficients θ_h in the equation (3) where the endogenous variables are either hotel stays or employment instead of prices). Heteroskedasticity-robust standard errors in parentheses are computed using a White-correction routine. Sample period: 1999m01 to 2024m12, excluding the Covid period 2020m03-2021m12, for all four regions. Significant at ***0.01, **0.05, *0.10.

Table B.11. Effects of weather-related disasters on imports (2SLS)

	T=0	T=1	T=2	T=3	T=4	T=5	T=6
Imports							
Agriculture (AZ)	2.42	3.00	3.50	2.65	3.25	3.78	2.10
	(2.43)	(3.66)	(4.18)	(3.61)	(4.14)	(4.33)	(3.52)
Extractive indus. (DE)	-14.01	-0.02	0.19	-4.38	-1.61	-12.71	-6.08
	(10.98)	(13.02)	(15.07)	(14.7)	(15.49)	(16.39)	(14.88)
Processed food (CA)	0.54	0.03	0.54	0.39	1.89	2.37	2.58
	(1.41)	(2.06)	(2.75)	(2.73)	(2.70)	(2.53)	(2.20)
Textile (CB)	-2.80	-5.33	-2.54	-2.12	-2.44	-4.49	0.45
	(2.67)	(4.19)	(4.99)	(3.75)	(4.01)	(3.65)	(3.38)
Wood (CC)	1.36	0.27	1.82	-2.14	-2.84	-6.00*	1.36
	(2.58)	(3.32)	(3.74)	(3.43)	(3.34)	(3.55)	(4.90)
Refined oil (CD)	5.02	9.81**	10.71**	10.70*	7.39	2.48	4.62
	(3.14)	(4.60)	(5.13)	(6.05)	(5.64)	(6.34)	(6.11)
Chemical products (CE)	-7.01**	-4.93	-5.38	-2.22	-3.35	-4.55	6.55
	(3.08)	(5.39)	(6.05)	(5.92)	(6.65)	(6.61)	(7.60)
Pharmac. goods (CF)	1.01	-4.24	-8.13	13.84	15.39	16.80	20.49
	(12.65)	(16.85)	(19.72)	(18.90)	(16.39)	(15.90)	(17.23)
Gum / plastic (CG)	-0.37	-4.75*	-2.26	0.21	4.34	4.28*	3.70
	(1.78)	(2.60)	(3.18)	(2.79)	(2.69)	(2.57)	(2.41)
Metals (CH)	-1.12	-5.40	-6.04	-7.99	-3.25	-1.86	-0.67
	(4.01)	(5.69)	(6.58)	(6.23)	(6.76)	(6.92)	(6.31)
Electronics (CI)	2.83	3.05	2.59	-6.05	-7.53	-5.21	1.43
	(5.40)	(7.17)	(8.73)	(7.64)	(8.24)	(8.50)	(8.24)
Electric equip. (CJ)	-1.26	-6.45	-7.59	-3.39	-2.37	-2.90	-12.36*
	(4.49)	(5.97)	(8.25)	(8.79)	(8.79)	(7.78)	(6.80)
Industrial machines (CK)	-7.28	-8.66	-13.01*	-7.48	-3.14	-1.87	-1.72
	(4.72)	(6.52)	(7.39)	(7.12)	(6.82)	(6.97)	(6.70)
Transport mat. (CL)	11.39	9.93	22.01*	4.68	3.86	-4.18	2.40
	(6.95)	(9.97)	(12.32)	(11.85)	(10.54)	(9.12)	(8.69)
Other manuf. (CM)	-3.13	-2.45	-0.25	1.36	-1.29	-5.33	-1.87
	(2.42)	(3.45)	(3.85)	(3.25)	(3.83)	(3.77)	(3.10)
Edition/Comm (JZ)	0.37	9.66	11.27	9.53	-7.47	-9.89	-4.97
	(5.05)	(8.61)	(9.16)	(7.92)	(6.25)	(6.40)	(5.90)
Techn. draw./art (MN -RU)	9.17	13.53	9.76	19.92	15.97	37.94	-0.79
	(18.54)	(28.31)	(32.29)	(30.31)	(34.44)	(35.01)	(31.72)
Total	2.84	2.57	6.29	4.92	5.26	2.14	3.39
	(2.25)	(3.37)	(4.08)	(4.15)	(3.79)	(3.70)	(3.39)

***Note*:** This table reports the estimated coefficients of the cumulative impulse responses of real activity measures to weather related disasters obtained from the 2SLS local projections model (coefficients θ_h in the equation (3) where the endogenous variables are imports by type of sectors instead of prices). Heteroskedasticity-robust standard errors in parentheses are computed using a White-correction routine. Sample period: 1999m01 to 2024m12, excluding the Covid period 2020m03-2021m12, for all four regions. Significant at ***0.01, **0.05, *0.10.

Table B.12. Alternative 2SLS specification not controlling for year fixed effects

	T=0	T=1	T=2	T=3	T=4	T=5	T=6
(A) Baseline							
Headline	-0.14	-0.11	0.11	0.11	0.13	0.12	0.20
Fresh food	0.99	6.71***	8.01***	4.59***	2.45	1.16	1.23
Other food excl. tobacco	-0.09	-0.21**	-0.11	-0.24	-0.28*	-0.11	-0.14
Manufactured products	-0.06	-0.38***	-0.13	0.05	-0.05	-0.10	-0.01
Services	-0.20*	-0.47***	-0.29**	-0.08	-0.04	-0.02	0.05
(B) No year FE							
Headline	-0.09	-0.05	0.28	0.20	0.06	0.03	0.21
Fresh food	0.66	7.46***	10.14***	5.76**	2.13	0.10	1.00
Other food excl. tobacco	0.02	-0.10	0.02	-0.11	-0.17	0.02	-0.13
Manufactured products	-0.03	-0.36**	-0.10	0.10	-0.16	-0.21	0.00
Services	-0.17	-0.5***	-0.28*	-0.06	-0.06	-0.06	0.15

***Note*:** Results for alternative specifications of local projections of consumer prices in a 2SLS setting as presented in equation (3). Panel (A) shows results for our baseline specification. Panel (B) shows results for a 2SLS specification controlling for region-specific quarter fixed effects, but not for year fixed effects. Standard errors are heteroskedasticity-robust and computed using a White-correction routine. Significant at ***0.01, **0.05, *0.10. Sample period: 1999m01 to 2024m12, excluding the Covid period 2020m03-2021m12, for all four regions.

Appendix C. Results using ground data

Meteorological records from ground weather stations are obtained from the Global Surface Summary of the Day (GSOD), a database derived from the Integrated Surface Hourly dataset. This source provides data for over 9,000 stations around the world beginning in 1929, with two to three stations matched to each region in our analysis (Figure C.1). Each weather station provides data on precipitation in 0.01 inches in cumulative terms per day and the maximum wind speed measured for one minute during the day in tenths of knots.

Figure C.1. Location of weather stations

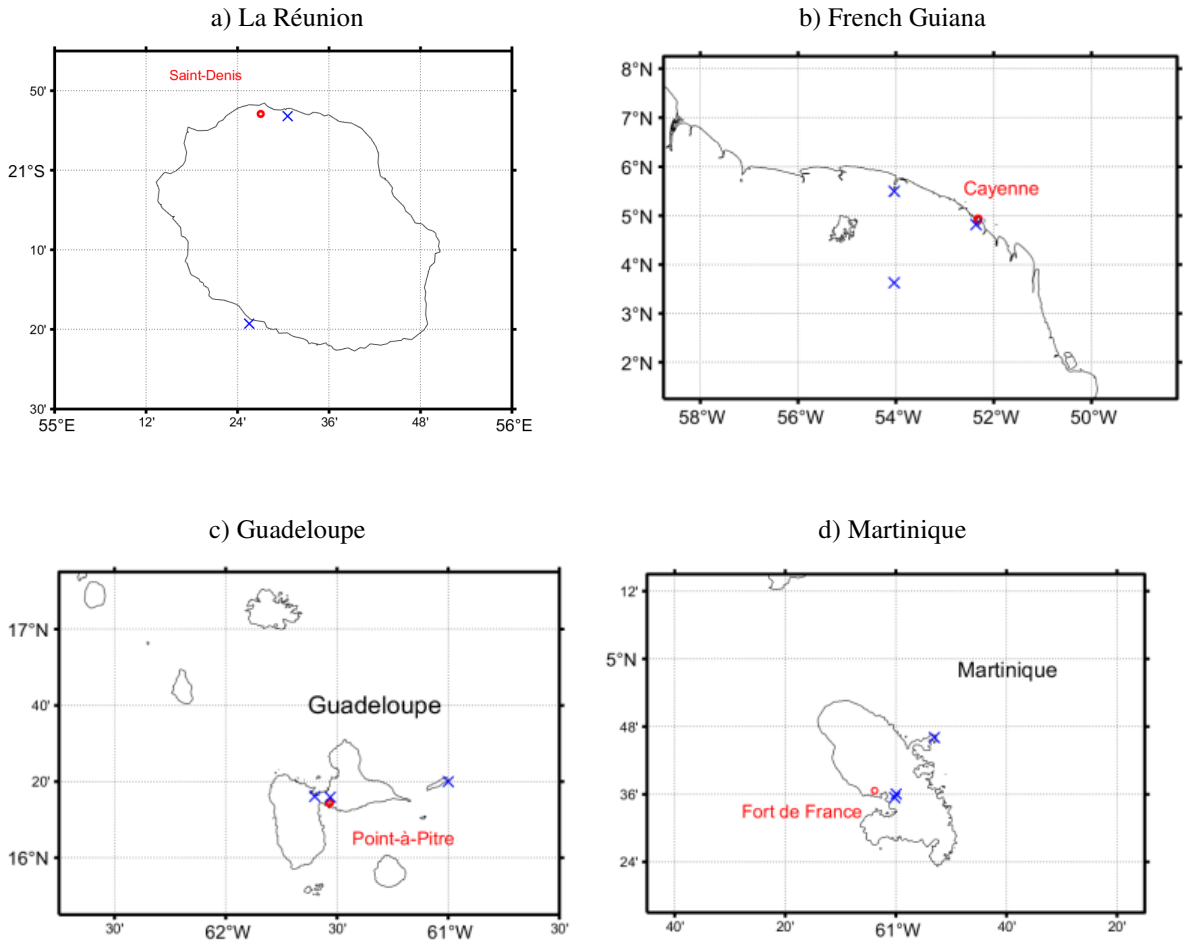

Note: Blue crosses mark the locations of ground weather stations from the Global Surface Summary of the Day (GSOD) database in La Réunion (St Denis Gillot, St Pierre Pierrefonds), Martinique (La Lamentin, Martinique Aime Césaire International Airport, Trinité Caravelle), Guadeloupe (La Desirade, Le Raizet, Point-à-Pitre International Airport), and French Guiana (Maripasoula, Rochambeau, St Laurent du Maron).

Figure C.2. Comparing remote sensing with ground weather station data

a) Wind speed, La Réunion, Feb-2007 **b) Rainfall, Guadeloupe, Nov-1999**

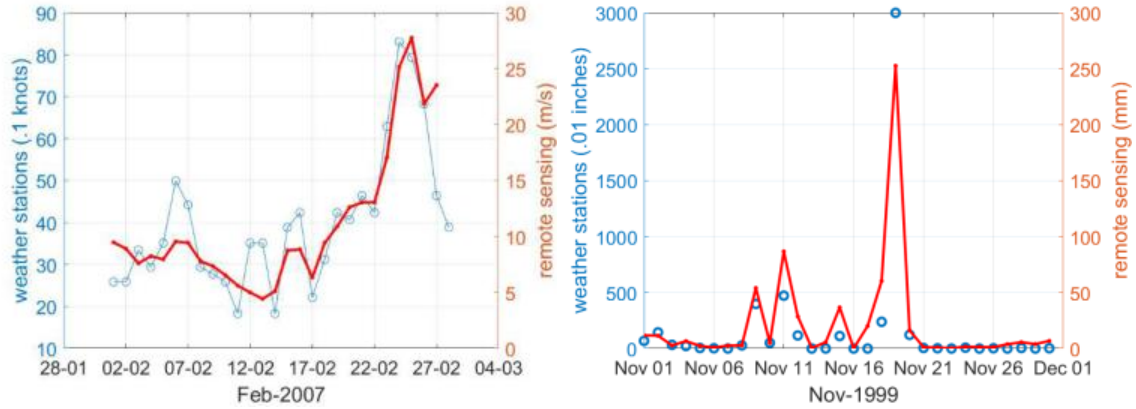

Note*:* Panel a) showing daily maximum wind speed in La Réunion in February 2007, Panel b) showing rainfall in Guadeloupe in November 1999. **Source***:* Remote-sensing wind speed (NOAA Cross-Calibrated Multi-Platform, CCMP; 0.25-degree grid in m/s; range from 0 to 30) and rainfall (NOAA Climate Prediction Center, CPC; 0.5-degree grid in mm). Ground station data from Global Surface Summary of the Day (GSOD) station data (wind in 0.1 knots; rain in 0.01 inches).

Table C.1. Relating administrative disasters to ground-level meteorological data

	(1)	(2)	(3)	(4)	(5)
Panel A: Marginal effects – Logit model					
Wind	0.052***			-0.079	-0.143
	(2.621)			(-0.851)	(-0.421)
Rain	0.001***			0.001***	0.002***
	(7.477)			(4.826)	(3.454)
$Wind^2$		0.009***		0.022	0.045
		(2.852)		(1.479)	(0.399)
$Rain^2$		0.000***		0.000*	0.000*
		(5.571)		(-1.757)	(-1.836)
$Wind^3$			0.002***		-0.002
			(3.051)		(-0.193)
$Rain^3$			0.000***		0.000
			(4.269)		(1.433)
Pseudo R^2	0.339	0.313	0.293	0.347	0.352
N	904	904	904	904	904
Panel B: 2SLS – 1st stage					
Pred prob.	1.037***	1.027***	1.027***	1.054***	1.065***
	(12.868)	(11.3)	(10.484)	(13.206)	(13.733)
Adj.R2	0.285	0.254	0.229	0.296	0.304
N	904	904	904	904	904
F-Stat	165.589	127.698	109.922	174.394	188.595

Note: Estimation results for first-stage equation (2) with dependent variable all natural disasters reported in EM-DAT and GASPAR as binary variable. All wind speed variables are expressed in m/s and all precipitation variables are expressed in mm. Wind corresponds to the maximum sustained wind speed maintained for one minute from the CCMP database per region and month. Rain is the maximum daily precipitation in mm per month and region as reported by the CPC Global Unified Gauge-Based Analysis of Daily Precipitation. T-stats are reported in parentheses. Standard errors are heteroskedasticity-robust and computed using a White-correction routine. Significant at ***0.01, **0.05, *0.10

Figure C.3. Main results with ground data– CPI components and headline CPI

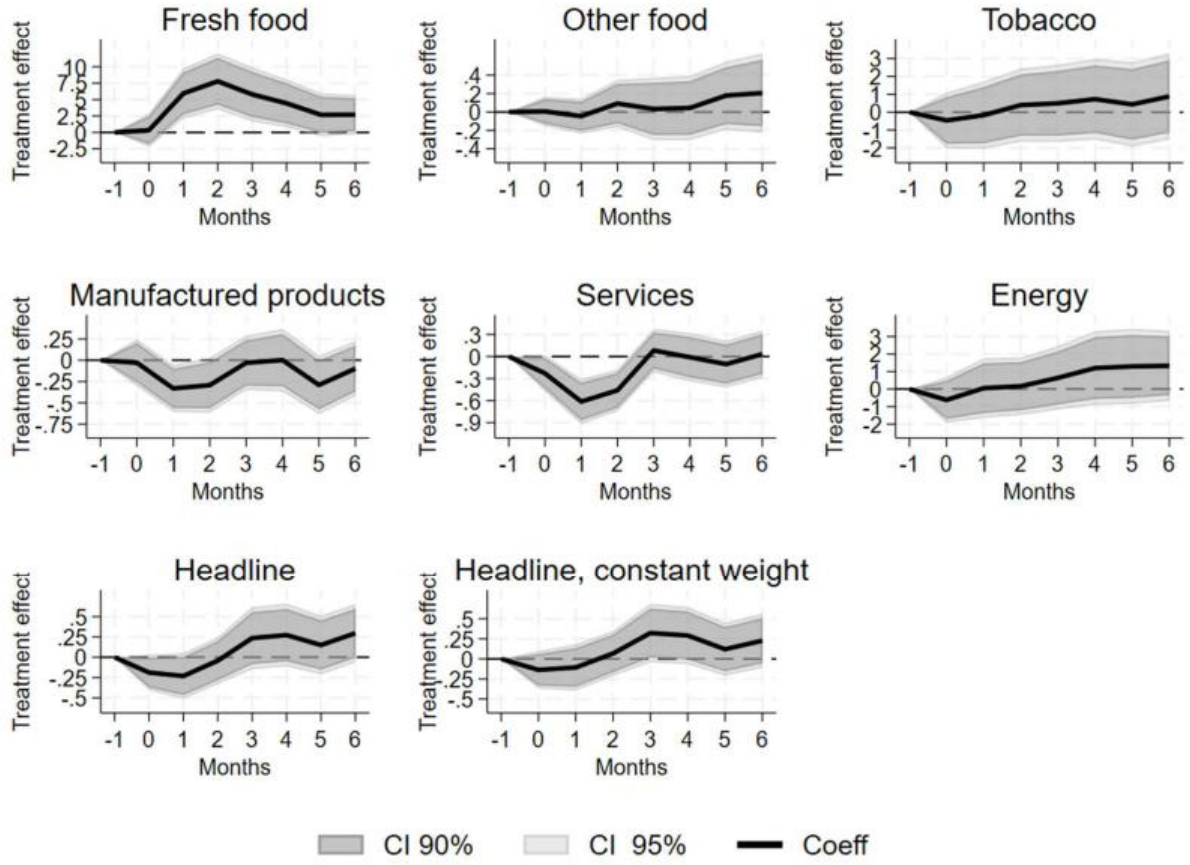

Note: Plotted are the cumulative impulse responses of CPI product components and headline to weather-related disasters (where meteorological data in the first step equation are ground data) obtained from our 2SLS baseline model; price effects (solid black line) are reported in percent; shaded areas show 90% (dark grey) and 95% (light grey) confidence intervals. Standard errors are heteroskedasticity-robust and computed using a White-correction routine. Months are expressed in distance to the natural disaster. Sample period: 1999m01 to 2024m12, excluding the Covid period 2020m03-2021m12, for all four regions.

Appendix D. The role of the estimated probability of a weather-related disaster for the price effects

In this Appendix, we explore how the estimated probability of a weather-related disaster affects the price effects obtained in our IV approach. To do so, we estimate the price effects of disasters for different thresholds of the estimated probability, which define the occurrence of a weather-related disaster.

We first define a series of more than 900 probability threshold values (*T*) uniformly defined between 0 and 1. For a given threshold value *T,* we define a binary variable $\mathbb{1}(\widehat{\omega_{i,t}} > T)$ equal to 1 if the predicted probability $\widehat{\omega_{i,t}}$ from the Logit model based on equation (1) is above this threshold and 0 otherwise. Then, for every threshold *T*, we run a local projection exercise (as in equation (3) on the price index for fresh food. We estimate as many local projection regressions as thresholds *T*, with the same set of controls as in our baseline specification (more than 900). The estimated equation can be written as follows:

$$\log\left(\frac{P_{i,t+h}}{P_{i,t-1}}\right) = \alpha_{2h} + \theta_h \mathbb{1}(\widehat{\omega_{i,t}} > T) + \rho_{2h} Z_{i,t} + \tau_{2h} Y_t \ldots + \delta_{2hy} + \mu_{2hq} + \gamma_{2hi} + \mu_{2hq} \times \gamma_{2hi} + \varepsilon_{2hi,t} \quad (10)$$

Figure D.1 plots the estimated coefficients θ_h in equation (10), for fresh food, at horizon *h=2,* obtained for the more than 900 values of thresholds (x-axis) (the dashed line corresponds to our baseline estimation obtained in our 2SLS model) whereas Figure D.2 plots the distribution of the price effects obtained across the more than 900 estimations. Several conclusions are worth being highlighted. First, the estimated price effect based on these discrete probability thresholds increases with the threshold. The effect goes from about 0 when the threshold is equal to 0 (meaning that virtually all observations are defined as a weather-related disaster) to 17.7% when the threshold is equal to 1 (meaning that only a few observations with the highest probability are treated as weather-related disasters). Second, the confidence interval contains the baseline estimated effect starting from a threshold probability of about 60%, this suggests that, above this value for the predicted probability, price effects are not statistically larger. Third, our baseline estimate is in the upper part of the distribution (Figure D.2).

Figure D.1. Price reactions of fresh food for a set of discrete shocks based on varying thresholds of estimated probabilities

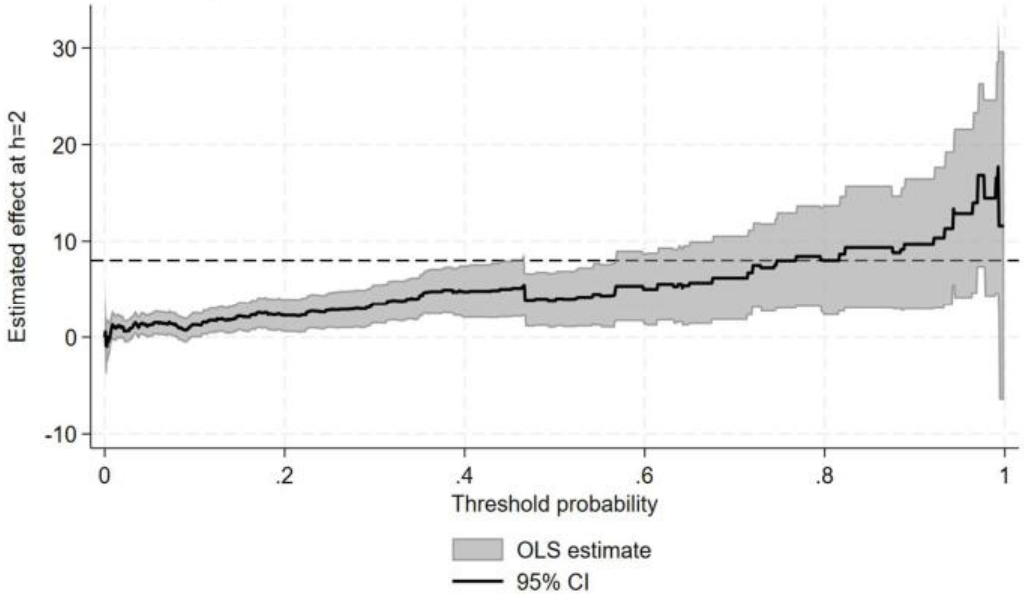

Note: Maximum estimated effect of OLS regressions for fresh food prices with shocks based on discretized probabilities estimated from Logit regression (1), with threshold varying from 0 to 1. Confidence intervals at the 95% level in grey. Standard errors are heteroskedasticity-robust and computed using a White-correction routine. The dotted line corresponds to our baseline estimated effect.

Figure D.2. Distribution of estimated effects on fresh food in the discrete shocks against the baseline effect

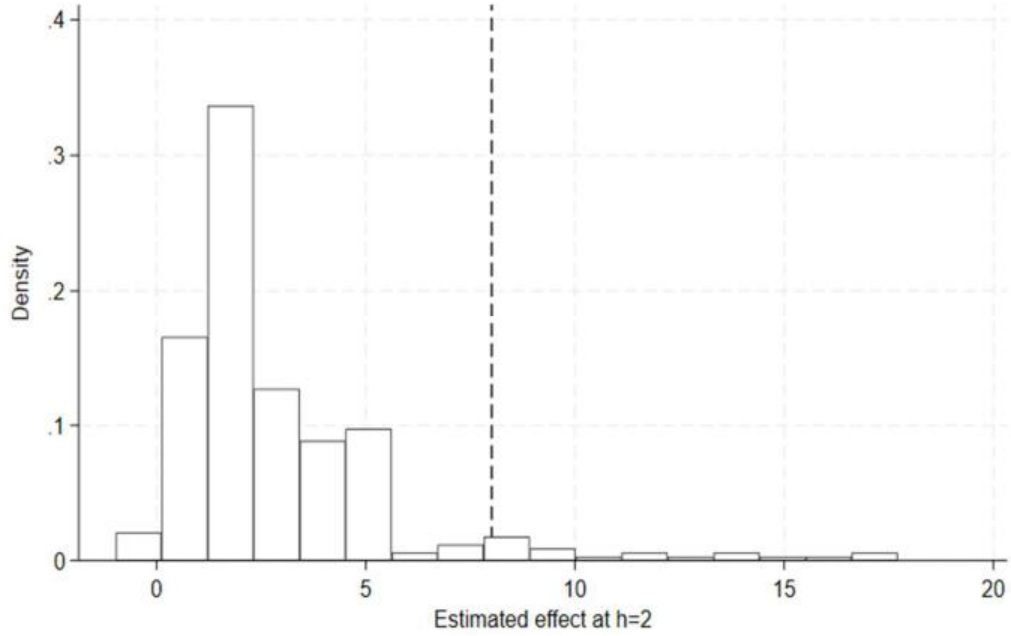

Note: Distribution of estimated coefficients represented in Figure D.1. The dotted line corresponds to the baseline 2SLS effect.

Appendix E. Estimating placebo effects

In this Appendix, we present results of different placebo regressions where we have randomized weather-related disaster shocks in both equations of our two-step model. We have run three distinct exercises.

E.1. Description of the placebo estimations and results

In a first exercise, we randomize the instrumental variables. Namely, we simulate rainfall and wind data from Gumbel laws of distribution (whose parameters are derived from the empirical distribution of rainfall and wind records across regions) since the Gumbel law is well suited to replicate the distributions of extreme events (see Section E.2 of this Appendix for additional methodological details). We run 100 2SLS estimations, each based on a distinct set of simulated data for instruments and using the actual observations for the treatment variable.

In a second exercise, we keep the actual values of the instrumental variables, but we randomize the treatment, drawing randomly 100 shocks from a uniform distribution. As in the previous exercise, we do not allocate them to regions in proportion to their observed frequency of disasters. We run 100 2SLS estimations, each based on a distinct set of simulated data for the treatment, but keeping the actual observations of the instrumental variables.

In a third exercise, we keep the actual values of the instrumental and treatment variables, and we compute the correct predicted probability of treatment in the first stage, but we randomly allocate this predicted probability across regions and over time between the first and second stage. We run 100 OLS estimations of the second stage, each based on a distinct set of randomizations of the predicted probability.

Figure E.1. Distribution of T-stats of placebo regressions

a) Randomization of instrumental variables | **b) Randomization of treatment variable** | **c) Randomization of predicted probabilities**

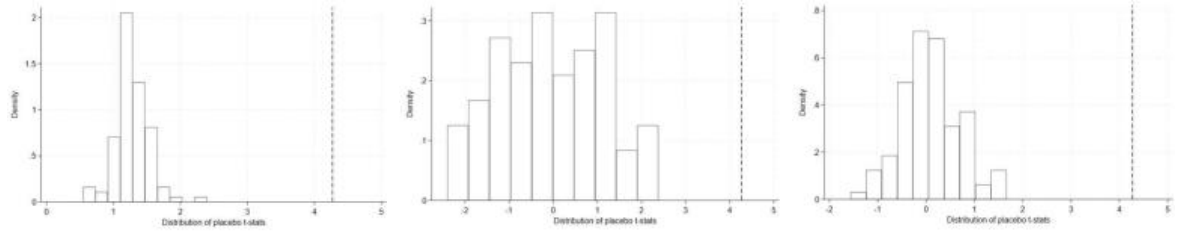

***Note*:** Distributions of T-stats of placebo tests. In Panel a), the randomized variables are the instrumental variables. In Panel b), the randomized variable is the treatment variable. In Panel c), the predicted probability is randomly allocated across regions between the first and the second stage. The dotted vertical lines correspond to the t-stat of the baseline estimation.

Figure E.1 plots the distributions of T-statistics for local projections of fresh food prices at horizon *h=2*, as well as the T-statistics from our baseline estimate (dashed vertical line). While the T-stat of the baseline estimate is equal to 4.3, 95% of those in the placebo estimates with randomization of instrumental variables are below 1.66 (Panel a), 95% of those in the placebo estimates with randomization of the treatment variable are below 1.98 (Panel b), and 95% of those in the placebo estimates with randomization of predicted probabilities are below 1.2 (Panel c).

E.2. Drawing random weather-related disasters for placebo estimations

Next, we describe how we draw random weather-related disasters for our first placebo estimation in which we instrument the actual administrative disasters by randomly generating them. We model the maximum observed monthly rainfall and wind speed using Gumbel distributions. The latter are part of generalized extreme value distributions, which are well suited to modelling extreme phenomena such as the ones we focus on.

For wind and rain, we generate 100 random draws from Gumbel distributions whose parameters match the empirical moments of the maximum wind and rain distributions. More specifically, the expected value and variance of a random variable following a Gumbel distribution of location parameter μ and of scale parameter β are defined as:

$$E(X) = \mu + \beta\gamma$$

$$V(X) = \frac{\pi^2}{6}\beta^2$$

where γ is Euler-Mascheroni constant (approximated by the value 0.5772156649). We therefore define $\hat{\beta}$ and $\hat{\mu}$ as:

$$\hat{\beta} = \sqrt{6} \times \frac{\widehat{sd(X)}}{\pi}$$

$$\hat{\mu} = \widehat{E(X)} - \hat{\beta}\gamma$$

where $\widehat{sd(X)}$ and $\widehat{E(X)}$ are empirical standard deviation and expected values observed for the variable X in our full sample of observations. Empirically, $\hat{\beta}$ and $\hat{\mu}$ are similar to the parameters estimated in Stata using the package extremes. Using these sets of parameters, computed both for observed maximum records of wind speed and rainfall, we randomly generate placebo values of maximum records of wind speed and rainfall for these values, defining them as:

$$Max_{placebo} = \max\left(\hat{\mu} - \hat{\beta} \times \ln(-\ln(\mathrm{U})), 0\right)$$

where U is a random draw in a uniform distribution [0,1]. Since random draws in a Gumbel distribution can take negative values, we truncate them at zero, to match the fact that maximum rainfall and wind speed cannot have negative values.

Table E.1. Empirical moments of maximum wind and rainfall and computed parameters of Gumbel distributions

	$\widehat{E(X)}$	$\widehat{sd(X)}$	$\hat{\mu}$	$\hat{\beta}$
Maximum wind speed	11.59	2.17	10.61	1.69
Maximum rainfall	46.77	33.88	31.52	26.42

In Figures E.2 and E.3, we plot the densities of placebo records (in grey), the density of observed records (in red), and the density of a random draw of a normal distribution with parameters of expected value and standard deviation equal to the empirical moments of maximum wind speed and rainfall (in blue).

Figure E.2. Placebo and observed maximum wind speed

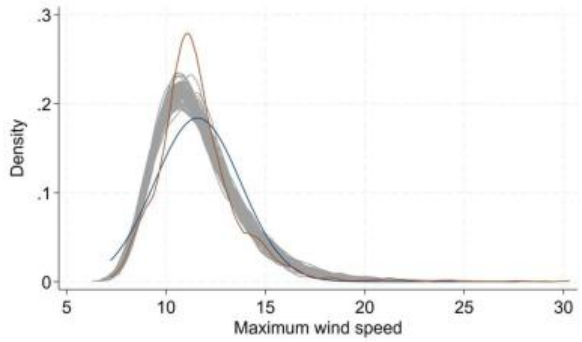

Figure E.3. Placebo and observed maximum rainfall

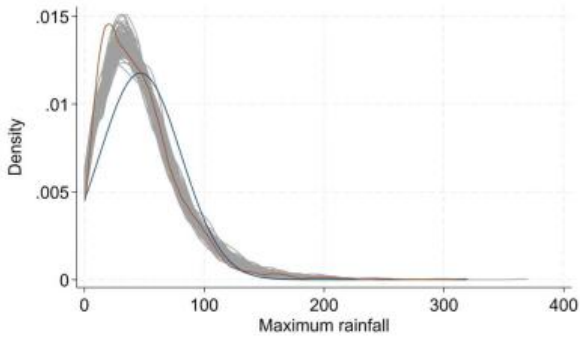

***Note*:** The grey curves represent 100 densities of random draws in Gumbel distributions matching the observed moments of maximum wind speed and maximum rainfall. Blue curves correspond to a random draw in a normal distribution. Densities of actual maximum wind speed and rainfall are plotted in brown.

In Figures E.4 and E.5, we plot the quantile-quantile (QQ) plots of our random draws against the observed distributions. Overall, our random draws match the distribution of observed maximum wind speed and rainfall reasonably well and are better suited to such data than a normal distribution.

Figure E.4. QQ plots of placebo and observed maximum wind speed

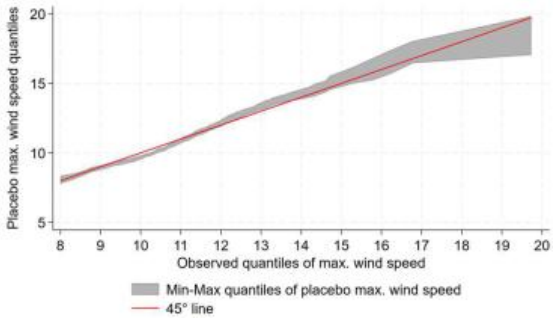

Figure E.5. QQ plots of placebo and observed maximum rainfall

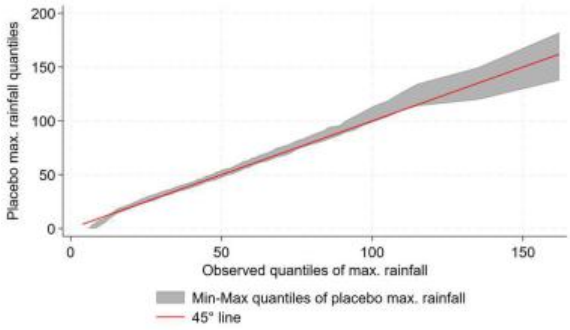

***Note*:** Plotted is the range of quantiles of placebo maximum wind speed (resp. placebo maximum rainfall) against the respective quantiles of observed maximum wind speed (resp. observed maximum wind speed).

Appendix F. Price effects and the CPI weight of fresh food

F.1. Varying the fresh food weight

The overall positive effect of natural disasters on inflation is mainly driven by the large effect on prices of fresh food products, which represent a small fraction of the CPI basket of goods (3.6% on average between 1999 and 2024). The share of fresh food products has continuously decreased over our sample period from 5.9% in 1999 to 2.7% in 2024 (Table A.4 in the Appendix). In this robustness exercise, we estimate the overall effect on inflation of natural disasters when we vary the share of fresh food.

Figure F.1. Baseline and alternative effects on CPI inflation

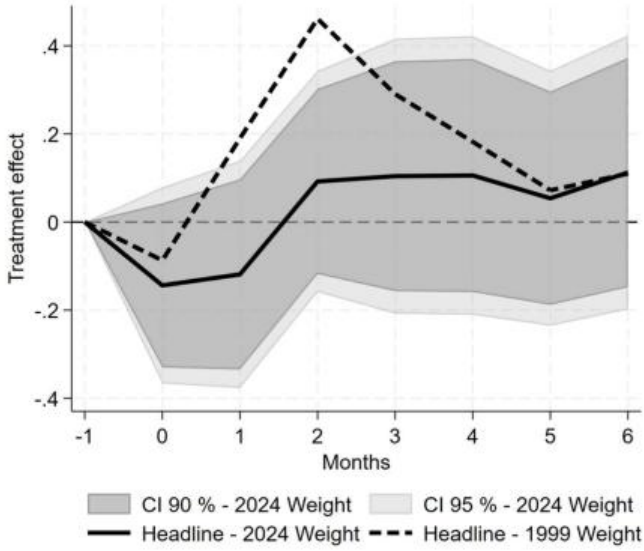

Note: Comparison of the baseline IV estimation for a reconstitution total CPI using weights of CPI components as of 2024 (solid line), and as of 1999 (dashed line). Treatment effects are expressed in percent. The shaded area represents the 90% and 95% confidence interval for the estimation using the 2024 weights. Standard errors are heteroskedasticity-robust and computed using a White-correction routine. The x-axis corresponds to the time horizon expressed in months since the disaster.

In Figure F.1, we show counterfactual effects on headline inflation, assuming different weights for fresh food. The blue line represents the effect estimated on a constant-weight headline, where each of the 6 main aggregates have throughout the whole sample a weight equal to their average value across regions in 2024. The shaded areas represent the 90% and 95% confidence intervals of this estimate. The red line represents the effect estimated on a constant-weight headline, where each of the 6 main aggregates have throughout the whole sample a weight equal to their average value across regions in 1999. This estimated is significantly higher than the one using 2024 weight, and reaches about 0.5% after two months, notably because of the higher weight of fresh food.

F.2. Differential effects depending on household income quintiles

In this Appendix, we evaluate the effect of weather-related disasters for different CPI basket composition, corresponding to different quintiles of income in regions, using the *Budget des familles* dataset from 2017. The main difficulty in merging the CPI data with the *Budget des familles* is that the *Budget des familles* consumption basket and the CPI aggregates we considered, though based on the same underlying classification (COICOP), have differing compositions. This prevents perfect mapping of the two sets of items. We therefore focus on the item that reacts the most strongly in our estimation, namely fresh food. However, reconciling the two datasets is not straightforward. Indeed, while INSEE publishes the CPI of fresh food and total CPI excluding fresh food, the share of fresh food in the consumption baskets is not available from the *Budget des familles* survey. Conversely, while the *Budget des familles* survey gives weight for total food (including tobacco), the food CPI published by INSEE excludes tobacco.

Table F.1. Share of food (inc. tobacco) in the household consumption basket, by quintile of income (2017)

	Guadeloupe	Martinique	French Guiana	La Réunion	Average
Total	15.8	16.0	15.8	17.0	16.2
1st quintile	19.8	19.9	21.2	23.3	21.1
2nd quintile	20.1	18.0	20.7	21.9	20.2
3rd quintile	16.5	16.5	16.2	17.2	16.6
4th quintile	15.8	15.3	15.2	15.7	15.5
5th quintile	12.4	13.9	12.2	14.5	13.3

Note: Share of food (including tobacco) in the household consumption basket (in % of total consumption), according to the *Budget des Familles* survey of 2017. The average across the four regions is computed as an unweighted mean.

We therefore resort to the following simple approximation. First, in the *Budget des familles* survey, for each quintile of income, and on average across the four overseas regions, we compute the percent deviation in the share of food (including tobacco), compared to the average share. Second, we apply these percent deviations to the average weight of fresh food observed in our sample. This gives us estimated weights of fresh food for each quintile. We therefore implicitly assume that the deviation of weights of fresh food between the quintiles and the average is the same as the observed deviation of weights of food including tobacco, and that the deviation of weights of food products observed in 2017 between the quintiles and the average is representative of the deviations that occurred between 1999 and 2024. Finally, we derive the weights of the remaining components of the CPI, making sure that i) their relative

weights are identical to that of the actual weight structure, ii) the sum of all weights including those of fresh food is equal to 100%. We then aggregate CPI components using this new structure, yielding a headline CPI for each quintile of income. Finally, we estimate the reaction of these quintile-specific CPI to weather-related shocks in our 2SLS-local projection framework (Figure F.2). We find a stronger reaction of the CPI corresponding to the basket structure of the first quintile (blue line, with the associated 90% and 95% confidence intervals in shaded areas), compared to that of the last quintile (red line), with a maximum difference of 0.15 pp.

Figure F.2. Baseline and alternative effects on CPI inflation by income quintile

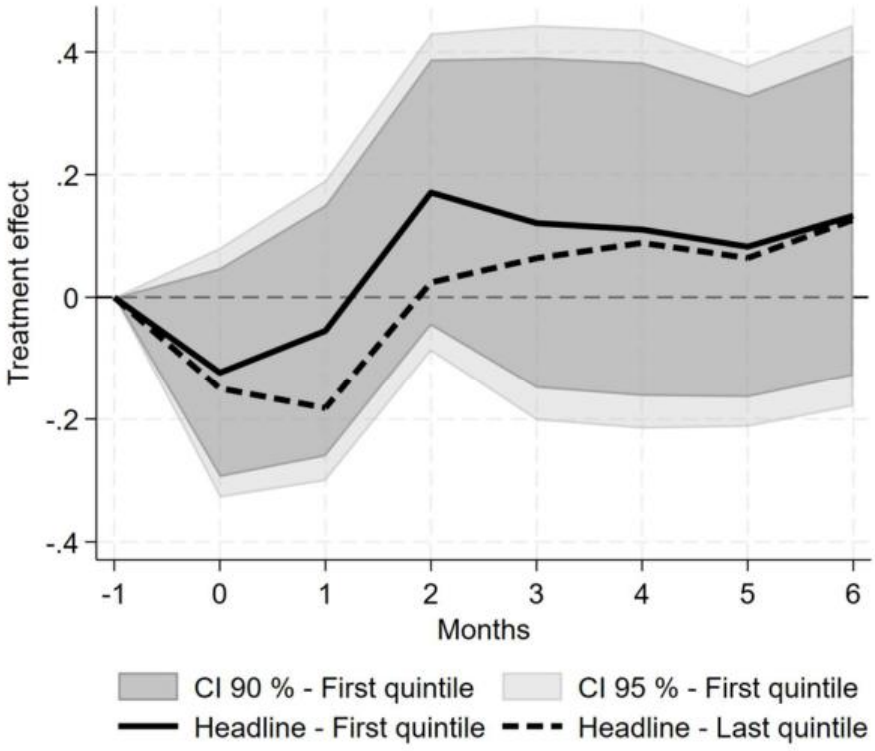

Note: Baseline IV impulse responses for constant-weight headline CPI reweighted by household-expenditure shares for the 1st (solid) and 5th (dashed) income quintiles (INSEE "Budget des familles" 2017). Treatment effects are expressed in percent. The shaded area represents the 90% and 95% confidence interval for the estimation using the weights of the first quintile. Standard errors are heteroskedasticity-robust and computed using a White-correction routine. The x-axis corresponds to the time horizon expressed in months since the disaster.

Appendix G. Construction of wind and rain damage functions

This Appendix provides complementary information on the construction of damage functions.

For the calibration of wind speed threshold value W^*, we choose to set this value at 15 m/s, which corresponds to the 95th percentile of the wind distribution in our sample. It is well known that remote-sensing data from CCMP is fairly accurate at low to moderate wind speeds (<15 m/s), but systematically underestimate high winds, in part because of spatial smoothing within fields from the numerical background model (Mears et al. 2022). This is a comparatively low threshold values of damage from extreme wind compared with the literature. Strobl (2012) and Heinen et al. (2018) set the threshold value at approximately 49 m/s. The higher value is due to the different underlying dataset, as these authors use the HURDAT data, which is collected from hurricane reconnaissance aircrafts that more accurately measure peak hurricane intensity. Also Emanuel (2011) uses a higher threshold value in a damage function at 26 m/s. We converted units to meters/second here, while the thresholds are defined in knots in Emanuel (2011) (50 knots) and in kilometer per hour in Strobl (2012) and Heinen et al. (2018) (177-178 km/h).

Unfortunately, the HURDAT dataset does not cover La Réunion. Applying the exact same thresholds from this literature to our wind data would not be consistent given the strong underestimation of wind speed above 15 m/s from remote sensing data. Further, it would lead to H_{it} being different from 0 for only few data points of our sample. However, for robustness we provide results with a threshold at 20 m/s which corresponds to the 98th percentile of the wind distribution in our dataset.

The calibration of the rainfall threshold values r^* follows Heinen et al. (2018). The threshold is based on precipitation of a cumulative amount of 112 mm over surface, cumulative over a three-day backward-looking window. Heinen et al. (2018) deducted this threshold from an intensity duration flood model and actual flood event data for Trinidad. We keep the same threshold in our case for all overseas territories.

Exposure weights ξ_{ij} are constructed from satellite nighttime light data from the U.S. Air Force Defense Meteorological Satellite Program (DMSP), obtained via the Earth Observation Group (Baugh et al., 2010). We use the version cleaned of background noise, averaged across the calendar year and corrected for percent frequency of light detection. Figure G.1, Panel a visualizes the data for the case of La Réunion. Figure G.1 Panel (b) shows nighttime light observations that are cleaned of observations above the ocean surface. We use geographic

information system software and freely available shapefiles on ocean surfaces by *Natural Earth* to geolocate the nighttime light and meteorological data jointly. The main motivation is to consider noise from coastal areas, such as ships or other coastal activities. We compute a proxy of economic activity in a weather cell j in region i as

$$\nu_{ij} = \sum_{n=1}^{N} NTL_{ijn} \times \mathbb{1}_{\{O_{ijn}=0\}}, \tag{G.1}$$

where NTL_{ijn} denotes nighttime light in region i in weather cell j and nighttime light grid cell n, and $\mathbb{1}$ denotes an index variable which takes the value of one if the nighttime light is recorded above land. Figure G.1 Panel (c) illustrates that the number of nighttime light observations N per weather cell j can vary substantially. The final weights are obtained by dividing nighttime light intensity in each weather cell j by total nighttime light intensity in region i:

$$\xi_{ij} = \frac{\nu_{ij}}{\sum_j \nu_{ij}} \tag{G.2}$$

Figure G.1, panel (d) illustrates the result, where brighter areas indicate higher values of ξ_{ij}.

Figure G.1. Nighttime light weights for La Réunion

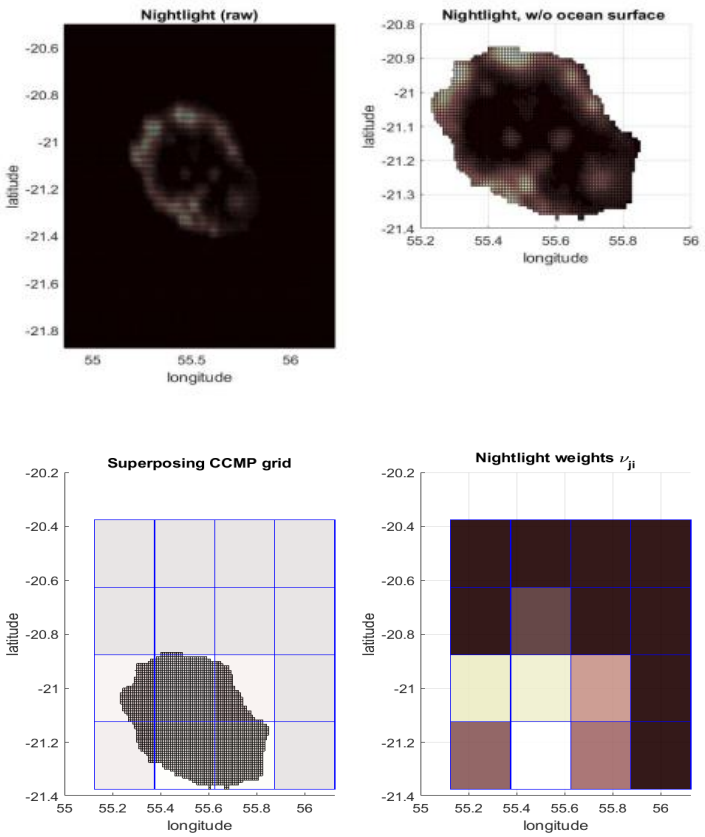

Note: Nighttime-light activity weights for La Réunion based on data of Defense Meteorological Satellite Program, cleaned from observations above ocean surface (based on Natural Earth coastlines). Weights are computed on the CCMP 0.25° grid as the normalized detection frequency within each cell (brighter = higher weight; weights sum to 1 over land cells).

Online Appendix References

Baugh, K., Elvidge, C. D., Ghosh, T., and Ziskin, D. (2010). "Development of a 2009 Stable Lights Product Using DMSP-OLS Data", *Proceedings of the Asia-Pacific Advanced Network*, 30(0), 114.

Emanuel, Kerry. (2011). "Global Warming Effects on U.S. Hurricane Damage." *Weather, Climate, and Society*, 3(4), 261–268.

Heinen, Andréas, Jeetendra Khadan, and Eric Strobl (2018). "The Price Impact of Extreme Weather in Developing Countries." *Economic Journal*, 129(619), 1327-1342.

Mears, Carl, Tong Lee, Lucrezia Ricciardulli, Xiaochun Wang, and Frank Wentz. (2022). "Improving the Accuracy of the Cross-Calibrated Multi-Platform (CCMP) Ocean Vector Winds." *Remote Sensing*, 17(14), 4230.

Strobl, Eric. (2012). "The Economic Growth Impact of Natural Disasters in Developing Countries: Evidence from Hurricane Strikes in the Central American and Caribbean Regions." *Journal of Development Economics*, 97(2012), 130-141.